



Norwegian University of  
Science and Technology

# Combined heat and power plant on offshore oil and gas installations

**Eirik Røberg Følgesvold**

Master of Science in Mechanical Engineering

Submission date: June 2015

Supervisor: Lars Olof Nord, EPT

Co-supervisor: Olav Bolland, EPT

Norwegian University of Science and Technology  
Department of Energy and Process Engineering



EPT-M-2015-23

**MASTER THESIS**

for

student Eirik Røberg Følgesvold

Spring 2015

Combined heat and power plant on offshore oil and gas installations

**Background and objective**

On offshore oil and gas installations the power demand is high. Process heat is also needed. In addition, the power plant should be flexible to be able to adjust to the needs of the oil and gas processes on the platform or FPSO. The current dominating technology is based on simple cycle gas turbines. Combined cycles with a gas turbine cycle combined with a steam bottoming cycle has emerged as one of the most attractive alternatives to meet the demands of the offshore installation.

The power-heat demand changes during the lifetime of the installation. For short duration changes, for example during off-loading, one could also choose to produce less heat and more power. In addition, different combined cycle plant configurations can be attractive depending on the needs of the installation, for example, a back-pressure steam turbine versus an extraction condensing steam turbine.

The overall objective of the Master's thesis is to make a detailed process model of a combined heat and power plant based on gas turbines and a steam bottoming cycle and subsequently simulate the process and generate results both at the design point and at off-design conditions (changes in power and heat load, changes in ambient conditions). The software to be used is Epsilon Professional.

**The following tasks are to be considered:**

1. Literature study on combined heat and power plants (CHP).
2. Evaluation and decision of CHP cycle configuration(s) to be studied.
3. Build-up of steady-state process model of the selected cycle(s).
4. Design point process simulation of the CHP cycle(s) including model validation.
5. Off-design simulations.
6. Sensitivity analysis.

Within 14 days of receiving the written text on the master thesis, the candidate shall submit a research plan for his project to the department.

When the thesis is evaluated, emphasis is put on processing of the results, and that they are presented in tabular and/or graphic form in a clear manner, and that they are analyzed carefully.

The thesis should be formulated as a research report in English with summary, conclusion, literature references, table of contents etc. During the preparation of the text, the candidate should make an effort to produce a well-structured and easily readable report. In order to ease the evaluation of the thesis, it is important that the cross-references are correct. In the making of the report, strong emphasis should be placed on both a thorough discussion of the results and an orderly presentation.

The candidate is requested to initiate and keep close contact with his/her academic supervisor(s) throughout the working period. The candidate must follow the rules and regulations of NTNU as well as passive directions given by the Department of Energy and Process Engineering.

Risk assessment of the candidate's work shall be carried out according to the department's procedures. The risk assessment must be documented and included as part of the final report. Events related to the candidate's work adversely affecting the health, safety or security, must be documented and included as part of the final report. If the documentation on risk assessment represents a large number of pages, the full version is to be submitted electronically to the supervisor and an excerpt is included in the report.

Pursuant to "Regulations concerning the supplementary provisions to the technology study program/Master of Science" at NTNU §20, the Department reserves the permission to utilize all the results and data for teaching and research purposes as well as in future publications.

The final report is to be submitted digitally in DAIM. Based on an agreement with the supervisor, the final report and other material and documents may be given to the supervisor in digital format.

- Work to be done in lab (Water power lab, Fluids engineering lab, Thermal engineering lab)  
 Field work

Department of Energy and Process Engineering, 14. January 2015



Olav Bolland  
Department Head



Lars Nord  
Academic Supervisor



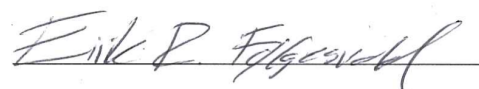


## Preface

This thesis was prepared at the Department of Energy and Process Engineering, Faculty of Engineering Science and Technology at Norwegian University of Science and Technology in fulfillment of a M.Sc. in Mechanical Engineering. The work was carried out in the period January 2015 to June 2015 under supervision of Associate Professor Lars. O. Nord and Professor Olav Bolland.

I would like to thank my supervisor Associate Professor Lars O. Nord for technical guidance and given thoughts.

Trondheim, 10-June-2015

A handwritten signature in black ink, reading "Eirik R. Følgesvold", written over a horizontal line.

Eirik R. Følgesvold





## Abstract

With the increased focus on reducing Norway's greenhouse gas emissions offshore, optimization of the power supply has become a focus area. Subsequently, steam bottoming cycles applied to gas turbines on offshore oil and gas installations has emerged as one of the most attractive alternatives to enhance efficiency and reduce emissions. The economic driving force of such modifications is the reduced CO<sub>2</sub> taxation. The steam bottoming cycle can be configured to deliver both heat and power to the offshore process and production facility. In this thesis, simulation work on two different combined heat and power configuration of the steam bottoming cycle are investigated. The aim of the study is to answer the research question: *“What are the positives and negatives of the backpressure- and extraction steam turbine for offshore combined cycle operation?”*

The combined cycles were designed and simulated in the process simulation software Epsilon Professional. Both the extraction- and backpressure steam turbine cycle had a single GE LM2500+G4 gas turbine as a topping cycle, and a once through steam generator to exploit the waste heat in the exhaust. The main objectives were to evaluate results at design, off-design and carry out a sensitivity analysis on the cycles. Additionally, possible reduction in CO<sub>2</sub> emission and taxation were discussed. At design the extraction steam turbine produced 8.2 MW, while the backpressure steam turbine output was 6.0 MW. Results showed that net thermal efficiency increased with 13.3 and 8.8 % compared to a simple cycle arrangement. The energy utilization factor for the extraction steam turbine reached 52.9 %, while the backpressure steam turbine achieved 74.2 %. Off-design results were displayed in diagrams illustrating the operational window. Electric power output was plotted against process heat delivered at a given supply temperature. Sensitivity analysis was carried out on both cycles.

The findings suggested that a backpressure steam turbine could be attractive for oil producing facilities with high demand of process heat. Large penalty in power output made it unsuitable for integration on facilities with process temperature demands above 120 °C. Results on the extraction steam turbine cycle suggested that an implementation towards facilities with less heat demand would be more attractive. Based on the results from the simulations, literature research and discussion, positive and negative remarks were made for each combined cycle configuration.



## Sammendrag

Det økende fokuset på utslippsnivået av klimagasser i Norge har resultert i et stort fokus på optimalisering av energiproduksjonen offshore. Som et tiltak for effektivisering har kombinerte kraftsykluser med damp stått frem som et av mest attraktive løsningene for reduisering av utslipp. De økonomiske drivkreftene for implementering av slik teknologi er de reduserte kostnadene i CO<sub>2</sub> avgifter. En kombinert kraftsyklus med damp kan bli modifisert til levere både varme og kraft til prosessering og produksjonsutstyret på offshore installasjonen. I denne oppgaven vil to forskjellige modifiseringer av en slik syklus bli nærmere undersøkt. De valgte kombinerte kraftsyklusene har henholdsvis en mottrykks dampturbin og en ekstraksjon dampturbin. Problemstillingen for oppgaven er: *”Hva er positivt og negativt ved bruk av mottrykk- og ekstraksjonsturbiner i en kombinert kraftsyklus offshore?”*

Syklusene ble designet og simulert programvaren Epsilon Professional. I begge syklusene ble GE LM2500+G4 bruk som toppsyklus mens damp ble generert i en OTSG. Hovedmålene var å evaluere resultater fra design, off-design og sensitivitetsanalyser. I tillegg ble reduksjoner i CO<sub>2</sub> utslipp og avgifter diskutert. Ved design oppnådde ekstraksjonsturbinen en kraftproduksjon på 8.2 MW, mens mottrykksturbinen oppnådde en kraftproduksjon på 6.0 MW. Resultatene viste en økning i den termiske virkningsgraden på henholdsvis 13.3 % og 8.8 % sammenlignet med enkeltstående operasjon av gassturbinen. Utnyttelsesgraden av tilført energi var henholdsvis 52.9 % og 74.2 % for ekstraksjon- og mottrykksturbin syklusene. Off-design resultatene ble fremstillet i diagrammer der netto generert kraft er plottet mot prosessvarme for en gitt suppleringsstemperatur. Sensitivitetsanalyse ble utført på begge syklusene.

Funnene antydte at en mottrykksturbin kan være attraktivt for en oljeproduiserende plattform med høyt varmebehov. Ved produksjon av prosessvarme ved temperaturer over 120 C, ble kraftproduksjonen så kraftig redusert at en mottrykksturbin ikke stod frem som et godt alternativ. Resultater fra ekstraksjonsturbinen antydte at en implementering kan passe seg best mot installasjoner som har lavere varmebehov, slik som produksjon av et gassfelt. Basert på resultatene fra simulering, litteraturstudie og analyse, så ble det laget en oppsummerende tabell med positive og negative merknader for hver av syklusene.



# Contents

<b>Preface</b> .....	<b>I</b>
<b>Abstract</b> .....	<b>III</b>
<b>Sammendrag</b> .....	<b>V</b>
<b>List of figures</b> .....	<b>XI</b>
<b>List of tables</b> .....	<b>XV</b>
<b>Nomenclature</b> .....	<b>XVII</b>
<b>1. Introduction</b> .....	<b>1</b>
1.1. Background .....	1
1.2. Objectives .....	2
1.3. Thesis organization .....	3
1.4. Risk assessment .....	3
1.5. Contributions .....	3
1.6. Limitations .....	4
<b>2. Cogeneration on offshore oil and gas installations</b> .....	<b>5</b>
2.1. Power generation .....	5
2.1.1. Gas turbines .....	5
2.1.2. Onshore power supply .....	6
2.2. Offshore heat and power requirement .....	9
2.2.1. Topside processing system .....	9
2.3. Reservoir engineering .....	13
2.3.1. Primary Recovery .....	13
2.3.2. Secondary recovery .....	16
2.3.3. Enhanced oil recovery processes .....	16
2.4. The energy trend.....	17
2.5. Emission trend and taxation .....	19
2.6. Existing facilities .....	22
2.6.1. Oseberg D.....	22
2.6.2. Eldfisk 2/7-E.....	23
2.6.3. Snorre B.....	24
<b>3. Thermodynamic methodology</b> .....	<b>27</b>
3.1. The 1 <sup>st</sup> law of thermodynamic .....	27
3.2. The 2 <sup>nd</sup> law of thermodynamic .....	28
3.3. Irreversibility and entropy .....	28
3.4. Process analysis .....	29
3.4.1. Isentropic compression and expansion .....	30
3.4.2. Polytropic compression and expansion .....	32
3.4.3. Compression and expansion calculation in Epsilon Professional .....	35
3.5. Heat transfer .....	35

3.6.	Definitions .....	36
3.6.1.	Power outputs .....	36
3.6.2.	Plant efficiencies .....	37
3.6.3.	Emission rates and cost .....	38
<b>4.</b>	<b>Power cycles .....</b>	<b>39</b>
4.1.	Brayton cycle.....	39
4.2.	Steam rankine cycle .....	41
4.3.	Combined heat and power cycles.....	43
4.3.1.	Extraction steam turbine cycle .....	43
4.3.2.	Backpressure steam turbine cycle .....	44
<b>5.</b>	<b>Cogeneration technology .....</b>	<b>45</b>
5.1.	Gas turbine .....	45
5.2.	Steam turbine.....	47
5.3.	Heat recovery steam generator .....	49
5.4.	Condenser.....	53
5.5.	Pumps .....	53
5.6.	Deaeration .....	54
<b>6.</b>	<b>Off-design operation and control.....</b>	<b>57</b>
6.1.	Gas turbine .....	57
6.1.1.	Axial compressor.....	58
6.1.2.	Axial turbine.....	60
6.1.3.	Combustor chamber .....	61
6.2.	Steam turbine.....	62
6.3.	Heat recovery steam generator .....	64
6.4.	Pump.....	64
<b>7.</b>	<b>Simulation methodology .....</b>	<b>67</b>
7.1.	Ebsilon Professional V-10.6.....	67
7.2.	General assumptions .....	69
7.2.1.	Ambient conditions .....	69
7.2.2.	Gas turbine .....	70
7.2.3.	Heat recovery steam generator .....	71
7.2.4.	Steam turbine.....	72
7.2.5.	Additional components.....	73
7.3.	Validation .....	74
7.4.	Extraction steam turbine model description.....	76
7.5.	Backpressure steam turbine model description .....	78
<b>8.</b>	<b>Results and discussion.....</b>	<b>81</b>
8.1.	Extraction steam turbine cycle .....	81
8.1.1.	Design case.....	81
8.1.2.	Off-design.....	84
8.1.3.	Sensitivity analysis .....	86
8.2.	Backpressure steam turbine cycle .....	92
8.2.1.	Design case.....	92

8.2.2. Off-design cases .....	95
8.2.3. Sensitivity analysis .....	97
8.3. Emission and taxation .....	102
8.4. Discussion .....	105
<b>9. Conclusions and further work .....</b>	<b>107</b>
9.1. Concluding remarks .....	107
9.2. Further work .....	108
<b>Bibliography .....</b>	<b>109</b>
<b>A. Appendices .....</b>	<b>113</b>
I. GE LM 2500+G4 Diagrams.....	113
II. Diagrams Validation Simulation .....	115
III. Extraction steam turbine cycle – additional results.....	116
IV. Backpressure steam turbine cycle –Additional results .....	119





## List of figures

Figure 2.1 General Electric LM2500+G4 gas turbine [10].....	5
Figure 2.2 Onshore power to FPSO, transformer on ship [2] .....	7
Figure 2.3 Onshore power to FPSO, subsea transformer [2] .....	7
Figure 2.4 Generalized topside processing system .....	9
Figure 2.5 Effect of primary recovery mechanism on an oil reservoir volume before and after production [25].....	14
Figure 2.6 Primary drivers: Pressure vs. Cumulative oil production .....	15
Figure 2.7 Primary recovery: GOR vs. Cumulative oil production .....	15
Figure 2.8 Illustrative curve for impacts of known events on energy intensity [29] .....	18
Figure 2.9 Source of emissions for offshore oil and gas production in Norway [1].....	19
Figure 2.10 Emission history and forecast for petroleum industry in Norway [1] .....	20
Figure 2.11 Oseberg-D combined cycle process layout [12] .....	22
Figure 2.12 Eldfisk 2/7-E combined cycle process layout [12] .....	23
Figure 2.13 Snorre B electrical connection scheme [40] .....	24
Figure 4.1 Brayton cycle [41] .....	39
Figure 4.2 T-s diagram for closed cycle gas turbine with irreversibilities [41] .....	40
Figure 4.3 Layout of combined gas turbine-steam power plant[41] .....	41
Figure 4.4 T-s diagram of ideal steam rankine cycle[41] .....	42
Figure 4.5 Layout of the extraction steam turbine cycle.....	43
Figure 4.6 Layout of the backpressure steam turbine cycle.....	44
Figure 5.1 LM2500+ G4 skid module [49].....	47
Figure 5.2 Horizontal drum based HRSG[51] .....	50
Figure 5.3 Vertical drum based HRSG [51].....	50
Figure 5.4 a) HRSG heat transfer at single pressure b) HRSG heat transfer at dual pressure [53] .....	51
Figure 5.5 Stand-alone deaerator [47].....	54
Figure 5.6 Deaerating condenser [56].....	55
Figure 6.1 Axial compressor characteristics [53].....	59
Figure 6.2 Characteristic curve for an axial turbine [53] .....	60
Figure 6.3 GE LM2500+G4 combustion chamber [47, 57].....	61

Figure 6.4 GE LM2500+G4 DLE operation principles [57].....	61
Figure 6.5 Combustion stability curve and the effect of combustion pressure [59] .....	62
Figure 6.6 Sliding pressure operation diagram [51].....	62
Figure 6.7 ST efficiency correction characteristic from Ebsilon Professional .....	63
Figure 6.8 Characteristic pump curve [45].....	65
Figure 7.1 Oseberg D validation simulation .....	75
Figure 7.2 Extraction steam turbine cycle – Ebsilon Professional model.....	77
Figure 7.3 Backpressure steam turbine cycle – Ebsilon Professional model.....	79
Figure 8.1 Energy balance for the extraction steam turbine cycle at design.....	81
Figure 8.2 T-Q diagram for HRSG in extraction steam turbine cycle .....	83
Figure 8.3 T-s diagram for extraction steam turbine cycle .....	83
Figure 8.4 Operational area for extraction of steam at 5 [bar].....	84
Figure 8.5 Effect of input parameters (1) – Extraction steam turbine cycle .....	87
Figure 8.6 Effect of input parameters (2) – Extraction steam turbine cycle .....	87
Figure 8.7 Sensitivity plot for cooling water temperature – Extraction steam turbine cycle...	88
Figure 8.8 Sensitivity plot for ambient temperature – Extraction steam turbine cycle.....	89
Figure 8.9 Sensitivity plot for pinch point temperature – Extraction steam turbine cycle .....	89
Figure 8.10 Sensitivity plot for GT exhaust pressure – Extraction steam turbine cycle.....	90
Figure 8.11 Sensitivity plot for 1 <sup>st</sup> stage ST efficiency – Extraction steam turbine cycle.....	91
Figure 8.12 Sensitivity plot for 2 <sup>nd</sup> stage ST efficiency – Extraction steam turbine cycle .....	91
Figure 8.13 Energy balance for backpressure steam turbine cycle at design.....	92
Figure 8.14 T-Q diagram for the HRSG in backpressure steam turbine cycle .....	94
Figure 8.15 T-s diagram for backpressure steam turbine cycle .....	94
Figure 8.16 Operational line for backpressure steam turbine at 2 [bar] Ts 120 [°C].....	95
Figure 8.17 Effect of input parameters (1) - Backpressure steam turbine cycle.....	98
Figure 8.18 Effect of input parameters (2) - Backpressure steam turbine .....	98
Figure 8.19 Sensitivity analysis ambient temperature - Backpressure steam turbine cycle ...	99
Figure 8.20 Sensitivity plot for ST efficiency - Backpressure steam turbine cycle.....	99
Figure 8.21 Sensitivity plot pinch point temperature difference - Backpressure steam turbine cycle .....	100
Figure 8.22 Sensitivity plot exhaust gas pressure - Backpressure steam turbine cycle .....	101
Figure 8.23 Sensitivity plot for feedwater temperature - Backpressure steam turbine cycle.	101

Figure 8.24 CO <sub>2</sub> emission rate .....	103
Figure 8.25 CO <sub>2</sub> taxation cost per MWh.....	104
Figure A.1 GE LM2500+G4 Load vs. Exhaust temperature diagram .....	113
Figure A.2 GE LM2500+G4 Load vs. Exhaust mass flow .....	113
Figure A.3 GE LM2500+G4 Power output for different ambient temperatures.....	114
Figure A.4 T-s diagram Oseberg-D simulation.....	115
Figure A.5 HRSG Q-T diagram Oseberg-D simulation.....	115
Figure A.6 Operational area for extraction steam turbine cycle at 1 [bar] T <sub>s</sub> 100 [°C] .....	116
Figure A.7 Operational area for extraction steam turbine at 2 [bar] T <sub>s</sub> 120 [°C] .....	117
Figure A.8 Operational area for extraction steam turbine at 8 [bar] .....	118
Figure A.9 Operational line for backpressure steam turbine at 1 [bar].....	120
Figure A.10 Operational line for backpressure steam turbine at 5 [bar].....	120
Figure A.11 Operational line for backpressure steam turbine at 8 [bar].....	121
Figure A.12 Backpressure steam turbine cycle - Steam turbine output vs. GT load - All backpressure levels.....	121
Figure A.13 Backpressure steam turbine cycle – Process heat vs. GT load - All backpressure levels.....	122



## List of tables

Table 2.1 Temperature of heating processes offshore.....	12
Table 2.2 Enhanced Oil Recovery [25, 27].....	17
Table 2.3 Trend for Norwegian CO <sub>2</sub> taxation for combusted natural gas in petroleum sector for years [3, 4, 37] .....	21
Table 2.4 Summarized data for the existing combined cycles.....	25
Table 5.1 Decision drivers for GT offshore and onshore [21].....	45
Table 5.2 Advantages for vertical and horizontal HRSG [50].....	50
Table 5.3 General trend for cost and efficiency for heat exchangers [50].....	51
Table 5.4 Offshore OTSG advantages and disadvantages .....	52
Table 7.1 Boundary Conditions Assumptions.....	69
Table 7.2 GE LM2500 +G4 Parameters.....	70
Table 7.3 OTSG simulation parameters.....	71
Table 7.4 Steam Turbine simulation parameters.....	72
Table 7.5 Additional machinery simulation parameters .....	73
Table 7.6 Validation results .....	74
Table 7.7 Extraction steam turbine parameters.....	76
Table 7.8 Backpressure steam turbine cycle parameters.....	78
Table 8.1 Results for extraction steam turbine cycle at design case .....	82
Table 8.2 Off-design results for extraction steam turbine 5 [bar] T <sub>s</sub> 150 [°C].....	85
Table 8.3 Selected input parameters for the sensitivity analysis of the extraction steam turbine cycle. ....	86
Table 8.4 Results for backpressure steam turbine at design point .....	93
Table 8.5 Results for backpressure steam turbine 2 [Bar] T <sub>s</sub> 120 [°C] .....	96
Table 8.6 Selected parameters for sensitivity analysis of backpressure steam turbine cycle ..	97
Table 8.7 Reference case – LM2500+G4 annual emission and taxation.....	102
Table 8.8 Summarized overview of major positives and negatives for the cycles .....	106
Table A.1 GE LM2500+G4 power output, fuel consumption and thermal efficiency at different loads.....	114
Table A.2 GE LM2500+G4 operational behavior for low ambient temperatures .....	114
Table A.3 Off-design results for extraction steam turbine 1 [bar] T <sub>s</sub> 100 [°C].....	116
Table A.4 Off-design results for extraction steam turbine 2 [bar] T <sub>s</sub> 120 [°C].....	117

Table A.5 Off-design results for extraction steam turbine 8 [bar] $T_s$ 175 [°C].....	118
Table A.6 Off-design results for backpressure steam turbine 1 [Bar] $T_s$ 100 [°C] .....	119
Table A.7 Off-design results for backpressure steam turbine 5 [Bar] $T_s$ 150 [°C] .....	119
Table A.8 Off-design results for backpressure steam turbine 8 [Bar] $T_s$ 175 [°C] .....	119

# Nomenclature

## Acronyms and Abbreviations

CC	combined cycle
CHP	combined heat and power
CDM	clean development mechanism
EOR	enhanced oil recovery
ER	emission rate
EUF	energy utilization factor
FLNG	floating liquid natural gas unit
FPSO	floating production storage and offloading unit
GE	General Electric
GOR	gas-oil-ratio
GT	gas turbine
HRSG	heat recovery steam generator
HP	high pressure
IP	intermediate pressure
JI	joint implementation
LNG	liquid natural gas
LP	low pressure
NCS	Norwegian continental shelf
NG	natural gas
NPD	Norwegian petroleum directorate
OTSG	once through steam generator
ST	steam turbine
TEG	triethylene glycol
WHRU	waste heat recovery unit
WOR	water-oil-ratio

## Latin Symbols

$A$	heat transfer area	$[\text{m}^2]$
$E$	energy	$[\text{J}]$
$e_s$	isentropic expansion correction term	$[-]$
$c$	velocity	$[\text{m}/\text{s}^2]$
$c_p$	heat capacity	$[\text{J}/\text{kgK}]$
$f_s$	polytropic expansion correction term	$[-]$
$g$	gravitational force	$[\text{kg}/\text{s}^2]$
$h$	entropy	$[\text{J}/\text{kg}]$
$H$	head	$[\text{kJ}/\text{kg}]$

$H_s$	isentropic head	[kJ/kg]
$H_p$	polytropic head	[kJ/kg]
$MW$	molar weight	[g/mol]
$\dot{m}$	mass flow	[kg/s]
$p$	pressure	[Pa; bar]
$Q$	heat duty	[J]
$R_0$	universal gas constant	[J/molK]
$s$	entropy	[J/kgK]
$T$	temperature	[k; °C]
$U$	internal energy	[J]
	overall heat transfer coefficient	[W/m <sup>2</sup> K]
$\dot{V}$	volume flow	[m <sup>3</sup> /s]
$v$	volume	[m <sup>3</sup> ]
$\dot{W}$	power	[W]
$x$	steam quality	[-]
$Z$	compressibility factor	[-]

### Greek Symbols

$\Delta T_{lm}$	log mean temperature difference	[k]
$\eta$	efficiency	[-]
$\kappa$	isentropic exponent	[-]
$\rho$	density	[kg/m <sup>3</sup> ]
$\sigma$	entropy production	[kJ/kgK]

### Subscripts

<i>amb.</i>	ambient
<i>aux</i>	auxiliary
<i>BP</i>	backpressure
<i>C</i>	cold
<i>comp.</i>	compressor
<i>cw</i>	coolingwater
<i>FW</i>	feedwater
<i>H</i>	hot
<i>gen</i>	generator
<i>GT</i>	gas turbine
<i>i</i>	inlet
<i>lm</i>	log mean temperature
<i>e</i>	exit
<i>ex</i>	exhaust
<i>mech</i>	mechanical



<i>p</i>	polytropic
<i>PP</i>	pinch point
<i>s</i>	isentropic
<i>SRC</i>	steam rankine cycle
<i>st</i>	steam turbine
<i>T</i>	temperature-pressure
<i>vap</i>	vaporization
<i>CV</i>	control volume
<i>v</i>	volume-pressure



# 1. Introduction

## 1.1. Background

As a result of the rising environmental awareness to the increasing levels of CO<sub>2</sub> in the atmosphere, the Norwegian government has taken steps to stimulate implementation of energy efficient technology on the Norwegian Continental Shelf (NCS). Petroleum activities on the NCS are responsible for 26 % of the total CO<sub>2</sub> emissions in Norway, where gas turbines (GT) accounts for 79 % [1]. Gas turbines provide mechanical drive, run generators and supply process heat on offshore facilities, and as of 2014, 167 gas turbines are installed [2]. As an incentive to implement more energy efficient technology, the Norwegian parliament in 2013 decided to significantly increase the CO<sub>2</sub> tax on combustibles from petroleum activity [3]. An increase of approximately 200 kr/ton emitted CO<sub>2</sub> was applied as a result of the recommendations in the environmental report “Klimameldingen” released by the Ministry Of Climate And Environment in 2012 [4]. Since then the tax has incrementally increased, and taxation cost for 2015 is approximately 428 kr/ton CO<sub>2</sub> emitted.

Due to increased cost of production, attention towards more sustainable power generation for offshore installations are now driven by both environmental and economic motives. Installation of onshore electric power supply has been a direct result from this, and is considered for all the new large infrastructural projects on the NCS. Applying gas turbines with a steam bottoming cycle has emerged as an attractive solution where onshore power supply is not economical feasible. Steam bottoming cycles recuperates waste heat from gas turbines to generate heat and power, thus enhancing power generation efficiency. The technology is common for onshore power plants, yet there only exist three offshore installations due to the strict sizing requirements, high cost and complex installation. Still the topic is of great interest and several papers, projects and concepts have been published over the last few years.

The EFFORT project from SINTEF and industrial partners [5] looked directly at the design and implementation of combined cycle (CC) systems for offshore installations. This work continues in the newly started COMPACTS, who is focusing on reducing weight and area requirement while improving operation reliability [6]. There have also been suggested large-scale power interconnection between platforms and/or Floating Production Storage and Offloading (FPSO) units to reduce emissions. The OPera project by DNV [7] proposed a semi descendent power hub installation with combined cycle technology to power offshore installations. Sevan Marine [8] developed a similar concept for an offshore power generation hub applied with carbon capture and storage technology. The idea is to have a main power hub of 8 gas turbines running on either field gas or supplied Liquid Natural Gas (LNG), exploit the heat from the exhaust in 4 steam bottoming cycles, and re-inject the captured CO<sub>2</sub> from the exhaust gas into a reservoir.

While many projects have studied combined cycles to enhance electricity production, little work has been focusing on options for cogenerative steam bottoming cycles. Offshore installations might experience rapid changes in both heat and power requirement, and off-design operation of gas turbines are common. Recognizing the increased need for efficient power production offshore, this thesis focuses on exploring two different cogenerative configurations of combined cycles for offshore oil and gas installations. The goal is to gain knowledge in the suitability for such systems in relation to offshore oil and gas production.

## 1.2. Objectives

The main scope of this thesis has been to design detailed process models, and simulate operation of two different offshore cogenerative power plants with a gas turbine and a steam bottoming cycle. Chosen cycles to be investigated were the extraction steam turbine and backpressure steam turbine cycle. Simulations were carried out in the process simulation software Ebsilon Professional [9]. The target was to determine offshore suitability by evaluating heat and power output, as well as operational flexibility and sensibility. Accordingly the research question for this thesis was defined as:

*“What are the positives and negatives of the backpressure- and extraction steam turbine for offshore combined cycle operation?”*

Technologies were evaluated in offshore viability with emphasis on:

- Efficiency
- Heat and power output
- Operational flexibility
- Integration with topside processing system
- CO<sub>2</sub> emission

Simulation results were to be presented in generalized heat vs. power output diagram for off-design operation. The diagrams will show the operational window for the combined cycle, process supply temperature, GT load, process heat and electric power output. Financial considerations towards taxation benefits will be evaluated with reference to Norwegian laws and policies. The author recognizes great variations in offshore operational conditions, thus consideration for other climates and areas are commented. As part of achieving the primary objective and answering the research question, the following tasks were completed:

- Literature study on Combined Heat and Power plants (CHP)
- Literature study on operational trends and contributing factors to heat and power demand during production lifetime of a field
- Design of process models in Ebsilon Professional
- Process model methodology validation
- Steady state simulation at design case and off-design

- Sensitivity analysis
- Evaluation of the results and cycle configurations
- Conclusion and suggestion for further work

### **1.3. Thesis organization**

In order to answer the research question the thesis was divided into 9 chapters. Following the introduction, a chapter on offshore cogeneration will provide the context necessary to understand the motivation, surrounding problems and operational variations during offshore power production. Chapter 3 will present the thermodynamic methodology and define parameters used in the simulations. In chapter 4 the power cycles are described and discussed based on thermodynamic principles. Chapter 5 will outline different technological options for cogeneration available including which one the author found suitable for the design and simulations. Chapter 6 discusses off-design operation theory for the technology chosen in chapter 5. Chapter 7 describes how the process simulations were carried out, design of the layout and presents the assumption on boundary conditions and machinery. Validation of the simulation methodology will also be presented in this chapter. Results are presented individually for the cycles in the first part of chapter 8, before it is followed by a joint discussion of the major findings related to the thesis objectives and theoretical framework. Conclusions and suggestions for further work are given in chapter 9, followed by bibliography and appendices.

### **1.4. Risk assessment**

No laboratory work or excursions was done during the making of this report. Therefore no risk assessment was carried out.

### **1.5. Contributions**

Main contributions from this work were:

- Design of two different process models of General Electric (GE) LM2500+G4 applied with steam bottoming cycles for offshore operation
- Calculation of design and off-design operation of process models for different process heat supply temperatures
- Heat and power output diagrams showing the operational window of the designed process models
- Sensitivity analysis of the cycles

## **1.6. Limitations**

- Dynamic operational behavior are not covered and outside the scope of this thesis
- Simplification in the design of cycles

## 2. Cogeneration on offshore oil and gas installations

Offshore oil and gas production are energy intensive processes and experiences variations in operating condition during a fields lifetime. In this chapter the context surrounding offshore heat and power production will be presented. The first section will cover the different options for offshore power and heat supply used today. The second section will attempt illustrate where the heat and power generally is required by study of the topside processing system. A short introduction to reservoir engineering is then given to provide insight in how different types of reservoirs affect the topside processing system. Potential environmental and financial benefits will be discussed in section 2.5, focusing on Norwegian taxation and emission policies. The chapter will end of with a presentation of the existing combined cycle facilities and how they are designed to meet power and heat requirements.

### 2.1. Power generation

#### 2.1.1. Gas turbines

The dominant power supply offshore is by the use of simple cycle gas turbines as seen in Figure 2.1. They provide mechanical drive for machinery and electricity generation. Process heat can also be produced when applied with a Waste Heat Recovery Unit (WHRU) on the exhaust flow. In 2008 there was 167 running gas turbines, predominantly in the range of 20-30 MW, with a combined power production capacity of approximately 3000 MW [2]. Processed gas at the installation is normally the preferred fuel. However, since this is not always available at startup, many of the turbines offshore are dual-fuel turbines. This means they can utilize heavier fuel such as diesel for startup.

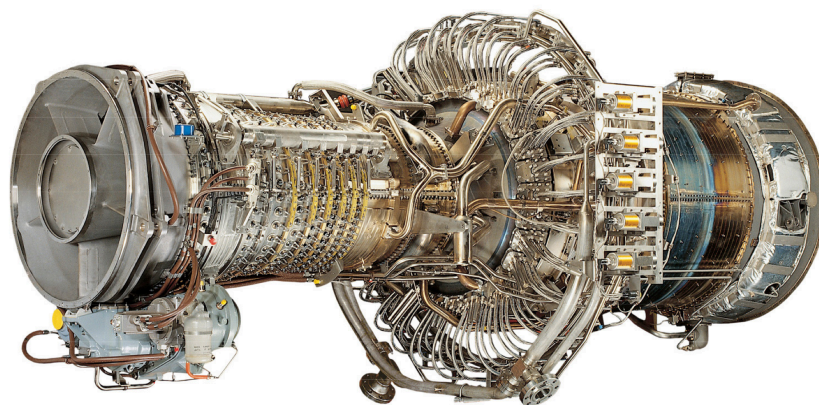


Figure 2.1 General Electric LM2500+G4 gas turbine [10]

Due to growing environmental concerns, CO<sub>2</sub> emissions from gas turbines have been at the center of public and academic attention. With increased CO<sub>2</sub> taxation many efficiency enhancing technologies and modulations have become economically feasible, one of such is

the cogenerative steam bottoming cycle. A cogenerative steam bottoming cycle would exploit unused heat in the gas turbine exhaust to produce both heat and power. Yet, there exists few steam bottoming cycles offshore and it is more common to increase the systems energy utilization by fitting a WHRU for process heat extraction. Today approximately 59 gas turbines are fitted with WHRU utilizing either hot oil or other mediums for process heat [11]. Exploiting the heat from exhaust gases are considered as one of the most environmentally friendly acts carried out towards lowering offshore CO<sub>2</sub> emissions [12]. Accordingly, combined cycles have emerged as an attractive solution to meet offshore heat and power demand while increasing the plants net thermal efficiency. However, for new installations on the NCS there exist other options as well.

### **2.1.2. Onshore power supply**

As an alternative to gas turbines, offshore installations can be powered by onshore power supply via electric cabling. Due to Norway's unique onshore electricity production dominated by hydropower, electrification by onshore power is considered by the majority to be environmental friendly. Besides the reduction in emitted CO<sub>2</sub>, the Norwegian Petroleum Directorate (NPD) [13] also emphasize on the benefits of improved safety and working environment. Gas turbines are still considered to be one of the main sources of potential ignition. Today it is required by law to consider onshore power supply during planning of new projects. Increased operational availability and reduced maintenance are other important advantages stressed by the NPD. Several offshore facilities have already been modified to onshore power supply [2]. Troll A, Ormen Lange, Gjøa and Vallhall, are all powered by this technology. Recently the Norwegian government also decided that onshore power supply should be chosen for the development of Utsirahøyden, the Johan Sverdrup field [14, 15]. At the same time it was also decided that surrounding fields (Gina Krogh, Edvard Grieg and Ivar Aasen) were to interconnect with the onshore power supply to Johan Sverdrup by 2022.

Currently onshore power supply is not technological achievable for offshore installations that are wind-turned. As a result the existing FPSOs are not under consideration for electrification [2]. The main reason is the under-development of swivel technology for long distance power supply due to transmission losses. However, concepts are being developed to assess this. One of them is to place the transformer on the ship itself, see Figure 2.2. This solves the problem regarding transmission losses but introduces possible problems related to mechanical tolerance in the swivel [2]. The oil filled transformer also introduces an extra risk of explosion. To avoid these problems another possible solution is to have the transformer placed on the sea bottom, see Figure 2.3. This solution has a high investment cost, and the major concerns are unknown reliability and complicated maintenance [2]. Another fallback for onshore power supply is the limitation in geographically operational area.



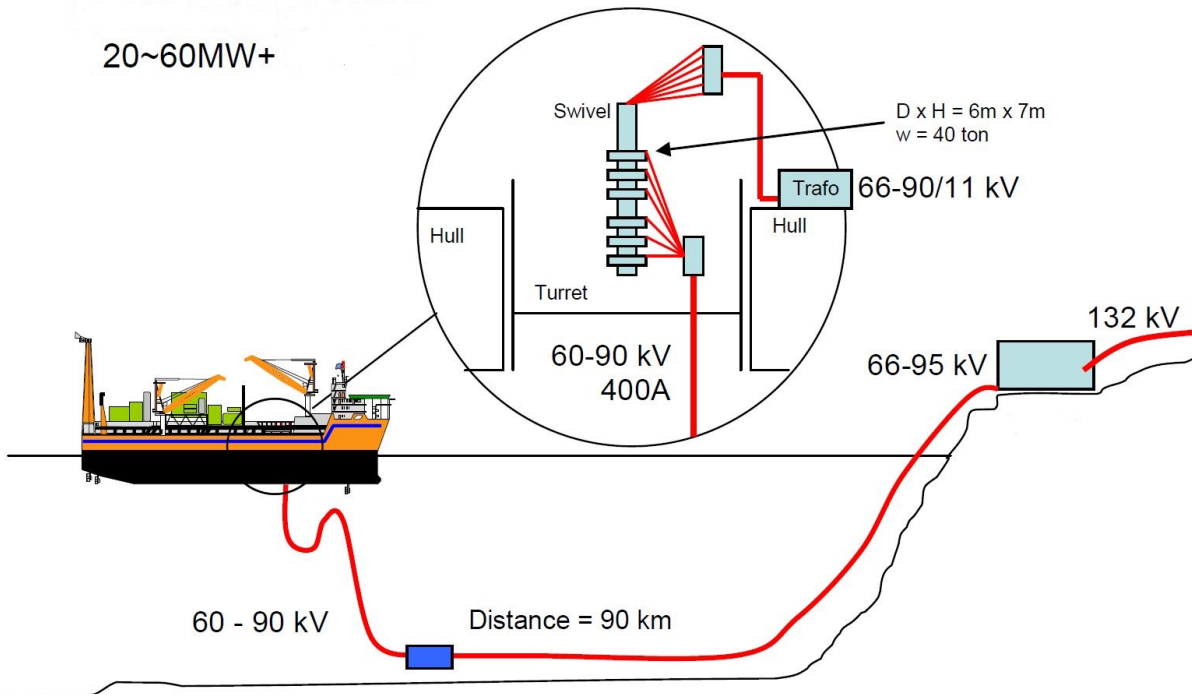


Figure 2.2 Onshore power to FPSO, transformer on ship [2]

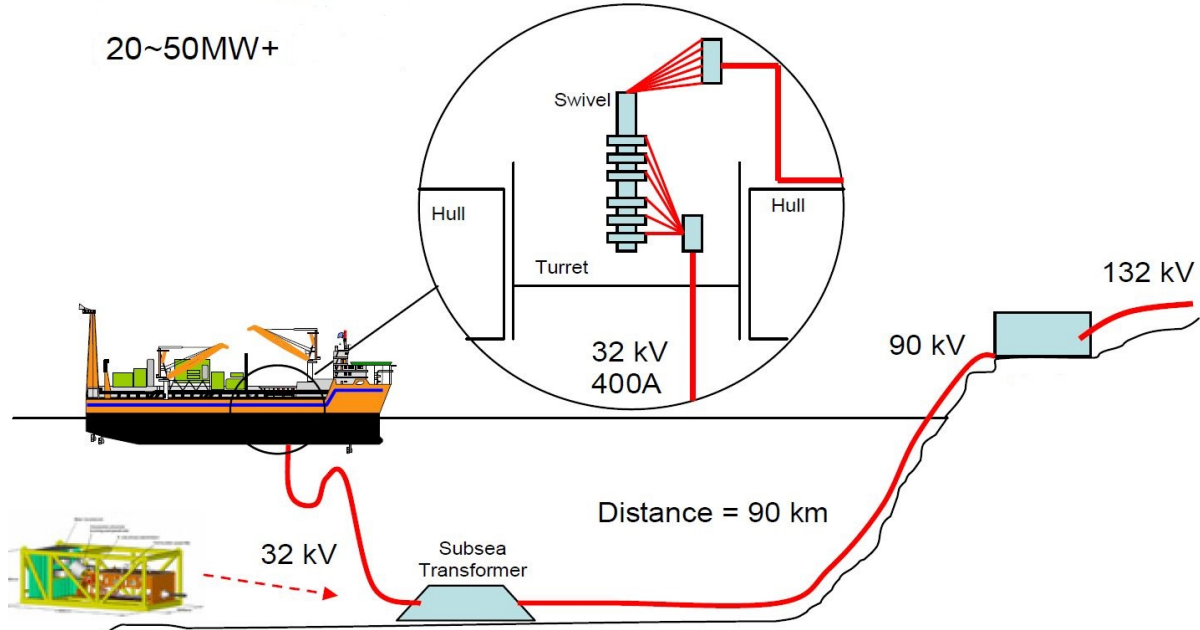


Figure 2.3 Onshore power to FPSO, subsea transformer [2]

In a report from SAFETEC [16], interviews of several operators showed a general positive attitude towards the increased implementation of onshore power supply. The report stated that few technical problems had been reported during installation and operation. However, many operators expressed themselves very skeptical to not utilizing gas turbines with some sort of heat recovery for production facilities with large process heat demand. NPD [13] recognizes the loss of heat extraction from gas turbines, resulting in natural gas fired boilers or electrical coils supplying the necessary process heat. For instance, Utsirahøyden will get its process heat from natural gas boilers, but have been requested to exploit electrical heaters as an alternative for future modifications [15]. Generally there have also been expressed a concern regarding where the delivered onshore electricity is produced. As the energy production from hydropower is to some extent season dependent, critical voices points to the absurdity by potentially supplying offshore installation with imported electricity from coal power plants abroad.

The decision of whether or not an offshore installation should be powered by gas turbines or have onshore power supply, is ultimately decided by the economical aspect. Economical benefits must surpass the traditional use of gas turbines. There have been reported difficulties and uncertainties in early planning for projects where economical benefits were not favorable but political pressure demanded onshore power supply [16]. In NPDs latest version of “Power from onshore to the Norwegian continental shelf” [2], infrastructural costs for onshore power supply are characterized as very high. Onshore power supply has the ability to supply several installations via the same cable. Uncertainties are reported to sustain well into project planning when several facilities were involved and where there had to be improvement on the onshore power distribution facilities/network [16].

The amount of parameters during planning makes it hard to predict when gas turbines are the better choice than onshore power supply. However, for deep-water developments and installations far from shore, it can be hard to justify the economical viability for onshore power supply. As stated in the introduction, some concepts centralized on having a combined cycle power hub facility offshore to enhance efficiency and reduce emissions. This shows that combined cycle technologies is of current interest for energy supply and emission reduction. In the next section a topside process facility will be examined in greater detail to pinpoint the processes heat and power requirements.

## 2.2. Offshore heat and power requirement

The required heat and power for an offshore installation is highly individual and relies on field characteristics, topside system and export requirement. The required heat and power can vary from ten up to several hundred megawatts combined [17]. In this section a generalized topside processing system will be presented and specific heat and power requirements discussed. The author emphasizes that this is a simplistic discussion only to highlight the major heat and power consumers on offshore facilities. On real facilities, special designs and configuration might show other trends than the one presented in this section. For simplistic reasons the production of LNG is not covered in this section, as the first Floating Liquid Natural Gas (FLNG) unit still is not deployed.

### 2.2.1. Topside processing system

In Figure 2.4 an overview of a topside processing system is presented to help the discussion.

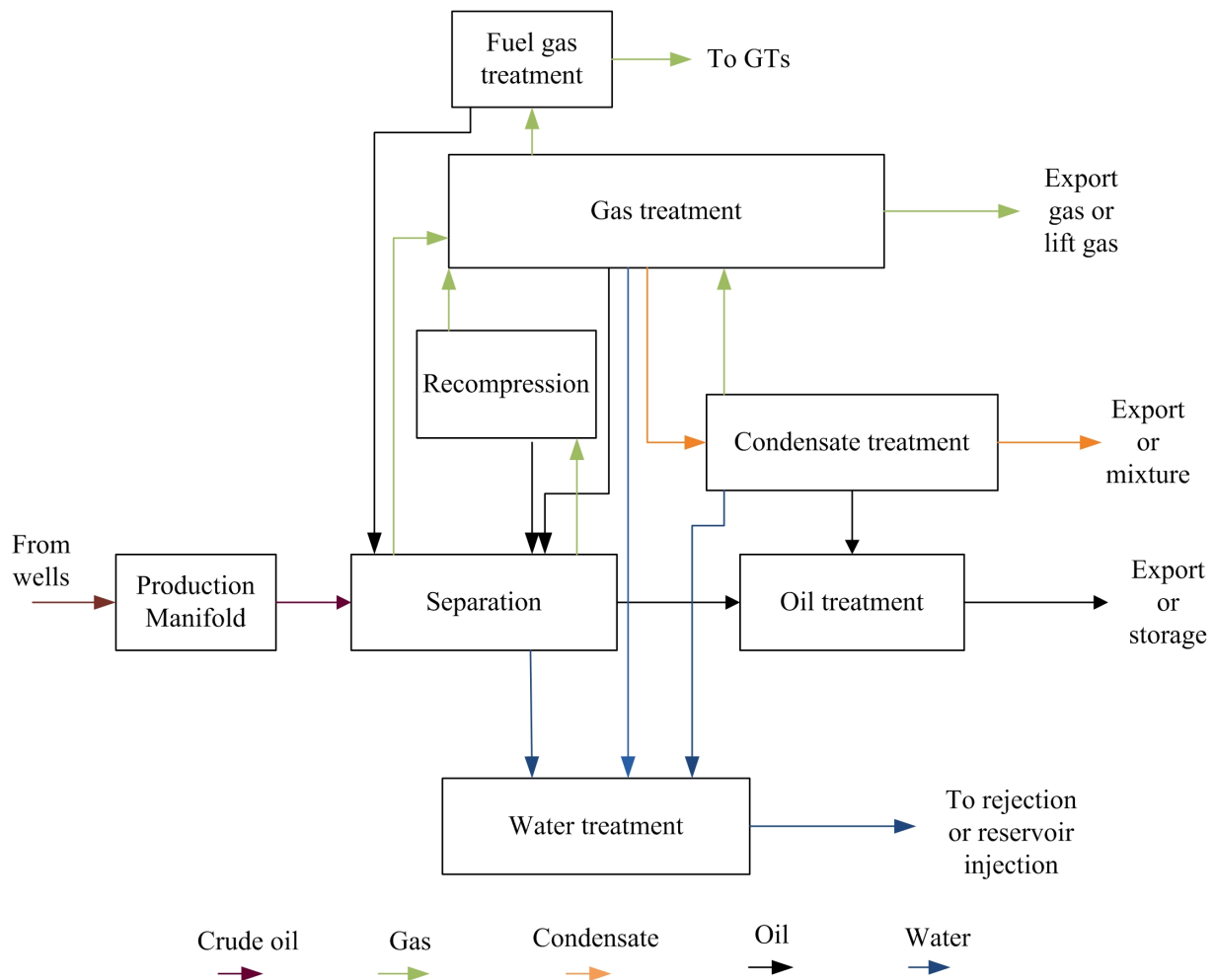


**Figure 2.4 Generalized topside processing system**

## **Production manifold**

This manifold includes necessary drilling, water injection, gas injection and gas gathering from different wells. Drilling is not a continuous operation and is one of the things that might add quite substantially to variations in power demand. The same goes for water and gas injection into the reservoir for enhanced oil recovery (further discussed in next section). It is common for the installation to have a separate production manifold to each separation train to allow better pressure handling and maximize production [18].

## **Separation**

From the production manifold crude oil enters the separation train to separate gas, oil and water. The number of separation train usually ranges between 1 or 2 on the NCS [18]. To ease the separation process, crude oil is either heated before or inside the separator to lower the viscosity. Depending on the type of reservoir the required process heat varies as the well flow inlet temperature is determined by ambient conditions and reservoir characteristic [17]. The composition itself also plays a major impact, as oil with higher viscosity requires more process heat. Temperatures can reach approximately 90-100 °C through the separation process, and this is considered to be the main process heat consumers for an offshore installation [17, 19]. Numbers of stages required for the separation process is typically 2-3 on the NCS, and are normally 3-phase with 3-5 minutes of liquid residence time [18]. As a comparison the number of separation stages on the Gulf of Mexico is usually 5, where only the last few stages are 3-phase [18]. The reason for higher number of stages is the stricter export specification of the oil from producing facilities in this region. Segregated gas and water is separately sent to the gas and water treatment facilities.

## **Oil Treatment**

After the separation train, oil is mixed with the recovered oil (and potentially condensate) from other treatment facilities. Compared to other regions, the temperature of the oil on the NCS can be quite high after separation. Oil is therefore cooled down to 25-30 °C before it is pumped to storage or exported to onshore refineries [19]. This is done to limit stresses in the export pumps [18].

## **Gas treatment**

From the separation stages hot gas is cooled and enters the gas treatment facility where accompanying oil and water is separated from the gas in a scrubber. As seen in Figure 2.4, oil is reinserted into the separation train and water is sent to treatment. The gas treatment facilities offshore varies a lot in complexity as the product might be sent onshore for further processing or inserted directly into an export pipeline. Depending on the export specification of the gas processing might include CO<sub>2</sub> removal, dehydration, sulfur removal and nitrogen removal. The reader may consult Campbell [20] for more exhaustive explanation of the different processes. Usually, gas treatment facilities only include dehydration, and only a few

facilities on the NCS treat gas to sales specifications [18]. Gas treatment primarily requires a lot of cooling and recompression work. The only specific process heat requirement is the regeneration of the Triethylene glycol (TEG) used for dehydration. Regeneration temperature differs upon choosing of the TEG, but can be expected to approximately 205 °C [19]. Compression lift for export is the final step for the system. Treated gas is boosted to required export pressure level and transported via pipelines running directly to the market or an onshore process facility. Required power for compression varies between 3-30 MW [21] and is one of the main power consumers on offshore facilities. If gas turbines provide power for the installation and/or has fired boilers, fuel gas is taken from the gas treatment facility as seen in Figure 2.4. Flue gas might undergo further scrubbing, heating up to about 60 °C and pressurization before entering the combustion chambers or boilers [19].

### **Condensate treatment**

It is not common for installations to have a separate condensate treatment facility. However, it has proven to be economically sustainable for some facilities where condensate was mixed with processed gas to meet sales gas specifications. Proximity to a gas pipeline was essential to surpass the economical penalty of additional advanced processing equipment [18]. For the few topside processing systems with a condensate treatment, additional process heat is required. The stabilization process separating lightweight hydrocarbons from condensate requires reboiling of the condensate. Temperature of the reboiling is in the range 180-200 °C and takes place in a stripping column. Facilities without a condensate treatment facility, mixes the separated condensate from other facilities with the oil and transports it to onshore processing facilities.

### **Recompression**

The recompression facility recompresses segregated gas from the later stages in the separation train before the gas is sent to the gas treatment facility. In the recompression unit scrubbers might be in place to extract accompanied oil and water from the gas. No specific heat consumers are found in this part of the process.

### **Water Treatment**

Water is collected from the different processes around the offshore facility and treated with hydrocyclones with a subsequent degassing vessel [18]. Treated water is then rejected into the sea or pressurized for reservoir injection. Water injection pumps are one of the main power consumers for offshore oil and gas facilities.

In Table 2.1 the required temperatures for process heat are listed. These numbers are based on case studies on offshore facilities.

<b>Process</b>	<b>Temperature range</b>	<b>References</b>
Fuel gas heating	40 → 60 [°C]	[19]
Crude oil heating 1 <sup>st</sup> separation stage	45 → 55 [°C]	[19]
Crude oil heating 2 <sup>nd</sup> separation stage	80 → 90 [°C]	[19]
Condensate stabilization column, reboiler	180 → 200 [°C]	[19]
Gas dehydration, TEG reboiler	205 [°C]	[18, 19]
CO <sub>2</sub> removal, amine regeneration	110 – 140 [°C]	[22]

**Table 2.1 Temperature of heating processes offshore**

By looking at the treatment facilities and reports on offshore processing systems, one can pinpoint the major heat and power requirements. As stated, not all of the treatment facilities previously discussed are common for an offshore installation on the NCS. Bothamley [18] states in his comparison that a normal oil producing offshore facility on the NCS contains an oil treatment facility and only dehydration process for the gas.

The primary heat requirement was found to be the crude oil heating for separation, reboiler for condensate stabilization and some for regeneration of TEG. Exergetic case studies on offshore facilities supports these findings, with heating required in separation trains being much higher than regeneration of TEG [23]. Nguyen et.al [24] pointed out the 3 dominating power consumers on offshore facilities to be in following order: the compression train, seawater injection pumps, and gas recompression or oil pumping for export.

## 2.3. Reservoir engineering

In the previous section a topside processing plant were presented and its heat and power requirements discussed. Heat and power required for processing are directly related to the Gas Oil Ratio (GOR) and Water Oil Ratio (WOR) in the well flow. During production these ratios will change depending on type of reservoir and recovery technique utilized at the site. Other boundary conditions such as reservoir temperature, pressure and fluid composition will also influence the topside production system. In this section, a short outline of reservoir characteristics will be presented and discussed. The aim is to pinpoint how recovery mechanisms and type of reservoir influence heat and power requirements. The term “recovery mechanisms” is associated to the operation recovery process utilized in production. Val Pinczewski [25] classifies the mechanisms into three groups:

- **Primary recovery** – water drive, gas cap expansion, solution gas drive and pressure depletion
- **Secondary recovery** - water and/or gas injection to maintain reservoir pressure
- **Tertiary recovery** – Enhanced Oil Recovery processes (EOR)

### 2.3.1. Primary Recovery

Hydrocarbon reservoirs are generally categorized into three different types based on fluid properties [25]:

- Oil reservoir
- Retrograde condensate gas reservoir
- Gas reservoir

The categorization is based upon reservoir temperature and pressure state, as well as the phase envelope given by the fluid composition. During production the surfacing well flow will experience a drop in pressure. If the well flow expands inside the phase envelope to the left of the critical point, the reservoir is categorized as an oil reservoir. If well flow expands to the right of the critical point, but still within the phase envelope, the reservoir is categorized as a retrograde condensate gas reservoir. A gas reservoir will not enter the phase envelope of the well fluid at all, expanding above and to the right of the envelope. As well fluid (or gas) is extracted from the reservoir the volume inside the reservoir must be replaced by something else. In Figure 2.5 it is illustrated how primary recovery mechanisms replaces the volume of oil in the oil reservoir. Note that size and segregation of components are purely illustrative.

## MATERIAL BALANCE ON ORIGINAL OIL VOLUME

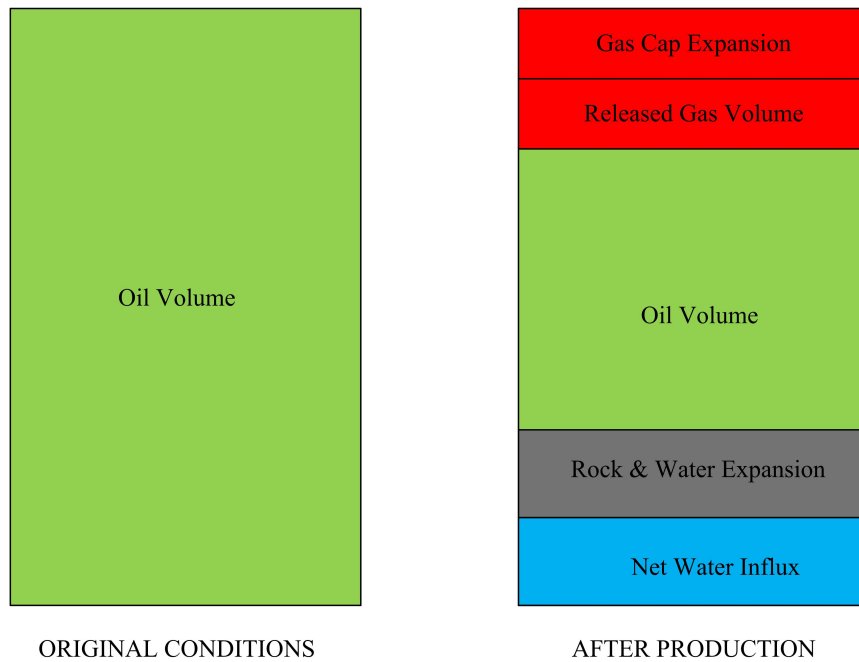


**Figure 2.5 Effect of primary recovery mechanism on an oil reservoir volume before and after production [25]**

Primary recovery mechanism is a term for the four driving factors that replaces the volume of extracted oil and gas. It is common to classify a reservoir not only by product, but also by which primary driving forces that are present within the reservoir.

- **Pressure depletion drive** – primarily fluid and rock expansion due to relieved pressure
- **Solution gas drive** – as pressure drops below bubblepoint, gas is released from the oil inside the reservoir and forms a gas cap above the oil
- **Gas cap drive** – reservoir with a gas cap initially above the oil zone
- **Water drive** – the oil or gas is in contact with an aquifer and during pressure depletion water replaces the oil and gas

Figure 2.6 illustrates how the different driving forces affects reservoir pressure against the cumulative produced oil. The figure shows that reservoirs containing a gas cap, or where a gas cap is formed during production, preserve a higher pressure level during production over a longer period of time. However, it does say anything regarding the GOR in the well flow. Figure 2.7 illustrates how the different driving forces are related to GOR during production. It shows that reservoirs driven by solution gas or gas cap drive, also experience the greatest change in GOR as well as maintaining a higher pressure level. This effect has to be taken into consideration in the design of the processing system. As the gas treatment facility uses a lot of power for compression work, varying GOR might suggest that compressors are running on sub-optimal operative conditions for substantial period of the production lifetime. Finding the



best point of design for the fields lifetime, or defined period, could increase the efficiency of the topside processing facility.

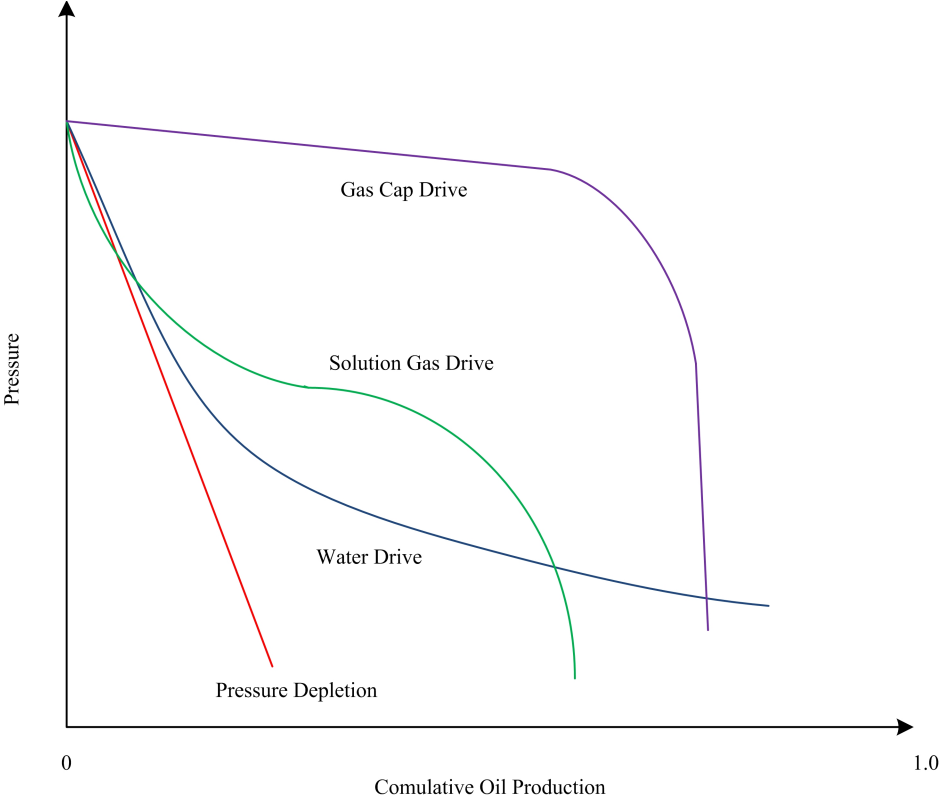


**Figure 2.6 Primary drivers: Pressure vs. Cumulative oil production**

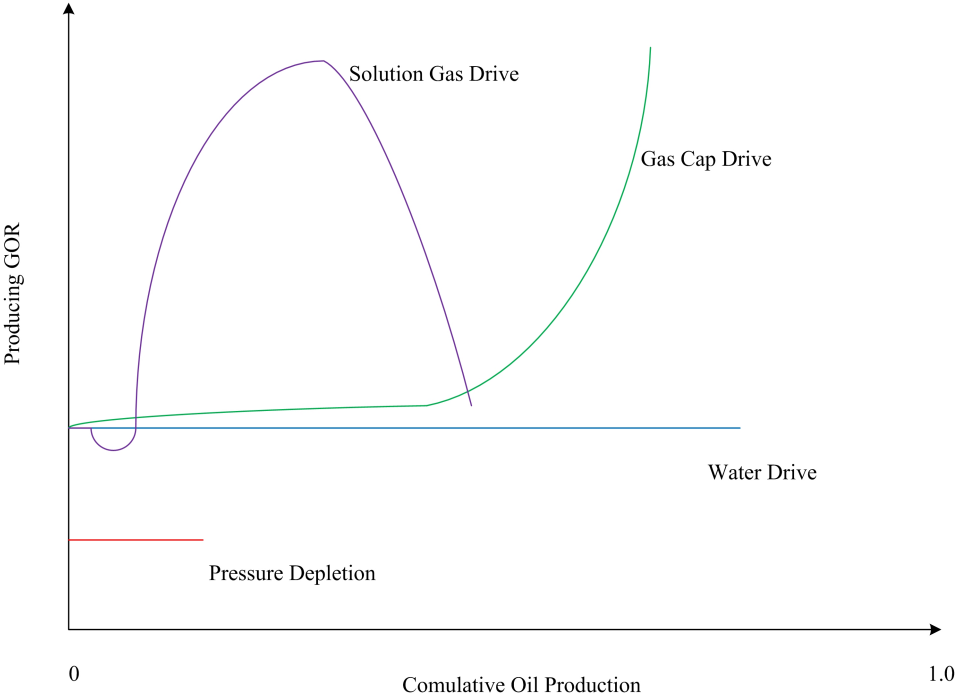


**Figure 2.7 Primary recovery: GOR vs. Cumulative oil production**

In the early petroleum days, oil and gas production were limited to only exploit the primary recovery drives. Today it is very common to actively increase a fields production output and lifetime by using secondary recovery techniques.

### **2.3.2. Secondary recovery**

The idea behind secondary recovery techniques is to maximize production throughput and are usually quite energy-intensive processes [19]. The most used method on the NCS is water flooding to maintain a high reservoir pressure and to drive oil towards the wellheads. Water injection will prolong the production lifetime of the field, but it will also gradually increase the WOR in the incoming well flow. Towards the end of production as much as 90 % of the surfacing well flow may consist of water [26]. Injected water must be pumped to a pressure level differentially higher than the hydrostatic reservoir pressure before injection. Seawater is normally used. Reuse of the cooling water from the topside processing facility will lower the power requirement for water lifting. This solution can be found be on the Eldfisk water injection platform, where the cooling water from the condenser is injected into the reservoirs [12]. Production water from the wells is usually not recommended due to the risk of deterioration in the reservoir. However, fresh seawater can be added to minimize the problem. Another secondary recovery technique is gas injection where natural gas (NG) is reinserted into the reservoir to maintain pressure level. The procedure requires extra compression work and additional cooling. It is also worth to mention gas lifting. The concept of gas lifting does not take place down in the reservoir, but the idea is to insert natural gas into the base of the production string or tubing [27]. Natural gas mixes with the “heavier” hydrocarbons from in the well stream and reduces viscosity for the incoming flow. This eases transportation to the topside facility.

### **2.3.3. Enhanced oil recovery processes**

The third and final method to increase production is referred to as tertiary recovery or Enhanced Oil Recovery (EOR). The primary and secondary recovery techniques are usually referred to as the conventional techniques, and EOR is any process apart from these [25]. EOR processes are carried out when the conventional recovery methods stops working and for immobilized oil in the reservoir. The EOR can be classified into three groups as shown in Table 2.2. Conduction of EOR measures might require additional and more complex process equipment topside, increasing the overall energy demand. CO<sub>2</sub> injection has been proposed as an EOR incentive for the future as it has shown promising potential in operator studies [28]. However the lack of access to sufficient volumes of CO<sub>2</sub> on several platforms has stopped further evaluation. Yet there has been reinserted CO<sub>2</sub> (for storage) into a reservoir from the Sleipner installation since 1996. NPD [28] states that reservoirs in the Norwegian Sea has sufficient capacity to store CO<sub>2</sub> from both onshore Norwegian sources as well as from northern Europe in the future. Hence, future trends might show an increase in the power requirement for gas reinsertion.

**Table 2.2 Enhanced Oil Recovery [25, 27]**

<b>Classification</b>	<b>Measure</b>	<b>Result</b>
Thermal	Steam injection	Reduced viscosity of the crude oil by heat easing the flow through reservoir.
	In-situ combustion	
Chemical Injection	Micellar polymer	Improved oil mobility by lower tension between water and oil
	Polymer	
	Caustic or Alkine	
Miscible Injection	Enriched hydrocarbons	Reduced viscosity of the crude oil and eased flow through the reservoir
	CO <sub>2</sub>	
	Nitrogen and Fluegas	

## 2.4. The energy trend

This section will attempt to bring all the information together to create an overview over what to expect in the energy trend for offshore facilities. From section 2.3 one can recognize how different types of reservoirs and driving forces could influence both the energy demand and the required topside processing system. Figure 2.6 illustrated that reservoirs with an initial gas cap or a forming gas cap will experience lower pressure depletion during production. However, these fields will have a much greater variation on the GOR that will influence the performance of the processing facility.

With secondary recovery techniques such as water flooding, production lifetime will be increased but at the cost of higher energy requirement for pumping work and gradually increasing WOR. A study by Vanner [29] concluded that a general increase in energy intensity for all types of field were to be expected on the NCS. The specification on export products will influence the heat and power demand for the installations. On the NCS most facilities exports unstabilized crude oil to onshore processing facilities. Other places such as the Gulf of Mexico exports stabilized crude oil and therefore have a higher requirement for processing heat [18, 30].

At oil reservoir producing facilities, maximum production rate is generally reached early in the production lifetime before gradually declining. The use of water injection is common on the NCS to maintain pressure in reservoir. Volume of injected water and corresponding power requirement can be assumed to be relatively stable over the production period [26]. The largest power consumers on an oil platform were found to be water injection pumps, gas compression, gas injection, export pumps, drilling and supportive systems. The largest heat consumer is the heat required for the separators. The long-term power demand can be relatively constant for an oil platform, but the decreasing production rate will increase the energy intensity for the installation [26, 31].

At gas reservoir producing facilities, power demand differs compared to oilfields during production lifetime. Gas is normally extracted from reservoirs by primary recovery drivers, thus a gradually decrease in pressure will occur [26]. It can prove necessary to lower the operation pressure in the processing facility to maximize the production output from the reservoir. This will lead to sub-optimal operation of equipment as well as increased compression work for export. By this one can say that the energy requirement will gradually increase during the production lifetime [26]. Figure 2.8 illustrates how the energy intensity changes for known events that might occur during production lifetime. It should be noted that the trend line is purely illustrative and that the impact of these events will vary depending on facility and reservoir type.

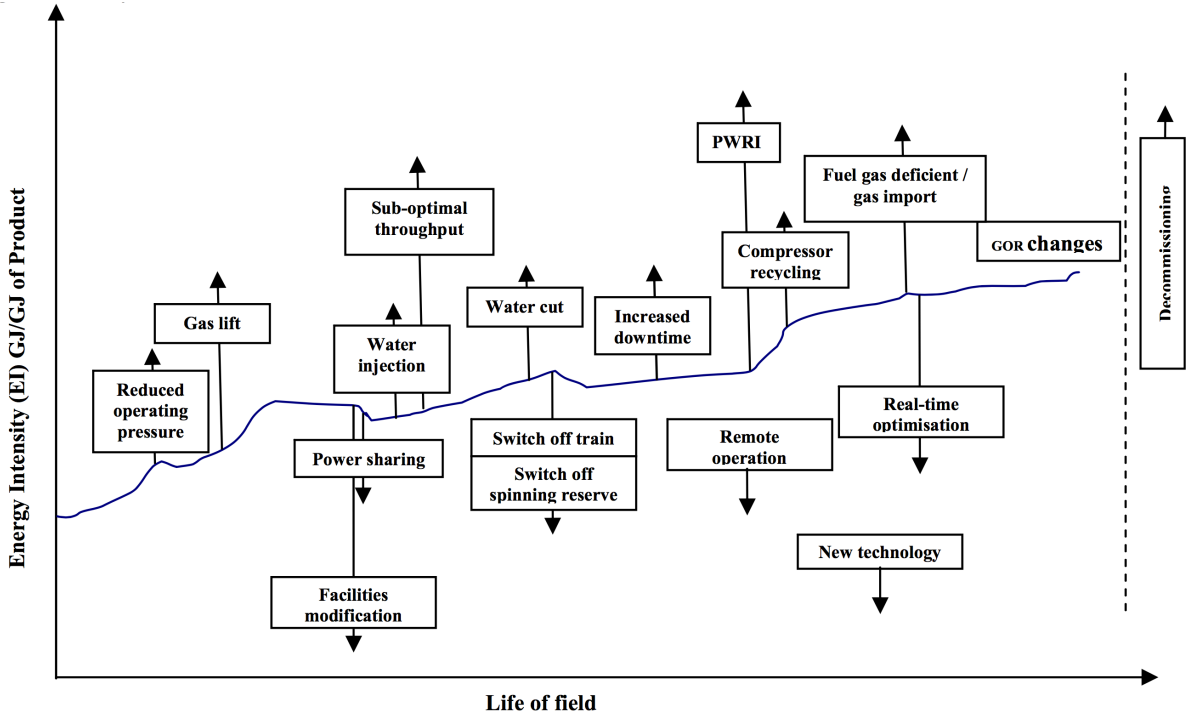
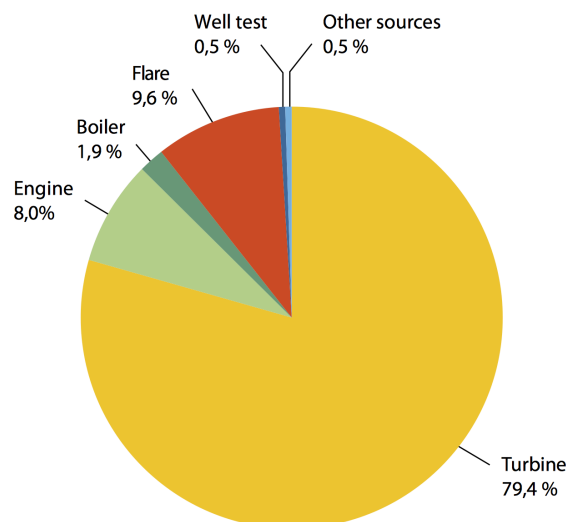


Figure 2.8 Illustrative curve for impacts of known events on energy intensity [29]

The implementation of a cogenerative combined cycle could increase the power and heat output while lowering fuel consumption per unit of produced power. The generated electricity could be used to meet variation in power demand, allowing gas turbines to operate at higher efficiency. A combined cycle could also meet the discussed increasing power demand occurring over the lifetime of a field. Process heat from the combined cycle could also benefit the systems efficiency by replacing fuel consumption if boilers are present. In the next section emission trend and policies on the NCS will be presented to show the how taxation cost and future emission targets affects operation.

## 2.5. Emission trend and taxation

Throughout the entire oil and gas production process, emissions of chemicals and gases are being released. In 2013, the Norwegian petroleum industry was responsible for 26 % of the total greenhouse gas emissions in Norway [32]. This makes the petroleum industry the largest source of greenhouse gas emissions, equivalent to approximately 14 million tons of CO<sub>2</sub> equivalents [32]. Further analysis carried out by the NPD revealed that 79 % of the emissions came from power generation with gas turbines [1], illustrated in Figure 2.9. These numbers show that there is great potential in improving energy efficiency for offshore power generation. Flaring is another excessive source of CO<sub>2</sub> emissions. Still, flaring is allowed due to necessary safety regulations. In order to minimize flaring, the government must approve the quantity of gas flared. The scientific reason for flaring and not simply venting the gas to the atmosphere is the greenhouse gas effect from different gases. Methane have, averaged over a 100-year period, 21 times higher global warming potential than CO<sub>2</sub> [33]. Interestingly though, in the early periods of petroleum production extensive flaring of gas was common as it was considered to be a non-valuable byproduct.



**Figure 2.9 Source of emissions for offshore oil and gas production in Norway [1]**

Since the early 90s Norway has had an excessive focus on emission control in the offshore section. Emissions are controlled by several national acts such as the Petroleum Act, the Sales Tax Act, the Greenhouse Gas Emission Trading Act, the Pollution Control Act, and since 1991 had the CO<sub>2</sub> taxation system to help boost the implementation of energy efficient equipment [1]. Norway was also part of the first Kyoto agreement in 2008, agreeing to reduce emission to 1 % above 1990-levels by 2012 [34]. At the end of the period the target was not met and emission licenses had to be bought to cover the difference [35]. Besides reducing its own emissions, Norway and other countries can reach their emission targets by emission licenses trading, Joint Implementation (JI) or the Clean Development Mechanism (CDM). In practice, this means that Norway has to buy emission licenses if they release more than promised. The Joint Implementation means that a country is also able meet their targets by

participating in projects abroad instead of domestic. CDM is the last way to reduce emissions by supporting and cooperating in sustainable project in developing countries. The first target of the Kyoto agreement was to reverse emission levels to the levels in 1990, corresponding to a total emission reduction of 5% of the emission levels in 2013 [32]. Since then, Norway has agreed to the second commitment of the Kyoto protocol (2013 - 2020), the Doha Amendment. The target is to reduce the annual emission levels to 84 % of the reference year 1990 until 2020 [36]. In March 2015 the government agreed to increase their targets further, by stating that they would reduce emission levels by 40 % of the reference year 1990 by 2020 [32]. In Figure 2.10 the emissions history and forecast from the petroleum sector can be seen. The figure shows that there is great potential for implementation of efficiency enhancing technology for power production.

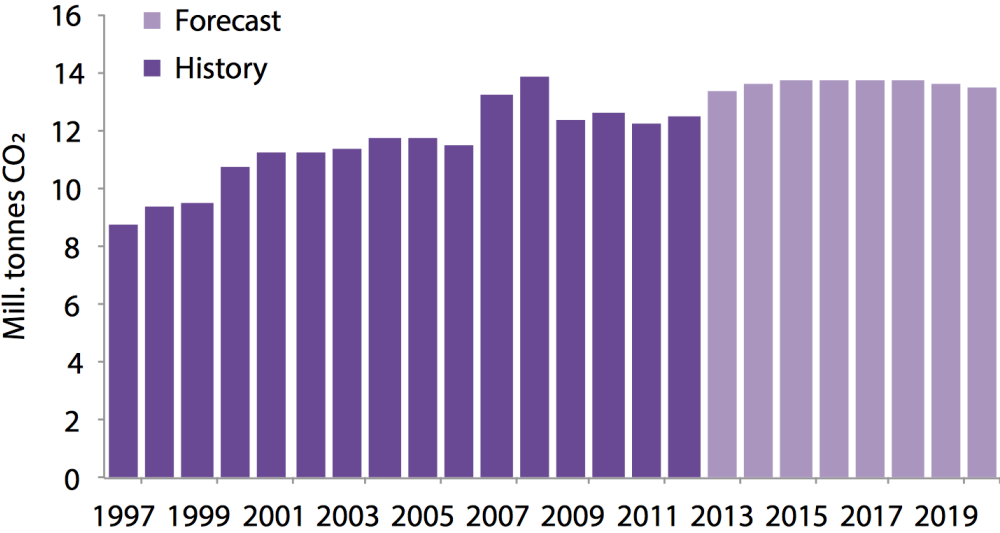


Figure 2.10 Emission history and forecast for petroleum industry in Norway [1]

One of the major driving forces for implementation of efficiency enhancing equipment on the NCS is the potential economical benefit towards the CO<sub>2</sub> taxation. Be aware that the CO<sub>2</sub> tax, for simplistic reasons, is calculated on how much natural gas or fuel that has been burnt and not on how much CO<sub>2</sub> emitted. The Norwegian Parliament decided in 2012 to drastically raise the CO<sub>2</sub> tax for petroleum activity from 0.49 to 0.96 kr/sm<sup>3</sup> burnt natural gas in the 2013 budget [3]. This was an increase of approximately 200 kr/ton CO<sub>2</sub> and was implemented as a result of the recommendations in the environmental report “Klimameldingen” from the Ministry Of Climate And Environment [4]. Since then, the CO<sub>2</sub> tax for natural gas has been growing steadily the last couple of years, and was raised to 1.00 kr/sm<sup>3</sup> burnt NG in the 2015 budget [37]. In Table 2.3 the taxation rates for the last 4 years are summarized. Note that there are specific tax costs for burning liquids on the NCS, but these values are not included in the table. Traditionally the cost per liter kr/L has matched the cost per standard cubic meter

kr/sm<sup>3</sup>. The last column includes the corresponding approximate cost per ton CO<sub>2</sub> emitted. Be aware that this value might change dependent on the composition of the combusted NG.

**Table 2.3 Trend for Norwegian CO<sub>2</sub> taxation for combusted natural gas in petroleum sector for years [3, 4, 37]**

<b>Year</b>	<b>Burned NG [kr/sm<sup>3</sup>]</b>	<b>Approximate cost for CO<sub>2</sub> [kr/ton]</b>
2012	0.49	210
2013	0.96	410
2014	0.98	419
2015	1	428

So far this chapter has described the different power solutions for power supply, where the heat and power demand is located on an offshore facility, how reservoir types influence the energy requirement over time, and presented the emission targets and taxation costs in Norway. By illustrating the variety of parameters for offshore power generation, the aim has been to provide an overview of where the potential benefits from applying combined cycle technology is. A cogenerative combined cycle could potentially lower the amount of NG combusted for heat and power production. Reduction in taxation and fuel cost being the economical driving forces. In the next section the current installed offshore combined cycle plants will be presented.

## 2.6. Existing facilities

As of today only three offshore combined cycle power plants are installed in Norway and are currently the only ones in the world. The cycles were put into operation between the end of 1999 and the middle of 2000 [12] The main distinction between the different installations is how each of them is designed to meet the platforms specific requirements and limitations.

### 2.6.1. Oseberg D

The first combined cycle is located at the Oseberg-D platform and uses two GE LM2500+ turbines as topping cycles. The original layout can be seen in Figure 2.11. The gas turbines delivers mechanical work to run two export compressors. In the figure, exhaust gas at 481 °C enters the double-intake single pressure drum based Heat Recovery Steam Generator (HRSG). In the summer of 2010 Aibel [38] replaced the drum type HRSG with a Once Through Steam Generator (OTSG). Interestingly, the steam turbine (ST) is not located at the same platform as the HRSG. Power from the steam turbine reduces the required power output from three Coberra 6000 turbines located at the utility area at the interconnected Oseberg Field Centre. Steam from the HRSG travels through a 400 meter long pipe before it enters the steam turbine. Due to the variations in operation loads on the GE LM2500+, electricity produced by the steam turbine varies. This variation is met by controlling the load on the Coberra 6000 generator sets at the Oseberg Field Centre. Included in the design is the possibility to extract process heat from the steam turbine at a value of 12 [MW].

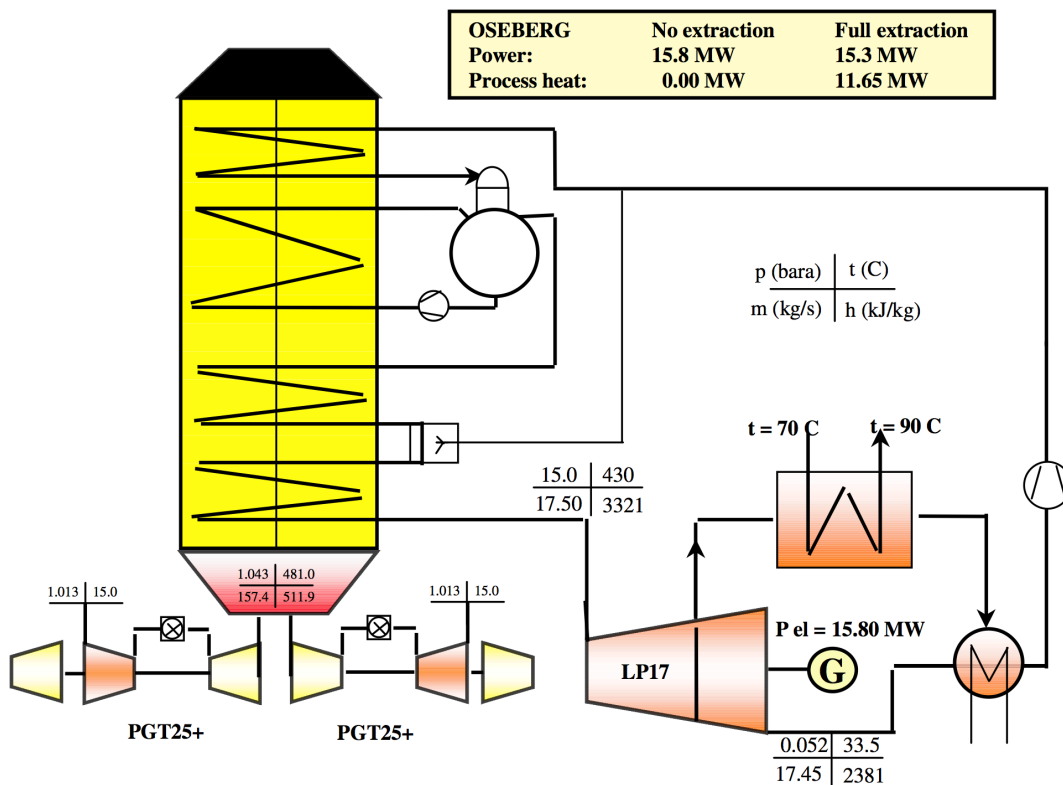


Figure 2.11 Oseberg-D combined cycle process layout [12]



## 2.6.2. Eldfisk 2/7-E

The second combined cycle is located at the Eldfisk Water Injection Platform and is the single producer of required electricity at the platform. The bottoming cycle is designed to deliver 10 [MW] of electricity. Original layout can be seen in Figure 2.12. In that design a triple inlet drum type HRSG was connected to two GE LM1600 gas turbines delivering mechanical work to the water injection pumps, and one GE LM2500 running a gas compressor. Besides producing steam for the bottoming cycle, steam was also provided to water treatment and processes on the platform. Since the original system was put into operation in 2000 the HRSG has been replaced with two cylindrical OTSGs delivered by HRS [39]. The new OTSGs have helically tubing along the walls and a bypass channel in the center. The LM2500 is connected to one of the OTSG and the two LM1600 to the other. As electricity demand and steam generation may vary from each other, 10 % excess steam is continuously produced to ensure sufficient controlling possibilities. This extra steam is guided through a bypass valve that has been fitted to lead some of the steam directly to the condenser. Worth mentioning is that the seawater used in the condenser, is the same water used for water injection to the reservoir. This clever design reduced the total amount work needed for the lifting of seawater.

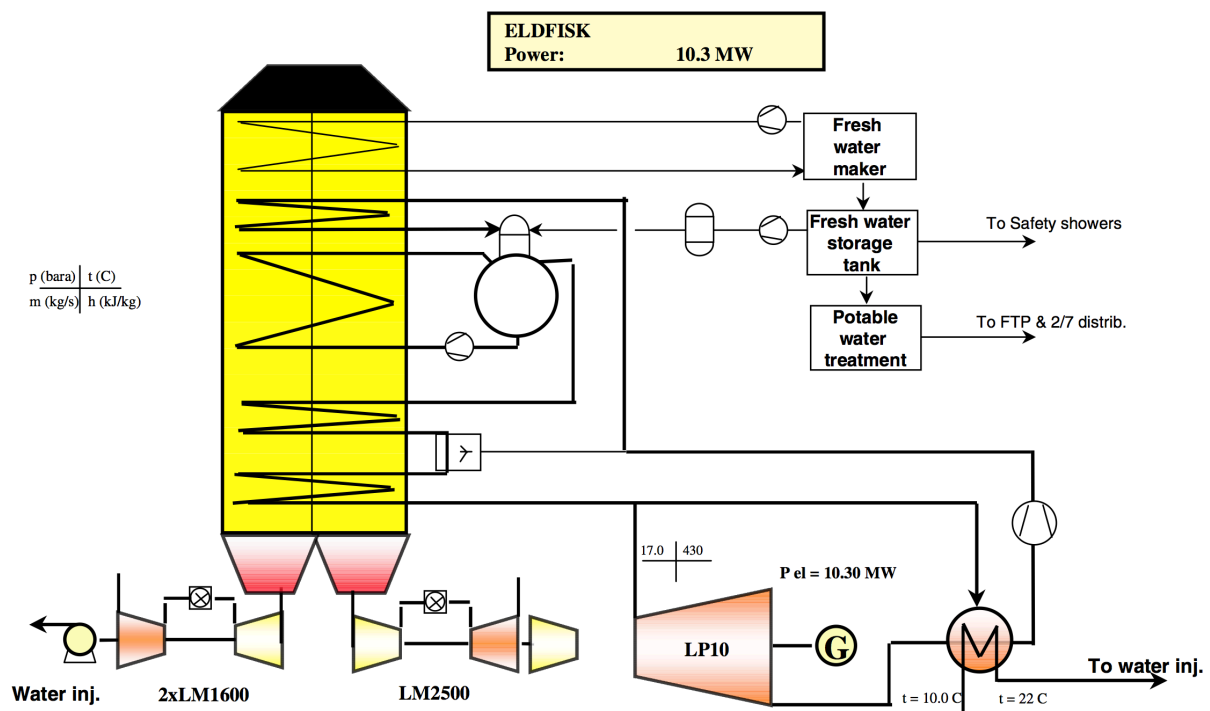


Figure 2.12 Eldfisk 2/7-E combined cycle process layout [12]

### 2.6.3. Snorre B

The final combined cycle installed offshore is located on Snorre B platform. In some ways the design looks familiar to the original Oseberg D design. The HRSG has a double intake and is placed on top of two GE LM2500+ gas turbines. The possibility to extract steam for heating purposes is also present. However at Snorre the steam is extracted at 6 bar and not 1 bar as on Oseberg D. At full extraction this stream of steam provides 8 MW of process heat, but the extraction reduces the electricity power generated from 17 to 15 MW at full load. The main operational strategy is to run the combined cycle continuously at full load to reduce costs. There is a 10.5 km electrical connection between the Snorre B platform and the Snorre TLP platform, where surplus electricity from the steam turbine is transferred. A layout of the interconnection, between gas turbines and electric motors on the platform, can be seen in Figure 2.13. On the Snorre TLP platform there are three simple cycle gas turbines that will be used to meet the remaining power demand. This electrical interconnection between the platforms is a way to ensure stable operation conditions for the combined cycle and maximizes the savings.

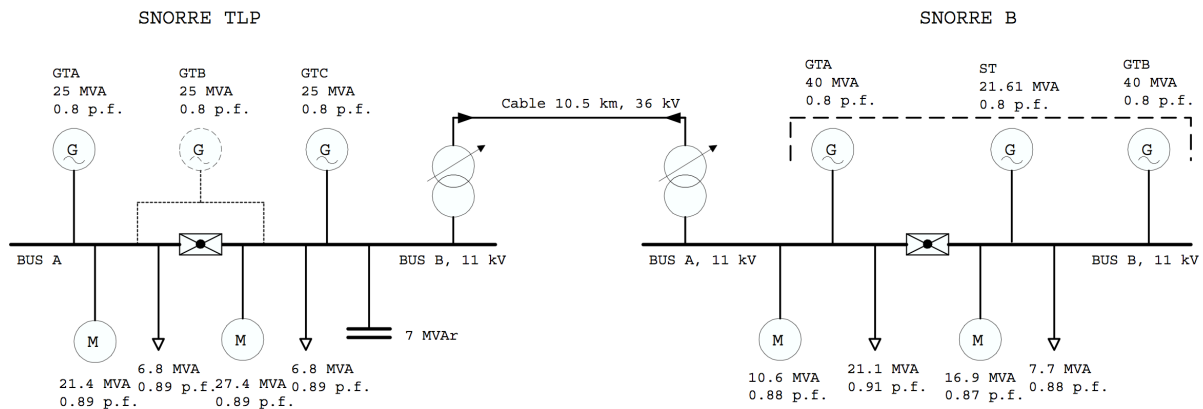


Figure 2.13 Snorre B electrical connection scheme [40]

At present, the technical challenges when implementing steam bottoming cycles are still currently one of the reasons why only three such cycles have been installed. Strict regulations regarding weight and spacing in retrofit planning are probably the biggest issues, and might not exceed the economical and environmental benefits. In Table 2.4 the data from the three existing CC are summarized.

**Table 2.4 Summarized data for the existing combined cycles**

<b>Data</b>	<b>Oseberg D</b>	<b>Eldfisk 2/7-E</b>	<b>Snorre B</b>
Gas Turbines	2x LM2500+	LM2500 2x LM1600	2x LM2500+
Steam Turbines Power [MW] (design point)	15.8 (88% GT load, no extraction) 14.3 (88% GT load, full process heat extraction)	10.3	17.3 (100% GT load, no extraction) 15.2 (100% GT, full process heat extraction)
Process Heat [MW]	11.7	-	8.0
Fuel Savings [MSm <sup>3</sup> /year] relative to GT	36	23	39
CO <sub>2</sub> Reduction [tons/year] relative to GT	80 000	50 000	92 000
HRSG	Original: Vertical flow, single pressure, double intake, bypass stack, four levels, forced circulation,  Updated: OTSG	Original: Vertical flow, single pressure, triple intake, bypass stack, five levels, forced circulation, dedicated level for fresh water maker,  Updated: Dual cylindrical OTSG, helically tubing, centered bypass	Vertical flow, single pressure, double intake, bypass stack, forced circulation, designed for floating production facility,



### 3. Thermodynamic methodology

Some of the most used thermodynamic concepts are worth repeated before going into the details of the cycles evaluated. The following chapter will briefly touch upon used methods and define parameters used in the report and simulations. Suggested reading for more detailed and elaborated explanation towards the thermodynamic concepts is “Fundamentals of Engineering Thermodynamic” by Moran and Shapiro [41].

#### 3.1. The 1<sup>st</sup> law of thermodynamic

One of the fundamental rules is the 1<sup>st</sup> Law of thermodynamic, conservation of energy in a closed system. This law states that for a closed system, the only way energy can change is by transfer of energy by work or by heat [41]. This relation can be expressed as:

$$\Delta E_{kinetic} + \Delta E_{potential} + \Delta U = Q - W \quad (3.1)$$

When simulating bottoming cycles, it can be defined as an open system with mass entering and exiting the system boundaries. For such systems the conservation law of mass must be applied, given in equation (3.2). The law states that mass cannot suddenly appear or disappear within a defined control volume [41].

$$\frac{dm_{CV}}{dt} = \sum_i \dot{m}_i - \sum_e \dot{m}_e \quad (3.2)$$

By equation (3.2) and the definition of work, the work term in equation (3.1) can be expanded.

$$\dot{W} = \dot{W}_{CV} + \sum_e \dot{m}_e (p_e v_e) - \sum_i \dot{m}_i (p_i v_i) \quad (3.3)$$

The term  $\dot{W}_{CV}$  is the energy transferred across the boundary of the control volume, and the other terms are the work transferred with the incoming and outgoing flow of the control volume. Instead of constantly evaluating the internal energy of a medium in relation to the volumetric work, a more convenient combination of the two is frequently used, defined as enthalpy, given by equation (3.4) [41].

$$h = u + pv \quad (3.4)$$

Since enthalpy is a non-measurable unit the values can be calculated by either using ideal gas laws, tables, or have a real gas approach using equations of state. Temperature, pressure and other possible measureable values are obtained and used to calculate the enthalpy difference

over a component or process. It is important to remember that enthalpy is not a defined value, and must always be seen in relation to a state condition. The scope of this thesis is to analyze the different cycles in a specific control volume and at steady state conditions. Applying the conservation of mass, expanded work term and enthalpy on a mass basis to the energy equation (3.1) gives:

$$\frac{dE_{CV}}{dt} = \dot{Q}_{CV} - \dot{W}_{CV} + \sum_i \dot{m}_i \left( h_i + \frac{c_i^2}{2} + gz_i \right) - \sum_e \dot{m}_e \left( h_e + \frac{c_e^2}{2} + gz_e \right) = 0 \quad (3.5)$$

Equation (3.5) states that the energy balance in the control volume over time is equal to the energy supplied or withdrawn by heat, work and energy in the mass flow across the control volume. At steady state this balance must be equal to zero.

### 3.2. The 2<sup>nd</sup> law of thermodynamic

A useful feature regarding the second law of thermodynamic is the ability to evaluate performance to an ideal case. The 2<sup>nd</sup> law of thermodynamic tells us something about the direction in which a process is allowed to go without the addition of external energy. The Kelvin-Planck statement of the law goes:

*“It is impossible for any system to operate in a thermodynamic cycle and deliver a net amount of energy by work to its surroundings while receiving energy by heat transfer from a single thermal reservoir” [41]*

This means that some energy extracted from the reservoir has to be released to the surroundings and considered as loss. As a result, there is no such thing as a perfect heat engine. The closest thing to a perfect engine is the Carnot engine. The Carnot efficiency (equation 3.6) presents the maximum efficiency of an ideal reversible thermal process between two thermal reservoirs. The temperatures in the equation are the temperatures at which heat is rejected  $T_C$  and supplied  $T_H$  to the reservoirs.

$$\eta_{carnot} = 1 - \frac{T_C}{T_H} \quad (3.6)$$

### 3.3. Irreversibility and entropy

Losses are always present in the real world and in thermodynamics these losses are referred to as *irreversibilities*. This includes friction, combustion, heat loss, spontaneous chemical reactions and others. When irreversibilities occur, it is not possible to reverse a process to its initial state without the addition of energy, as stated by the 2<sup>nd</sup> law of thermodynamic. To be

able to get a measurement of where in a cycle the losses occur, the property entropy is very useful. Entropy is defined by equation (3.7) [41] :

$$S_2 - S_1 = \left( \int_1^2 \frac{\delta Q}{T} \right)_{\text{int.rev}} \quad (3.7)$$

Entropy is a state function that tells how much the system has lost its ability to provide work between two states. The generation of entropy by internal irreversibilities must always be positive according to the 2<sup>nd</sup> law of thermodynamic. This implies that when the entropy generation term is equal to zero, there are no irreversibilities present within the control volume, also referred to as an isentropic process. Equation (3.8) gives an entropy balance at steady state for an open control system.

$$\frac{dS_{CV}}{dt} = \sum_j \frac{Q_j}{T_j} + \sum_i \dot{m}_i s_i - \sum_e \dot{m}_e s_e + \dot{\sigma}_{CV} = 0 \quad (3.8)$$

This balance accounts for the transfer and production of entropy in a given control volume and for steady state condition this must be equal to zero. In this thesis entropy will be used in T-s (temperature-entropy) diagrams. These diagrams are a common presentation of thermodynamic cycles, and provide a good visualization of losses and process flow.

### 3.4. Process analysis

When performing process calculations on real gases there are essentially two main types of calculation methods for an analytical approach, the isentropic process and the polytropic process. The polytropic process has for many years been the preferred method of approach and is implemented in industry standards. The simulation software used in this thesis utilizes isentropic efficiency as the specification input for a steam turbine, thus both methods are presented in this report. The main difference in the analysis between ideal and real gas is that the isentropic exponent  $\kappa$  and the polytropic exponent  $n$  are no longer a constant. The exponents are segregated into temperature-pressure ( $\kappa_T, n_T$ ) and pressure-volume ( $\kappa_v, n_v$ ) exponents, which must be distinguished. This section will highlight the formulas used for the compression and expansion process in the two approach methods. The suffix 1 and 2 will represent the inlet and outlet of a compressor, and the suffix 3 and 4 will be the inlet and outlet of an expander/turbine.

### 3.4.1. Isentropic compression and expansion

As previously stated, the isentropic process is has no irreversibilities occurring during the process. The isentropic pressure-temperature relation for a real gas is expressed by equation (3.9) [42]:

$$\frac{T_{2s}}{T_1} = \left( \frac{p_2}{p_1} \right)^{\frac{\kappa_T - 1}{\kappa_T}} \quad (3.9)$$

Isentropic volume-temperature relation for the real gas is expressed in equation (3.10) [42]:

$$pv^{\kappa_v} = const \quad (3.10)$$

The isentropic temperature exponent ( $\kappa_T$ ) expressed in equation (3.11) can be derived from equation (3.9). It states that a change in the isentropic temperature exponent is related to the change in temperature and pressure along a given isentropic efficiency path.

$$\kappa_T = \frac{1}{1 - \frac{p_1}{T_1} \left( \frac{\partial T}{\partial p} \right)_{\eta_s}} \quad (3.11)$$

The isentropic volume exponent ( $\kappa_v$ ) expressed in equation (3.12) can be derived from equation (3.10). It states that a change in isentropic volume exponent is related to the change in pressure and volume at a given isentropic efficiency path.

$$\kappa_v = - \frac{v_1}{p_1} \left( \frac{\partial p}{\partial v} \right)_{\eta_s} \quad (3.12)$$

Because the exponents are continuously changing throughout the compression, an exact calculation of the compression work is not possible. Averaged values of the exponents by the inlet, mid and outlet value, can improve the calculation. However, even though averaged value of the exponents are used, the approach does not take into account all the changes for the isentropic volume exponent  $\kappa_v$  [42]. To compensate for this, the isentropic head correction factor ( $f_s$ ) is introduced.



$$f_s = \frac{h_{2s} - h_1}{\frac{\kappa_v - 1}{\kappa_v} [p_2 v_{2s} - p_1 v_1]} \quad (3.13)$$

To find an expression for the isentropic enthalpy change for a compressor, one starts off with the approximation shown in equation (3.14).

$$H_s = \int_1^{2s} v dp \approx \frac{\kappa_v}{\kappa_v - 1} [p_2 v_{2s} - p_1 v_1] \quad (3.14)$$

By assuming a constant volume-pressure exponent, one can derive an expression for isentropic enthalpy change for compression by equation (3.10), equation (3.13) and the compressibility factor given by equation (3.15).

$$Z = \frac{pvMW}{R_0 T} \quad (3.15)$$

The result is often referred to as the formula for isentropic head, and is given by the equation (3.16) [42].

$$H_s = h_{2s} - h_1 = f_s \frac{\kappa_v - 1}{\kappa_v} \frac{Z_1 R_0 T_1}{MW} \left[ \left( \frac{p_2}{p_1} \right)^{\frac{\kappa_v - 1}{\kappa_v}} - 1 \right] \quad (3.16)$$

By multiplying with the mass flow, the value for isentropic work of the compressor can be calculated, equation (3.17).

$$\dot{W}_{s,comp} = \dot{m}_1 H_s = \dot{m}_1 f_s \frac{\kappa_v - 1}{\kappa_v} \frac{Z_1 R_0 T_1}{MW} \left[ \left( \frac{p_2}{p_1} \right)^{\frac{\kappa_v - 1}{\kappa_v}} - 1 \right] \quad (3.17)$$

The expression for isentropic efficiency for a compression process is then given by equation (3.18). By assuming an isentropic efficiency, the real compressor work can be calculated through the given relation beneath.

$$\eta_{s,comp} = \frac{\dot{W}_{s,comp}}{\dot{W}_{comp}} = \frac{\dot{m}_1 (h_{2s} - h_1)}{\dot{m}_1 (h_2 - h_1)} \quad (3.18)$$

Calculation of the expansion process is similar as to the compressor side. The averaged values of the isentropic exponents are calculated, but also the here there is need for an isentropic

correction factor for changes in the isentropic volume-pressure exponent. The isentropic expansion correction term is defined as [42]:

$$e_s = \frac{h_3 - h_{4s}}{\frac{\kappa_v}{\kappa_v - 1} [p_3 v_3 - p_4 v_{4s}]} \quad (3.19)$$

By similar method as with the compression the enthalpy change for an isentropic expansion becomes:

$$H_s = h_3 - h_{4s} = e_s \frac{\kappa_v}{\kappa_v - 1} \frac{Z_3 R_0 T_3}{MW} \left[ 1 - \left( \frac{p_4}{p_3} \right)^{\frac{\kappa_v - 1}{\kappa_v}} \right] \quad (3.20)$$

The work delivered from the expansion process thus becomes:

$$\dot{W}_{s,turbine} = \dot{m}_3 H_{s,turbine} = \dot{m}_3 e_s \frac{\kappa_v}{\kappa_v - 1} \frac{Z_3 R_0 T_3}{MW} \left[ 1 - \left( \frac{p_4}{p_3} \right)^{\frac{\kappa_v - 1}{\kappa_v}} \right] \quad (3.21)$$

By equation (3.22) the definition for an isentropic efficiency for an expansion process becomes:

$$\eta_{s,turbine} = \frac{\dot{W}_{turbine}}{\dot{W}_{s,turbine}} = \frac{\dot{m}_3 (h_3 - h_4)}{\dot{m}_3 (h_3 - h_{4s})} \quad (3.22)$$

### 3.4.2. Polytropic compression and expansion

The polytropic process can be seen as incremental isentropic compressions along the actual compression line defined by the polytropic efficiency of the compressor [42]. The polytropic exponents vary through both the expansion and compression process, and as a consequence the polytropic approach will never be perfect. Due to the diverging pressure lines in the enthalpy-entropy (h-s) diagram for a real gas, the polytropic process will give a more accurate results than the isentropic approach.

Polytropic temperature-pressure and volume-pressure relations are defined by equation (3.23) and (3.24) [42]:

$$\frac{T_2}{T_1} = \left( \frac{p_2}{p_1} \right)^{\frac{n_T-1}{n_T}} \quad (3.23)$$

$$pv^{n_v} = \text{const.} \quad (3.24)$$

The definition of the temperature-pressure exponent ( $n_T$ ) can be derived from equation (3.23). Equation (3.25) states that changes in temperature-pressure exponent is dependent on variation in temperature and pressure along a given polytropic efficiency curve.

$$n_T = \frac{1}{1 - \frac{p_1}{T_1} \left( \frac{\partial T}{\partial p} \right)_{\eta_p}} \quad (3.25)$$

Similarly the pressure-volume exponent is related to the changes in pressure and volume along the given polytropic efficiency curve. Equation (3.26) can be derived from equation (3.24).

$$n_v = - \frac{v_1}{p_1} \left( \frac{\partial p}{\partial v} \right)_{\eta_p} \quad (3.26)$$

The calculations of the values for polytropic temperature and volume exponents are by industry standards carried out by Shultz method [43]. It is basically a better approach to find values of the exponent that adjust the polytropic compression process closer to the real compression process.

To find an expression for polytropic head one starts with the approximation shown in equation (3.27).

$$H_p = \int_1^2 v dp \approx \frac{n_v}{n_v - 1} [p_2 v_2 - p_1 v_1] \quad (3.27)$$

By assuming constant polytropic volume exponent, along with equation (3.24) and equation (3.15), an expression for polytropic head can be derived. The derived expression is given by equation (3.28) [42]. A correction factor for the pressure-volume exponent is necessary and it is defined similarly as the correction factor for isentropic compression in equation (3.13).

$$H_p = f \frac{n_v}{n_v - 1} \frac{Z_1 R_0 T_1}{MW} \left[ \left( \frac{p_2}{p_1} \right)^{\frac{n_v-1}{n_v}} - 1 \right] \quad (3.28)$$

Equation (3.28) is only valid when the polytropic volume exponent is defined by [42]:

$$n_v = \frac{\ln\left(\frac{p_2}{p_1}\right)}{\ln\left(\frac{v_1}{v_2}\right)} \quad (3.29)$$

Multiplying the mass flow with the polytropic head in equation (3.28), the expression for required compressor work becomes:

$$\dot{W}_{p,comp} = \dot{m}_1 H_{p,comp} = \dot{m}_1 f \frac{n_v}{n_v - 1} \frac{Z_1 R_0 T_1}{MW} \left[ \left(\frac{p_2}{p_1}\right)^{\frac{n_v-1}{n_v}} - 1 \right] \quad (3.30)$$

With this expression the polytropic efficiency for a compression process can be derived:

$$\eta_{p,comp} = \frac{H_p}{H} = \frac{h_{2p} - h_1}{h_2 - h_1} \quad (3.31)$$

By similar method as described above, the expression for polytropic change in enthalpy for an expansion process can be derived. Equation (3.32) shows the polytropic head for an expansion process. However, note that no expansion correction term is included.

$$H_p = \frac{n_v}{n_v - 1} \frac{Z_3 R_0 T_3}{MW} \left[ 1 - \left(\frac{p_3}{p_4}\right)^{\frac{n_v-1}{n_v}} \right] \quad (3.32)$$

The polytropic efficiency defined for an expansion process then becomes [42]:

$$\eta_{p,turbine} = \frac{H}{H_p} = \frac{h_3 - h_4}{h_3 - h_{4p}} \quad (3.33)$$

### 3.4.3. Compression and expansion calculation in Ebsilon Professional

In Ebsilon Professional both polytropic and isentropic efficiencies are used to calculate the output of components. However, there seem to be a majority of components that require assumed isentropic efficiencies. The methods for calculation in Ebsilon Professional are based on the principles presented in the previous sections. By the energy equation (3.5) for a process in steady state, the change in enthalpy will determine the value for the heat and/or work transferred. In Ebsilon Professional a calculation step does not calculate all the parameters described in the isentropic and polytropic approach. The software uses an extensive industry standard libraries of enthalpy and entropy values for gases and liquids at a given pressure, temperature etc. (see section 7.1. for more details regarding the software). The calculations in the software will then only be dependent on interpolation and iteration with the values in the tables. However, the calculative principles described in the previous section are valid for calculations and is presented to provide an in depth introduction to how real gas thermodynamic differ from the ideal gas approach.

### 3.5. Heat transfer

The relation between temperature difference and heat transfer area can be seen by equation (3.34). By increasing the log mean temperature difference the heat transfer area can be reduced.

$$Q = UA\Delta T_{lm} \quad (3.34)$$

The log mean temperature difference are defined by the following formula [44]:

$$\Delta T_{lm} = \frac{\Delta T_{hot} - \Delta T_{cold}}{\ln\left(\frac{\Delta T_{hot}}{\Delta T_{cold}}\right)} \quad (3.35)$$

The HRSG efficiency is determined as the enthalpy difference of the steam divided by the enthalpy difference of the exhaust gas.

$$\eta_{HRSG} = \frac{h_{gas,in} - h_{gas,exit}}{h_{gas,in} - h_{gas,amb}} \quad (3.36)$$

### 3.6. Definitions

In this last section the parameters used in this thesis is defined.

#### 3.6.1. Power outputs

Gas Turbine power output was defined as net work delivered to the shaft multiplied with the generator and mechanical efficiencies.

$$\dot{W}_{shaft,GT} = \dot{W}_{turbine} - \dot{W}_{comp} = \dot{m}_3(h_3 - h_4) - \dot{m}_1(h_2 - h_1) \quad (3.37)$$

$$\dot{W}_{GT} = (\dot{W}_{shaft} \eta_{gen} \eta_{mech})_{GT} \quad (3.38)$$

Steam turbine power output was defined as the work produced by the steam turbine multiplied with the generator and mechanical efficiencies.

$$\dot{W}_{ST} = (\dot{W}_{turbine} \eta_{gen} \eta_{mech})_{ST} \quad (3.39)$$

To avoid liquid formation in the last stages in of the steam turbine a minimum required steam quality value was determined. Steam quality is defined as the mass of vapor in the flow divided by the total mass of the flow [41].

$$x = \frac{m_{vapor}}{m_{liquid} + m_{vapor}} \quad (3.40)$$

Pump work for an incompressible fluid, such as water, is given by [45]:

$$\dot{W}_{pump} = (\dot{m}_1 H) \eta_{pump} \eta_{motor} = (\rho_1 \dot{V}_1 H) \eta_{pump} \eta_{motor} \quad (3.41)$$

The term  $\eta_{pump}$  is either the isentropic or polytropic efficiency of the pump, depending on software calculative approach.

### 3.6.2. Plant efficiencies

The thermal efficiency of the gas turbine was defined as the GT power output divided by the mass flow of fuel multiplied with its Lower Heating Value (LHV).

$$\eta_{GT} = \frac{\dot{W}_{GT}}{\dot{m}_{fuel} LHV_{fuel}} \quad (3.42)$$

The thermal efficiency of the steam bottoming cycle was defined as the power output from the steam turbine divided by the heat in the exhaust from the gas turbine.

$$\eta_{SRC} = \frac{\dot{W}_{ST}}{\dot{m}_{fuel} LHV_{fuel} (1 - \eta_{GT})} \quad (3.43)$$

Net plant power output was defined as the work provided by the GT and ST and subtracted with the auxiliary power requirements. In the auxiliary power requirement all pumps in the system were included.

$$\dot{W}_{net,plant} = \dot{W}_{GT} + \dot{W}_{ST} - \dot{W}_{aux} \quad (3.44)$$

The thermal efficiency of the combined cycle was defined as the net power output divided by the fuel input multiplied with its lower heating value. The relation is given by equation (3.45).

$$\eta_{net,plant} = \frac{\dot{W}_{net,plant}}{\dot{m}_{fuel} LHV_{fuel}} \quad (3.45)$$

Useful process heat from the cycles was defined as the latent heat of steam, equation (3.46). The available superheat was extracted in the simulations and regarded as a loss.

$$\dot{Q}_{process} = \Delta H_{vap} \quad (3.46)$$

The Energy Utilization Factor (EUF) is a parameter which tells how much of the energy from the burnt fuel that is being utilized either by power generation or by process heat [46].

$$EUF = \frac{\dot{W}_{net,plant} + \dot{Q}_{process}}{\dot{m}_{fuel} LHV_{fuel}} \quad (3.47)$$

### 3.6.3. Emission rates and cost

CO<sub>2</sub> emission rate ( $ER$ ) from the plant was defined as the annual emitted CO<sub>2</sub> in the exhaust divided by annual electrical produced megawatt hour.

$$ER_{power} = \frac{\dot{m}_{CO_2,exhaust}}{\dot{W}_{net,plant,annual}} \quad (3.48)$$

The annual taxation cost of burning fuel offshore is given by equation (3.49), where the annual fuel consumption ( $f$ ) is multiplied with the tax rate ( $l$ ).

$$CO_{2,tax} = f \left[ \frac{sm^3}{year} \right] \cdot l \left[ \frac{kr}{sm^3} \right] \quad (3.49)$$

An interesting and easy comparable relation is the taxation cost per produced megawatt hour for electricity produced, given by equation (3.50)

$$CO_{2,tax} = \frac{f \cdot l}{\dot{W}_{net,plant,annual}} \quad (3.50)$$



## 4. Power cycles

This chapter will describe the combined cycles concepts before moving on into more technical details in Chapter 5. The chapter starts of with an explanation of the Brayton cycle, often referred to as the simple cycle gas turbine. It is then followed by a run-through of the steam Rankine cycle, and in the last two sections the combined heat and power cycles chosen for simulations are described.

### 4.1. Brayton cycle

As stated in section 2.2, the common method of energy production offshore is by the use of simple cycle gas turbines, in thermodynamics referred to as the Brayton cycle. As seen in Figure 4.1 the gas turbine power cycle consists of a compressor, a combustion chamber and turbine sections.

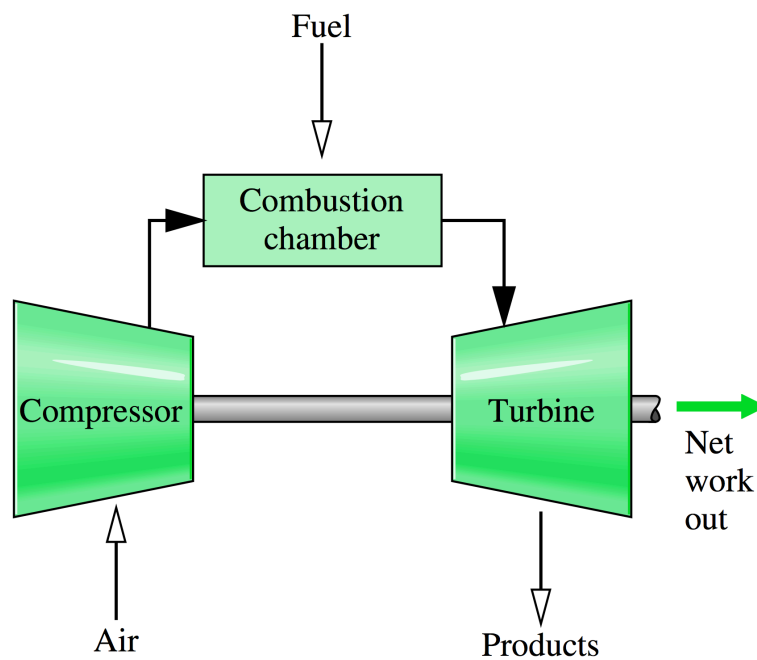
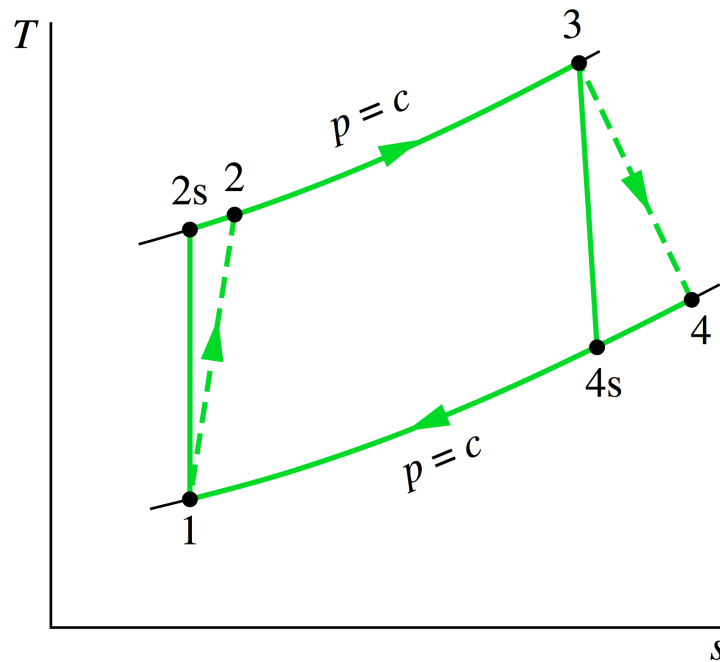


Figure 4.1 Brayton cycle [41]



**Figure 4.2 T-s diagram for closed cycle gas turbine with irreversibilities [41]**

The cycle is illustrated better when looking at the T-s diagram in Figure 4.2. With reference to the figure the Brayton cycle goes:

- (1-2) The compressor increases the pressure level of air
- (2-3) The air is sent to the combustion chamber where air and fuel combusts.
- (3-4) Energy in the hot exhaust is converted into mechanical energy in the turbine section through expansion. First turbine section extracts energy to run the compressor, and the second turbine section is used to run a generator or machinery for mechanical work.

The 2s state and 4s state are the isentropic end states, illustrating how an irreversible compression and expansion looks compared to a real process. The entropy difference between state 2 and 2s is the production of entropy through the compressor, or in other words; the sum of irreversibilities explained in section 3.3. In a real gas turbine there might also be pressure drops present, such as through the combustion chamber and inlet filter. This is not shown in Figure 4.2.

## 4.2. Steam rankine cycle

The bottoming cycles to be examined in this thesis are modifications of the Steam Rankine Cycle. Figure 4.3 illustrate how the steam cycle is connected with the topping cycle and how heat in the exhaust is transferred. The steam Rankine cycle consists of an HRSG, steam turbine, condenser and a pump. The cycle itself is quite similar to the Brayton cycle but includes a phase change of the working medium and a closed cycle arrangement. With relation to Figure 4.3 the cycle goes:

- (9-6) Water is pumped to specified pressure level
- (6-7) Water is heated up in the heat exchanger (HRSG). The fluid undergoes phase transition and the steam is then superheated.
- (7-8) The steam is expanded through the turbine and mechanical work is extracted.
- (8-9) Steam then runs through the condenser before water then reenters the pump.

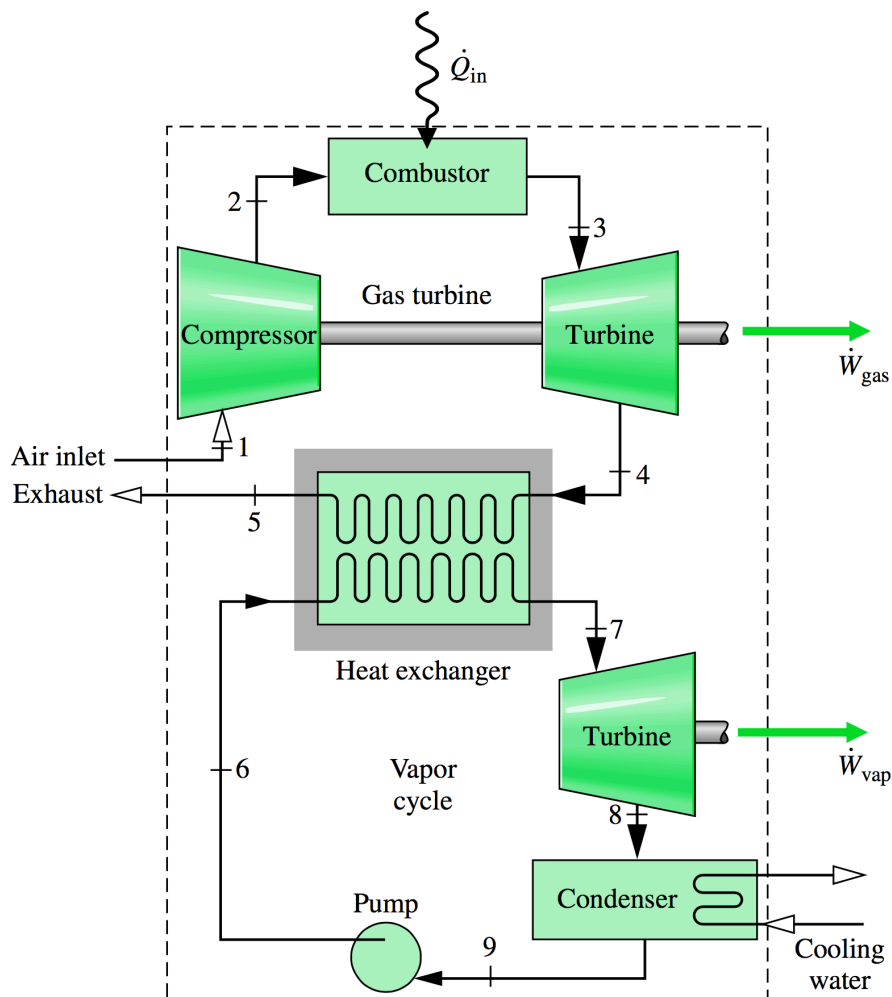
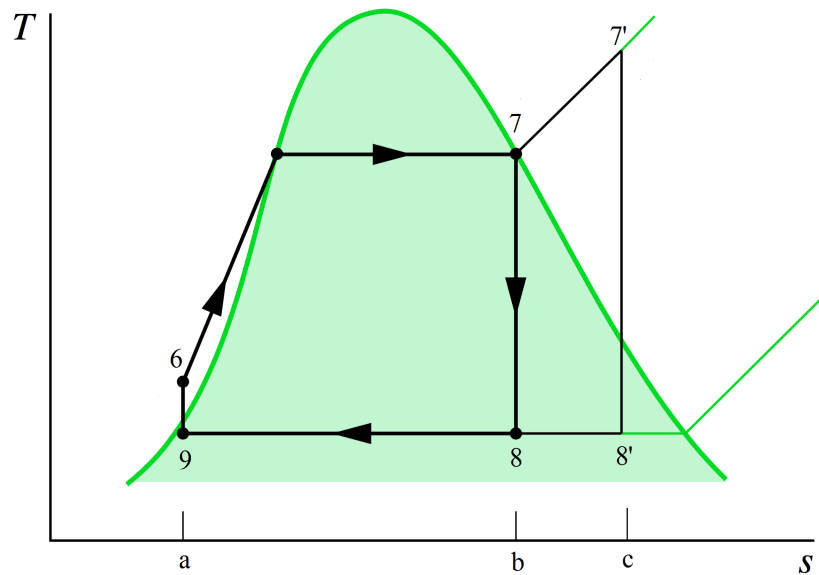


Figure 4.3 Layout of combined gas turbine-steam power plant[41]



**Figure 4.4 T-s diagram of ideal steam rankine cycle[41]**

The T-s diagram in Figure 4.4 illustrates how the cycle operates in and out of phase regions, though it does not show irreversibilities occurring in real situations. Two different expansion paths are drawn in the figure (7-8 and 7'-8') illustrating the benefit of superheating. Superheating is the additional heating (7-7') of the steam along a constant pressure line. This moves the steam away from the phase envelope, and allows the expansion to last longer in the gas phase region. The steam quality, as defined by equation (3.40), must be of certain value to avoid droplet formation in the flow through the last turbine sections. Droplet formation could cause erosion, corrosion, lower the efficiency and increase the need for maintenance. A common practice is to keep the steam quality above 0.90 when exiting the last turbine stages [41]. It can be seen from the Figure 4.4 that an increase in the steam pressure would require supplementary superheating to be able to stay within required steam quality at the outlet for a given condensation pressure level. It is therefore important to find the pressure ratio over the turbine that delivers the best overall thermal efficiency but still enables a good operation within safe conditions. The available condensing pressure subsequent to the turbine plays a major part in these design evaluation. Available cooling temperature on the site will determine the minimum outlet pressure on the outlet of the steam turbine. This is further discussed in section 5.4.

### 4.3. Combined heat and power cycles

Chosen CHP cycles evaluated in this thesis are the steam extraction cycle and the backpressure cycle. In the two following sections the layout of the cycles will be presented.

#### 4.3.1. Extraction steam turbine cycle

The extraction steam turbine cycle is somewhat similar to the steam Rankine cycle shown in Figure 4.3, major difference being the extraction configuration for the turbine. In Figure 4.5 the layout of the extraction steam turbine cycle is illustrated in a closed loop design. Extraction of steam (14) can be carried out by holes through the casing or from the piping between stages as shown in the figure. The cycle has the option to vary the amount of process heat delivered, which is controlled by a control valve. This flexibility could potentially ease operation but comes at the price of limited power generation through the later turbine stages. The process heat will be equal to the latent heat extracted between points (14) and (15), available heat in the superheated region is considered as a loss. Saturated water returning from process is reintroduced (15) after the low pressure (LP) pump through a mixing valve.

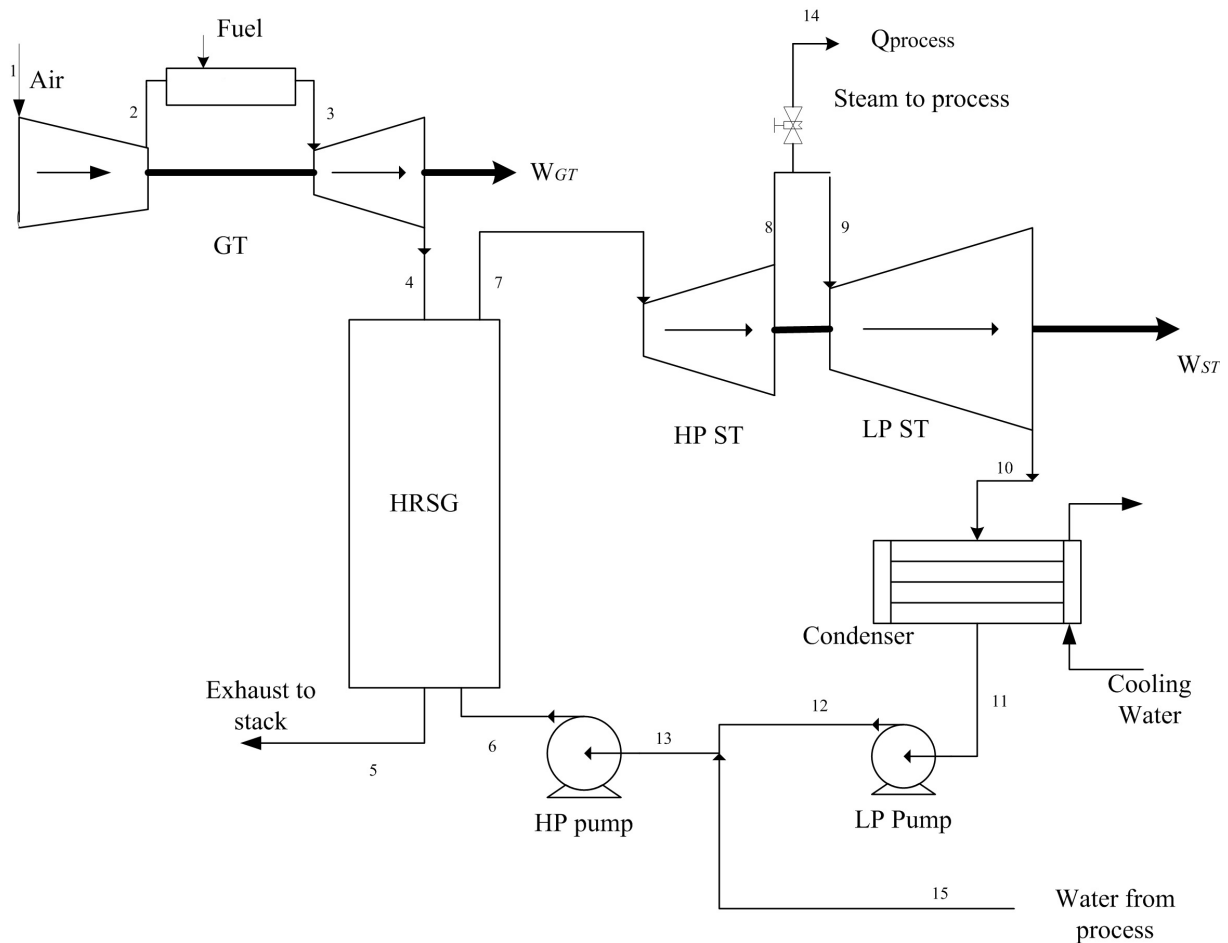
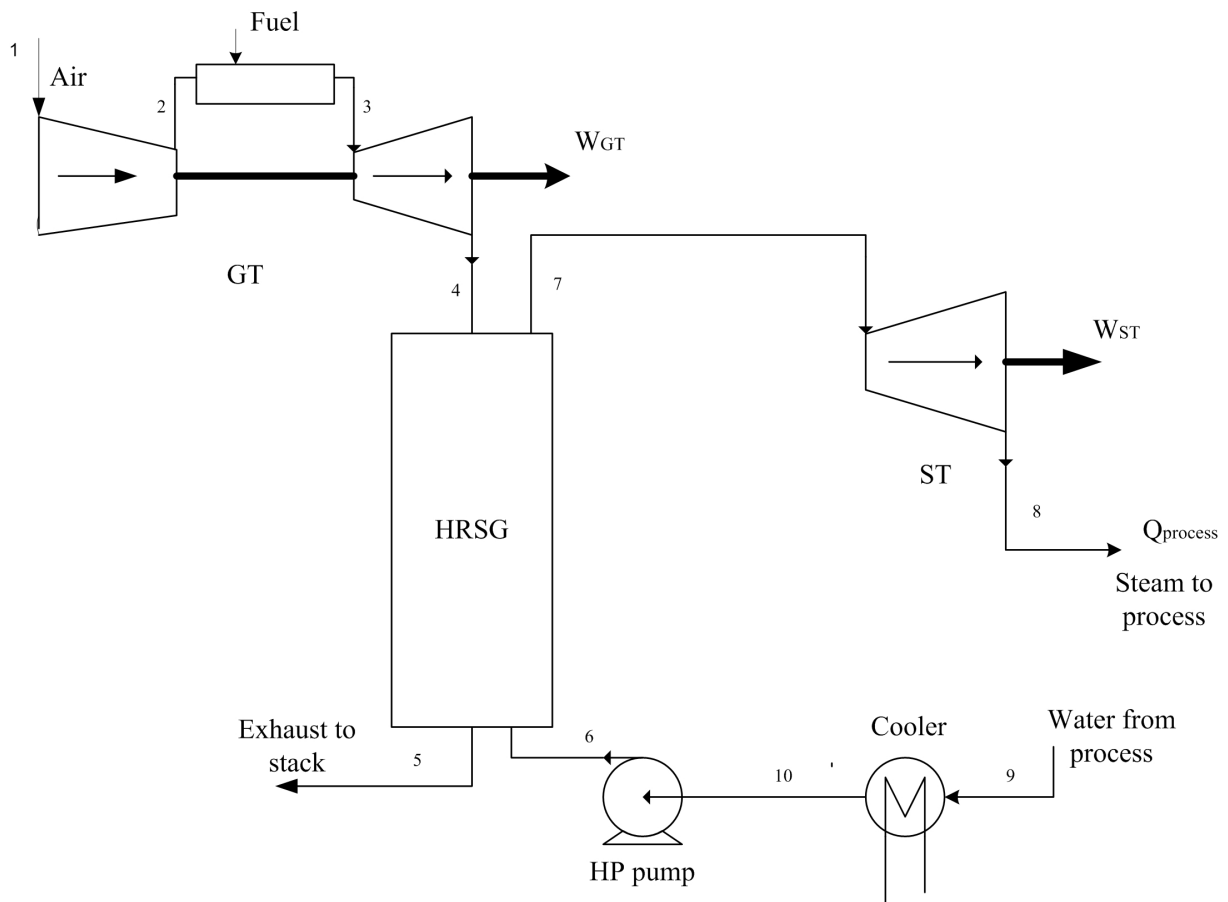


Figure 4.5 Layout of the extraction steam turbine cycle

### 4.3.2. Backpressure steam turbine cycle

In Figure 4.6 the layout of the backpressure steam turbine cycle is shown in a closed loop design. This cycle is different from the steam extraction cycle in the sense that all of the steam passes through the steam turbine before available latent heat is extracted in process facilities. Consequently this means that electric power generation is limited, as the pressure level at the turbine exit must be higher to deliver required process heat temperature. Another consequence of this is the electric power output being fixed with a specific amount of process heat. However, this might not necessarily be a bad thing as the heat in the steam could be better utilized compared to rejection in a condenser. The returning saturated water from process (9) is sent through an aftercooler, as the temperature is still quite high.



**Figure 4.6 Layout of the backpressure steam turbine cycle**

In this chapter the layout of the cogenerative bottoming cycles and topping cycle has been presented. In order to make the cycles suitable for offshore conditions the different alternatives for CHP technology must be addressed. The next chapter focuses on which technology that deems suitable for offshore conditions and how the author justifies the choices made.

# 5. Cogeneration technology

The following sections will present some of the different options for the major components in a cogenerative power plant. Options were evaluated for offshore operation and suitability. This is to provide a consistent line of arguments to why the chosen technological solutions seemed appropriate for offshore usage. The scope of this thesis is not big enough to cover all the in depth analysis of what is being presented here. Reasoning for the choices made are primarily done by evaluation of previous studies, sizing considerations and analytical evaluation for implementation with offshore systems.

## 5.1. Gas turbine

### Industrial vs. Aero-derivative

For gas power plants there are generally two types of gas turbines available, the industrial and the aero-derivative. Gas turbines for offshore operation generally have power outputs in the range of 10-35 MW and have axial flow through the compressor and turbine [21, 47]. For onshore power plants high efficiency and low maintenance costs are primary decisions drivers. Since produced power is the main product, maintaining a low cost of operation becomes crucial for business. In offshore operation the produced power is a necessity for the production of oil and gas products. Hence, availability, ruggedness and weight-to-power ratio are of great importance in order to keep a stable production and minimize area requirements. Reducing downtime by simple maintenance and repair are also of great interest for the offshore operators. Although efficiency previously was of less importance, taxation schemes and increased production costs for mature fields have lead to an increased focus on the efficiency in power production. Primary drivers for gas turbine selection for onshore and offshore conditions are summarized in Table 5.1.

**Table 5.1 Decision drivers for GT offshore and onshore [21]**

Offshore	Onshore
<ul style="list-style-type: none"> <li>▪ High power-to-weight ratio</li> <li>▪ Ruggedness</li> <li>▪ Availability/Reliability</li> <li>▪ Efficiency not critical (earlier)</li> <li>▪ Simple maintenance and repair</li> <li>▪ Off-design performance</li> </ul>	<ul style="list-style-type: none"> <li>▪ Cost of electricity</li> <li>▪ High efficiency</li> <li>▪ Cost of operation and maintenance</li> </ul>

The aero-derivative gas turbines main advantage is the high power-to-weight ratio compared to the industrial type. The reason for the low weight comes from its origin, old jet engine designs. In simple terms, the redesign from old flight engines was a removal of the big fan in front and a replacement of the nozzle with a separate power turbine section at the back. Common practice for offshore gas turbine maintenance is a replacement of the whole machinery. Performing maintenance onshore lowers the required downtime for the production

facility. For heavy industrial gas turbines this would be a non-practical option and maintenance would have to be carried out offshore. The aeroderivative GT has been, and still is, the preferred option for power generation on offshore installations [47, 48]. However, lightweight industrial types options are available and have become more competitive [21]. When aeroderivative gas turbines were chosen for offshore utilization, they were considered more advanced in material, efficiency and maintainability than industrial gas turbines. Today, one might consider them as to be equally advanced, due to the economic importance of onshore large-scale industrial gas turbines [47]. Nevertheless the aeroderivative gas turbines still has an advantage for offshore operation and is the chosen type for the simulations in this thesis.

### **GT chosen for simulation: GE LM2500+G4**

For the simulations carried out in this thesis, the aeroderivative gas turbine General Electric LM2500+G4 was chosen (shown in Figure 2.1). The +G4 model is the latest addition in the LM2500-series which are of one of the most commonly used GT on the NCS [48]. The design is a modified version of the old General Electric CF6 Aircraft Engine with over 278 million operational hours by 2005 [10]. The main advantages with the GE LM2500+G4 for offshore operation can be summarized as:

- High power to weight ratio
- Compact by volume
- Proven reliability
- High efficiency, 38%
- High power output, 34 MW
- Fast start-up

The most common way to install equipment on offshore installations is by skid modules. A typical skid module looks similar to a shipping container, and this eases installation and platform logistic. In Figure 5.1 the skid module for the GE LM2500 +G4 is included for illustrative purposes. As stated, this allows for replacement of gas turbines and performing maintenance onshore. The GE LM2500 +G4 skid module contains the following equipment [21]:

- Gas turbine
- Fuel System
- Starter equipment
- Bearing lube oil system
- Driven equipment
- Generator



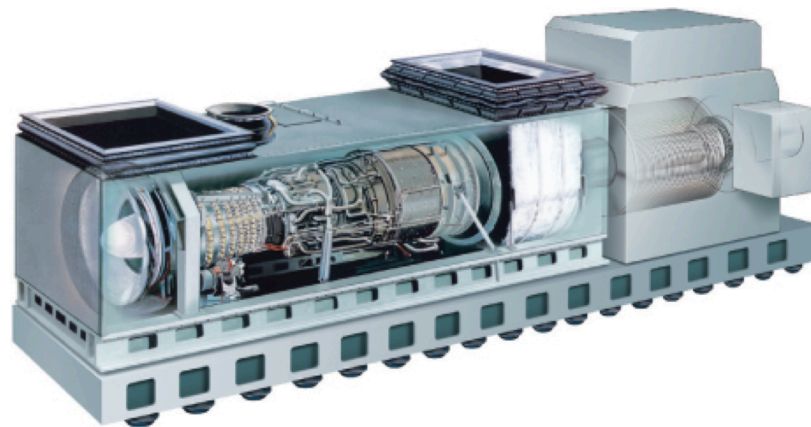
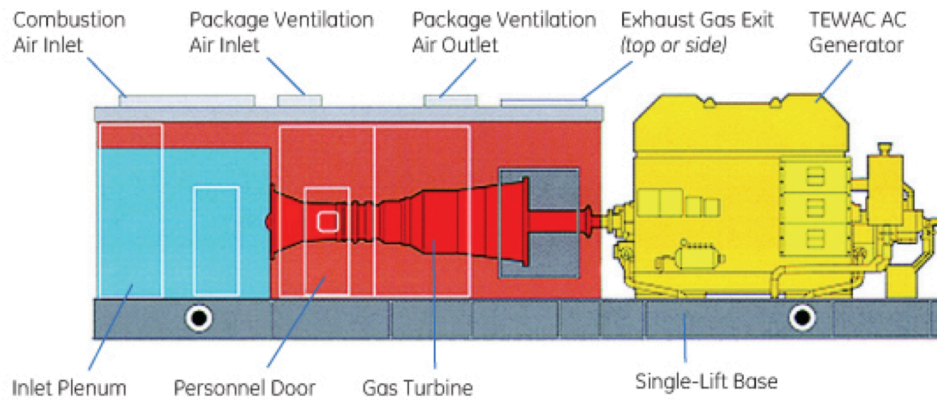


Figure 5.1 LM2500+ G4 skid module [49]

## 5.2. Steam turbine

As no component library from producers was available in the Epsilon Professional software, the chosen steam turbine for the simulation was a generalized steam turbine component within the software. The component was configured to act and operate as an extraction and a backpressure steam turbine to the best of knowledge. Configurations are further discussed in section 7.2.4. This section will discuss important characteristics for a steam turbine for offshore utilization and briefly present necessary equipment.

There exist a lot of different options for steam turbines on the market today. All from standardized to tailored machinery for specific plants. To simplify one can say that a steam turbine consists of four basic parts; the rotor, the stator, nozzles or flow passages and the frame for supporting the machinery [50]. In advanced onshore power plants steam turbines often consists of three different stages, high pressure (HP), intermediate pressure (IP) and low pressure (LP). This allows for good operational control and eases reheat and process heat extraction. A steam turbine operated as part of a combined cycle will have lower power output, pressure level and live steam temperature. For a modern power plant steam turbines have to meet the following criterias [50, 51]:

- Ability to operate over a wide range of steam flows
- High efficiency over a large operation window
- Possibility to handle reheat
- Fast startup
- Short installation time
- Floor-mounted installation

For offshore operation the first two points are of particular importance. Due to operational fluctuations on the gas turbine load, the steam turbine will experience changes imaginably more swiftly and often compared to onshore plants. As for reheat, the cycles investigated in this paper are not considered appropriate for such configuration. Reheat is most often installed between the HP and IP stage, suggesting reheating at pressure levels of 20-40 bar. Due to the lower pressure level for offshore combined cycles, applying reheat was considered as non-feasible. A major disadvantage would be the extra weight and area required for equipment, keeping in mind the increased volume flow of reheating at low pressure. As for the last two points, the installation of the steam turbine would be done with the already mentioned skid modules. Kloster [12] stated in his paper that a steam turbine skid can be assumed to require approximately the same area as a GT skid. His weight estimations for a steam turbine in the range of 15-20 [MW] were approximately 150 -175 tons and should consist of the following:

- Steam Turbine
- Generator
- Speed reduction gear
- Lubrication oil system incl. pumps
- Hydraulic system incl. pumps
- ST monitor and control system
- Condenser with condenser pump

Additionally the steam turbine system also requires an external water treatment plant, feedwater pump skid and a feedwater tank.

### **5.3. Heat recovery steam generator**

One of the most essential components in the combined cycle is the Heat Recovery Steam Generator. The HRSGs main function is the production of steam from the available heat in the GT exhaust. Many models are available on the market today, and this section will discuss the different options and how they fit into offshore operation.

#### **Fired vs. Unfired**

Depending on steam requirements and/or heat requirements, the HRSG can take three different forms:

- Unfired
- Supplementary-fired
- Exhaust-fired

In the supplementary- and exhaust-fired models additional burners are installed within the HRSG. Reasons for installing supplementary firing are to ensure steam production at required amounts and temperature when fluctuations in the inlet temperature occurs [50]. High supply temperature decreases the heat transfer area in the HRSG, seen by equation (3.34). As area is very costly offshore, supplementary firing could potentially lower cost of the HRSG. However, the need for better alloys to withstand higher temperatures and additional area for supplementary combustion must be taken into consideration [50]. Due to the high exhaust temperature from the GE LM2500+G4 and the avoidance of extra fuel consumption, an unfired HRSG was chosen for the simulations. If the supply temperature were lower, then the fired version could have been more interesting. Generally, the unfired version is the most preferred choice for combined cycle configurations [51].

#### **Vertical vs. Horizontal**

The two major characterizations for the construction are vertical and horizontal orientation. In the horizontal drum based HRSG shown in Figure 5.2, gravitational forces ensures natural circulations through the vertical tubing, thus no circulation pumps are required [51]. In the vertical drum based HRSG in Figure 5.3, tubes are horizontal suspended within the casing and circulation pumps can only be avoided when special design considerations are carried out. Table 5.2 summarizes advantages for the different designs, and as of today the vertical orientation is the preferred option for offshore installations.

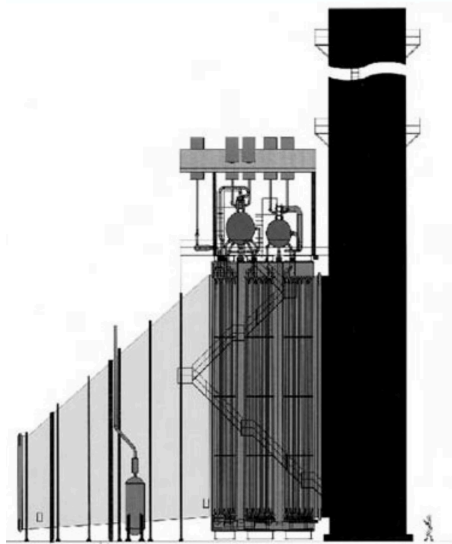


Figure 5.2 Horizontal drum based HRSG[51]

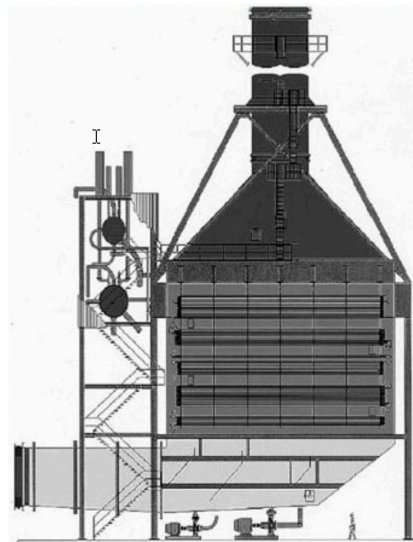


Figure 5.3 Vertical drum based HRSG [51]

Table 5.2 Advantages for vertical and horizontal HRSG [50]

Horizontal	Vertical
<ul style="list-style-type: none"> <li>▪ Natural circulation</li> <li>▪ Allows dryout due to vigorous circulation</li> <li>▪ Allows for compact steel structure</li> </ul>	<ul style="list-style-type: none"> <li>▪ Requires less footprint area</li> <li>▪ Less vulnerability to thermal cycling problems</li> <li>▪ Smaller tube diameter with circulation pumps</li> <li>▪ Less subjective to steam blockage in economizer</li> </ul>

### Single pressure vs. multiple pressures

During phase change in the evaporation, an unfavorable thermal match occurs through the HRSG. A characteristic bend in the heat transfer curve is one of the reasons development of other bottoming cycles utilizing different working fluids. Examples of such cycles are the Organic Rankine Cycle, the Kalina cycle and the supercritical CO<sub>2</sub> cycle. To improve thermal matching and increase thermal efficiency, modern onshore steam power plants use reheating at up to 3 different pressure levels. Figure 5.4 illustrates how the reheat process improves the match between heat transfer curves. In Table 5.4 the general assumed increase in power output and cost are shown for different configurations of HRSG. Even though multiple pressure levels seem to offer greater efficiency, the live steam pressure of a combined cycle makes the reheat process unsuitable option. In their paper, Nord and Bolland [52] suggested the best option for offshore installations to be a single pressure steam generator. They calculated that a 3 % penalty in efficiency could be expected. However, the weight reduction was calculated to be 2/3 of the compared dual-pressure system, making it the best choice.

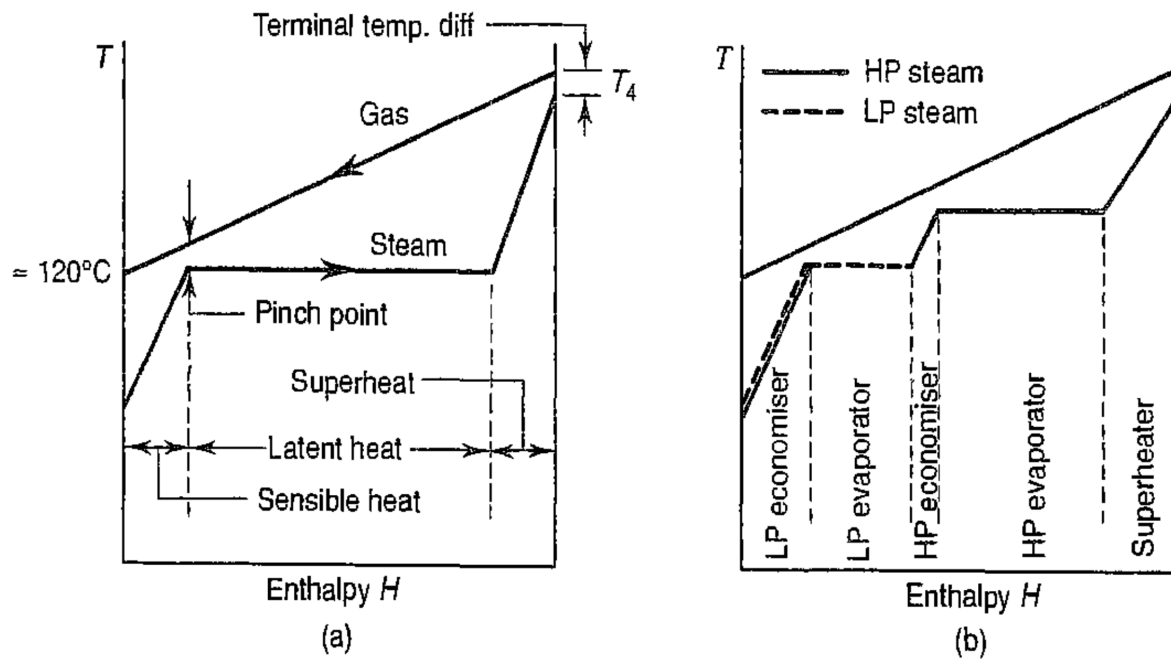


Figure 5.4 a) HRSG heat transfer at single pressure b) HRSG heat transfer at dual pressure [53]

Table 5.3 General trend for cost and efficiency for heat exchangers [50]

Type of Process	Increase in cost	Increase in efficiency	Increase in Power
Single Pressure HRSG	1.0	1	1
Single Pressure OTSG	0.98	1	1
Dual Pressure HRSG	1.025	1.015	1.015
Triple Pressure HRSG	1.03	1.02	1.02
Dual Pressure Reheat HRSG	1.04	1.035	1.035
Triple Pressure Reheat HRSG	1.035	1.027	1.027

### Once Through Steam Generator

The last alternative for the major design aspects of the offshore HRSG is having a Once Through Steam Generator (OTSG) or a traditional drum based system. In the simulations the once through steam generator design was chosen based on the development in recent years. Both the Oseberg D facility and the Eldfisk have replaced their old drum based systems with new OTSGs. In addition, similar works on combined cycles offshore [52, 54, 55] tend to choose the OTSG for its advantage in weight and area requirements compared to a drum based system.

In the OTSG the whole heat exchanger is basically one long piping where the zones for economizing, evaporation and superheating are drifting during variation in operational load. A major advantage is the weight reduction through the removal of circulation pumps, drums

and bypass stack [52]. In order to remove the bypass stack, the piping must be of high quality alloy so that the system can operate in dry condition. The increase in piping cost are recovered from the installation and construction cost by not having drums, circulation pumps, bypass stack or bypass damper valves [50]. The main cost driver for the system is the amount of heat exchange surface installed and type of alloy utilized [51]. A common indicator of heat exchange surface is the minimum pinch point selected in the evaporator. As the pinch point temperature decreases, surface area requirements increase exponentially while amount of generated steam increases linearly [51]. Choosing of pinch point must be assessed from both an operational and economical viewpoint. Table 5.4 highlights the pros and cons for the offshore OTSG.

**Table 5.4 Offshore OTSG advantages and disadvantages**

<b>OTSG</b>	
+ No bypass stack	- Reduced power output
+ No drum	- More advanced water treatment
+ Decrease in cost	- Expensive materials
+ Decrease in area requirement	
+ Less water consumption	
+ Smaller water treatment plant	
+ Ability to “run dry”	

### **Summarizing**

Based on the discussion above the chosen design for steam generation was the vertical unfired once through steam generator. The OTSG stands out as the most attractive option due to its reduced weight and area requirement compared to a drum based system. The vertical orientation minimizes area footprint and installation on top of the gas turbine would be a preferable approach to installation. Gas turbine exhaust temperature was considered to be of sufficient level, thus supplementary firing options within the OTSG was not assessed. The OTSG removes the necessity of drums, bypass stack and circulation pumps. In the paper from Nord and Bolland [52] the optimized once through steam generator for offshore usage was calculated to weight approximately 110 tons. Lastly, the offshore installation skid of the OTSG should include the following [12]:

- Once Through Steam Generator
- Inlet and outlet connections
- Single lift structure
- Instruments and instruments valve
- Piping incl. security valves
- High pressure pump

## 5.4. Condenser

There exists primarily four different cooling options for combined cycle system: direct water cooling with condenser, air-cooled condenser, wet cooling tower and dry cooling tower. Installation of a cooling tower or an air-cooled condenser offshore would not be a practical or economical option, due to the sheer size of the installation. The proximity of seawater favor the direct-water cooling condenser. These condensers consist of a bundle of tubes with cooling water flowing inside. Steam enters the condenser, and condensation occurs around the tubes. Temperature of available cooling water is one of the major design restrictions for steam power cycles, as it determines the minimum pressure for condensation. Since condensers allow for condensation to occur below atmospheric pressures, the corresponding condensation temperature can be much lower than 100 °C. Consequently, this allows for a larger enthalpy drop through the steam turbine. Accordingly, more energy are converted into mechanical energy [51]. Although minimizing pressure level can be favorable for power production, the size and weight of the condenser and steam turbine increases. Therefore, it can be assumed that condensation pressure levels offshore would be higher compared to onshore plants. The increased thermal driving force would lower the size of the condenser, as seen by equation (3.34).

## 5.5. Pumps

Number of pumps required for a combined cycle power plant varies with the number of pressure levels, type of HRSG and layout of the water treatment plant. The high-pressure feedwater pump and the lifting pumps for seawater are the major pumps for an offshore installation. The high pressure feedwater pump is usually a multistage centrifugal pump with electric drive [50]. If the plant experience large variation in operational load, variable speed configuration on the pump might be beneficial in order to vary feedwater supplied to the HRSG. This could be a suitable option for offshore installations where rapid changes in GT load might occur. HP pumps are subjected to high temperatures during operation and might experience corrosion and cavitation problems [50]. Due to the importance of this pump, a backup pump is usually installed. Seawater lifting pumps are generally assumed to experience a more stable load, as many processes on the installation continuously require cooling water. These pumps usually have a very large volume flow compared to other pumps on the facility. Other pumps worth mentioned within the power plant are circulation pumps for the water and support system such as lubrication and water treatment.

## 5.6. Deaeration

The deaeration process is necessary to remove unwanted dissolved gases from the condensate water. During operation in vacuumed pressure levels, leakages of gases into the system will always occur. Additional dissolved  $\text{CO}_2$  and  $\text{O}_2$  in the feedwater increases the risk of corrosion throughout the system [51]. Presence of these gases also reduces the heat transfer capabilities. A thermal blanket is formed along the piping by the non-condensable gases, resulting in increased thermal resistance through the HRSG [47]. In order to protect processing system and maintain high efficiency, deaeration is required.

In the stand-alone deaerator seen in Figure 5.5, water enters at the top and is heated by steam through a trayed section. Water droplets are heated to saturation point and dissolved incondensable gases are carried to the top of the deaerator for ventilation [51]. At the bottom of the deaerator it is common to have a buffer tank of deaerated saturated water. Injected steam forms a protective layer that prevents any reabsorption of  $\text{O}_2$  and  $\text{CO}_2$  to the treated water in the buffer tank. Depending on the pressure level inside the deaerator it is referred to as a pressurized or vacuum deaeration process.

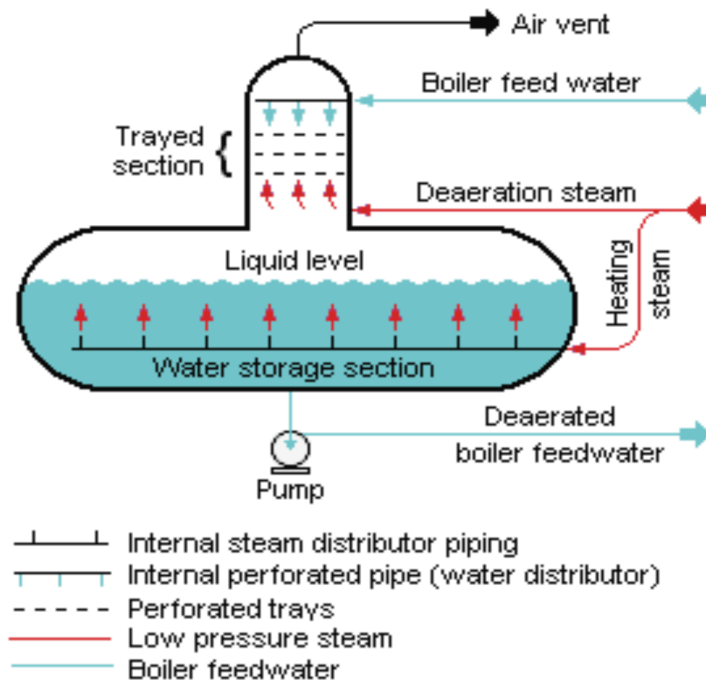


Figure 5.5 Stand-alone deaerator [47]

On offshore installation where area requirements are critical, an interesting alternative is to have the deaeration process carried out inside the condenser. Condensers can be fitted with evacuation equipment that removes the unwanted dissolved gases during condensation [51], illustrated in Figure 5.6. In their work, Athey et al. [56] used a vacuum deaerator condenser venting system on an cogenerative combined cycle and achieved  $\text{O}_2$  levels lower than required specification. As in the stand-alone deaerator, steam forms a protective layer prohibiting reabsorption of gases. Having the deaeration process in the condenser could



potentially reduce the overall area footprint. However, there was not found any research or analysis for weight and footprint comparison of the two options. For the process simulations a stand-alone deaerator component has been excluded from the models for simplistic reasons. This simplification was done due to uncertainties in the variations of water treatment facilities offshore.

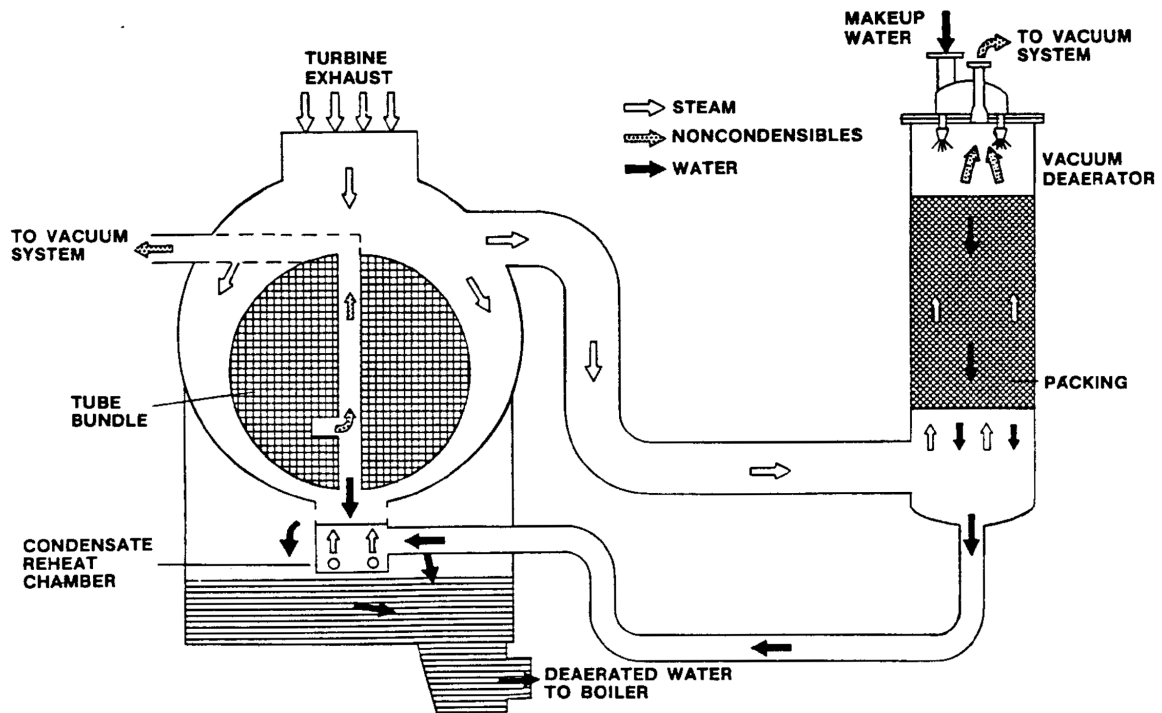


Figure 5.6 Deaerating condenser [56]

The aim of this chapter has been to present different technological options for a cogenerative combined cycle power plant. This section does not cover every aspect of the technological options, but the major components have been discussed. Technologies chosen for the simulations were based on literature studies and recommendations from previous work. It was attempted to provide a good line of argument for the choices made. Not all choices will affect the results, as the process simulations are a simplified version of the reality. With the thermodynamic theory in chapter 3, explanation of the CHP cycles in chapter 4, and the chosen technology in this chapter, the foundation for a good simulation is almost in place. But before the assumptions for the simulations can be made, it is important to clarify some aspects of how a combined cycle operates during off-design. Therefore, the next chapter is devoted to off-design operation and control.



## 6. Off-design operation and control

One of the thesis objectives for the simulations is to map off-design operational behavior of the cogenerative combined cycles. This chapter is devoted to present off-design theory for the different components. Offshore oil and gas production might lead to great variation in the power generation. Accordingly, knowledge in off-design behavior of the plant is important. To maintain predictable and stable operation, knowledge in both dynamic and steady state behavior must be assessed. Dynamic simulation of large plants can be costly and difficult. Therefore, it is common to use operational experience from similar plants along with steady state simulation, as a prediction for the dynamic behavior [51]. Dynamic behavior is beyond the scope of this thesis and will not be assessed. This chapter will give an introduction to the analytical method for off-design operation of gas turbine, steam turbine, HRSG and pump. Note that theory presented related to the chosen technologies from Chapter 5.

### 6.1. Gas turbine

The number of variables for a gas turbine performance calculation is too extensive to make a common characteristic performance chart. The following non-dimensional parameters are used to evaluate performance over the compressor (sub notation 01-02) and turbine (sub notation 03-04) [53]:

- $p_{02} / p_{01}$  Pressure ratio
- $m\sqrt{T_{01}} / p_{01}$  Non-dimensional mass flow
- $N / \sqrt{T_{01}}$  Non-dimensional speed
- $T_{01} / T_{02}$  Temperature ratio

With these parameters, experiments have shown that the most useful plots are the pressure and temperature ratio plotted against the non-dimensional mass flows. This can be carried out using the non-dimensional speed as a parameter. By the formula for isentropic efficiency, equation (6.1), one can construct characteristic lines for at a constant speed for a given isentropic efficiency [53]. These are plotted against pressure ratio and non-dimensional mass flow. The curves are created individually for both the compressor and turbine, and will be discussed in the next sections.

$$\eta_c = \frac{T_{02}' - T_{01}}{T_{02} - T_{01}} = \frac{(p_{02} / p_{01})^{(\gamma-1)/\gamma} - 1}{(T_{02} / T_{01}) - 1} \quad (6.1)$$

The author was unable to construct characteristic charts due to constrains in the component library used in simulation software. Instead general characteristic charts from literature are used.

### 6.1.1. Axial compressor

In Figure 6.1 a general axial compressor characteristic is drawn by the method previously described. The solid lines represent the lines of operation at a given constant rotational speed and isentropic efficiency. There are two occurring events limiting the operation area for compressors and turbines; choking and surging.

Surging occurs along the left-hand extremities and is characterized by a sudden drop in delivery pressure [53]. The sudden drop in pressure can cause pulsating flow, heavy vibrations and possible backflow within the compressor section. Surge must be avoided, as high temperature flames from the subsequent combustor chamber will destroy the compressor parts upstream if backflow occurs. For an axial compressor the surge points are reached before the lines of operation reaches their maximum efficiency point. Consequently the preferred points of operation are closer to the surge line. However, there is always installed an anti surge systems and a safety limit in order to avoid surge.

Choking is the right-hand extremity in Figure 6.1. Choking occurs when the mass flow has reached its maximum value given the downstream stagnation conditions [41]. To obtain a higher mass flow, one must either decrease the pressure ratio or increase the rotational speed. Axial compressors has a smaller operational area compared to radial compressors [53]. The non-dimensional speed curves does not allow for large variations in mass flow, and at large rotational speeds the lines becomes very steep. The lower graph of Figure 6.1 is the plotted isentropic efficiency against the non-dimensional mass flow for different rotational speeds. Such a plot provides a good indication of when one should increase the rotational speed to maintain high efficiency over the compressor.

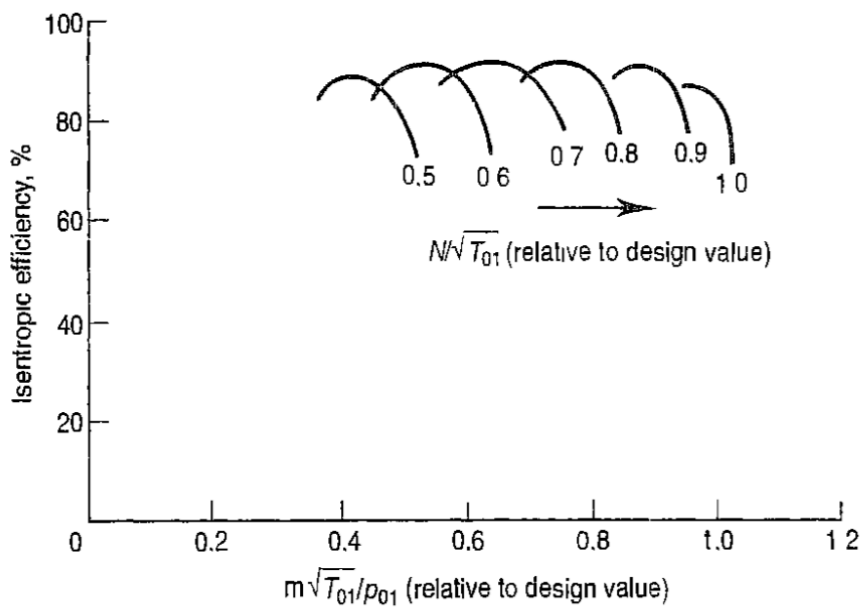
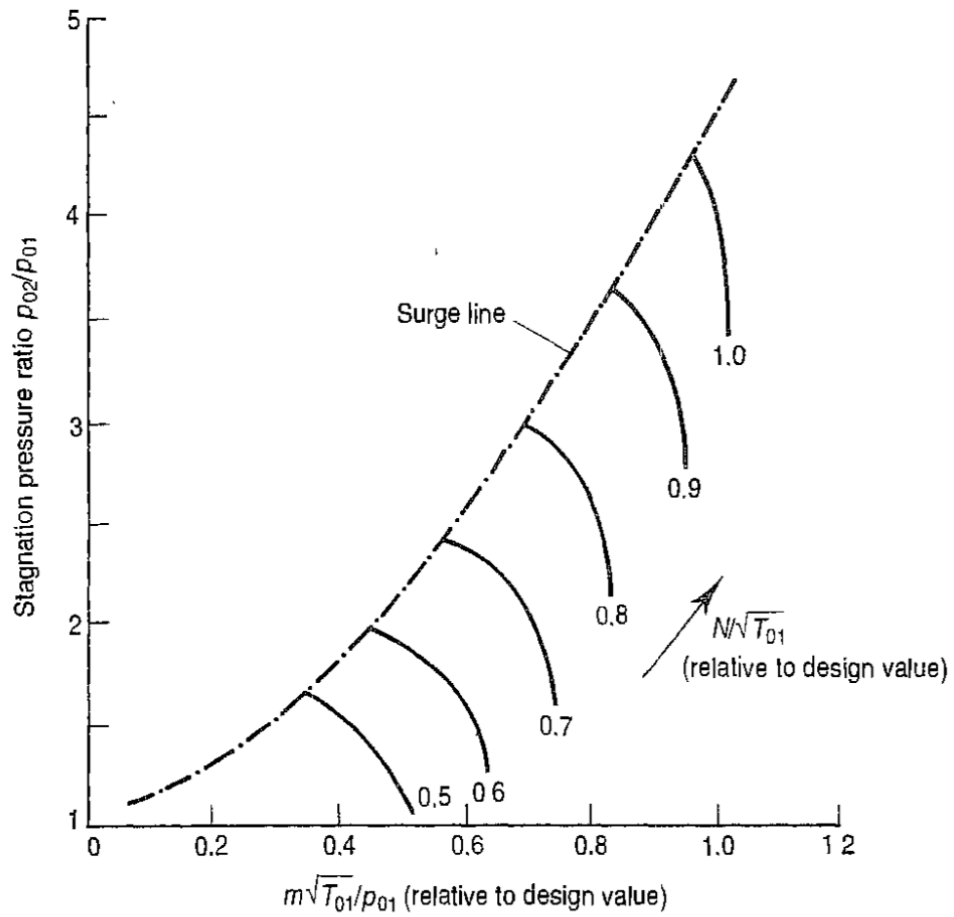


Figure 6.1 Axial compressor characteristics [53]

### 6.1.2. Axial turbine

With the same method as described, a turbine characteristic chart can be constructed with non-dimensional parameters. In Figure 6.2 the turbine characteristic curves are illustrated in two diagrams. In the upper diagram the speed lines are plotted against pressure ratio and turbine efficiency. In the lower diagram the speed lines are plotted against the pressure ratio and the mass flow. It can be observed that the turbine reaches choked condition rather quickly, and that turbine efficiency is constant for a large part of the speed lines. In a gas turbine it is common to run the turbine section with a speed line value 0.8 – 1.0 and at choked conditions [53]. The explanation for the small variation in efficiency is the blades ability to operate over a range of incidence angles without much increase in the loss coefficient [53].

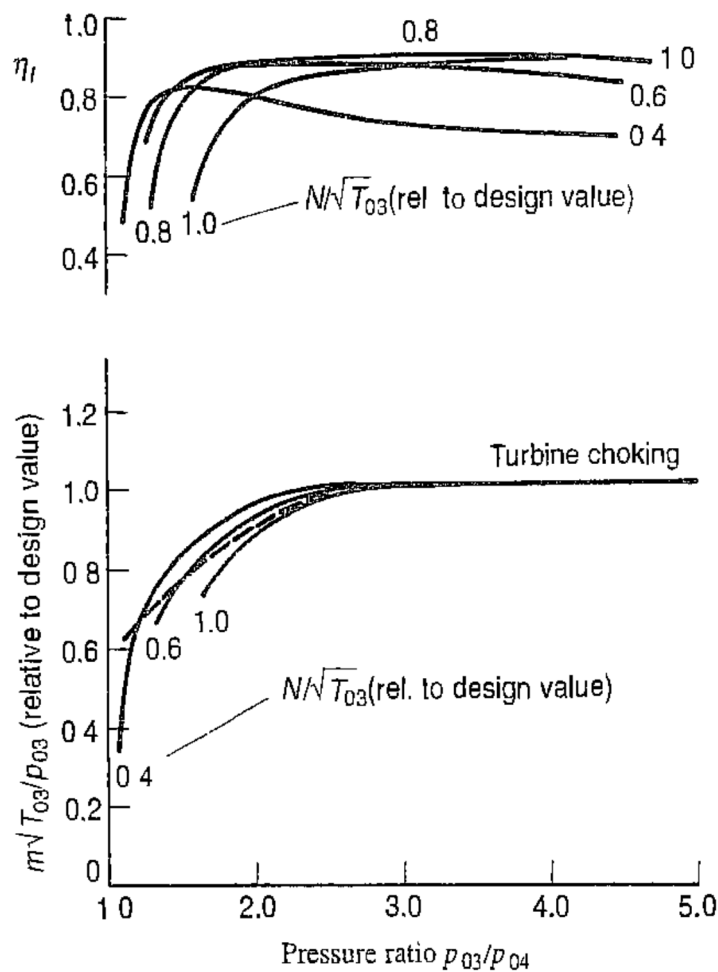


Figure 6.2 Characteristic curve for an axial turbine [53]

From the lower image in Figure 6.2 one can observe a maximum value for the mass flow  $m\sqrt{T_{03}}/p_{03}$  is reached due to choking. Axial turbines are normally operated in choked conditions and the most common place for choking is in the nozzle throat [53]. As with the compressor, this means that mass flux will not increase with a higher-pressure ratio. In

equation (6.2) the choked nozzle equation is presented for two different operating conditions [47]. This equation is commonly used for calculations to determine the inlet pressure of the turbine to find the compressor pressure ratio.

$$\frac{p_3}{p_{3,design}} = \frac{\dot{m}_3}{\dot{m}_{3,design}} \sqrt{\frac{T_3}{T_{3,design}} \frac{MW_{3,design}}{MW_3}} \quad (6.2)$$

### 6.1.3. Combustor chamber

One major control strategy to control gas turbine power output is through fuel input. Operational load determines how many reaction zones that are active with corresponding mass flow of fuel input. Figure 6.3 illustrates the combustion chamber for the GE LM2500+G4. The system has Dry Low Emission (DLE) combustion which aims for low NO<sub>x</sub> emission by controlling the flame temperature without the addition of water in the combustion chamber [53, 57]. As seen in Figure 6.4 regulating premixing zones (A-B-C) in the combustion chamber controls the flame temperature within a narrow temperature window for all power outputs. Maintaining a stable exhaust temperature is very beneficial for operation of the steam bottoming cycle.

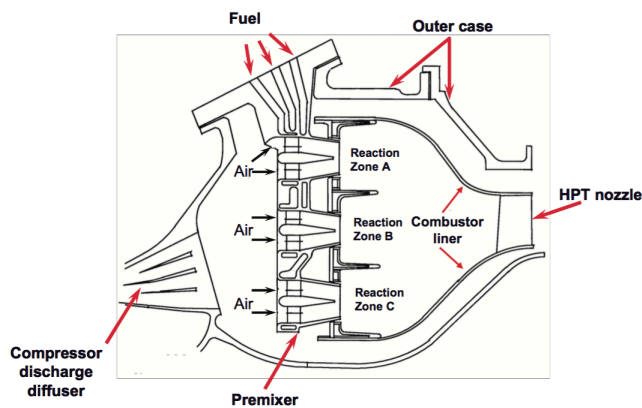


Figure 6.3 GE LM2500+G4 combustion chamber [47, 57]

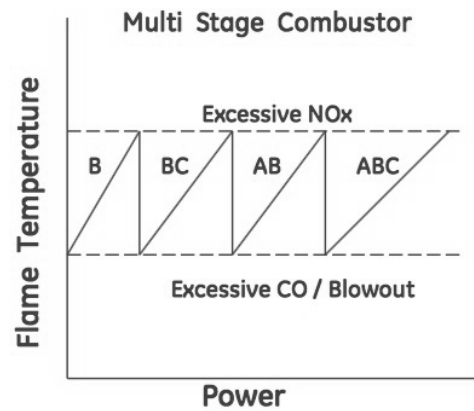
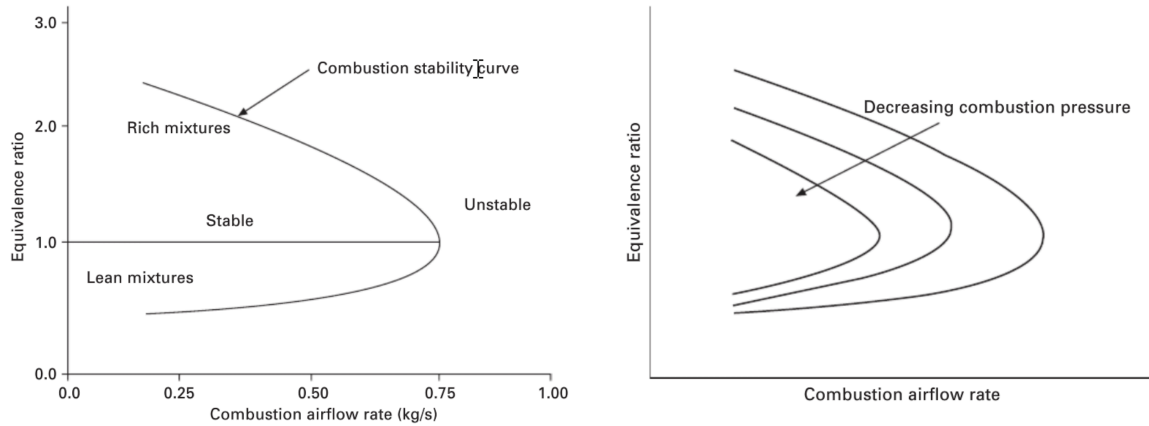


Figure 6.4 GE LM2500+G4 DLE operation principles [57]

All combustion chamber have an air-fuel ratio limit for when combustion becomes unstable. Figure 6.5 shows an example of how a stability curve will look for a combustion chamber. If the airflow rate becomes too high, the flame becomes unstable and could potentially blow out. If the air-fuel ratio is too low, the increased inlet temperature for the turbine could potentially cause sever damage to the blades. It is common for control systems to have a upper limit in change of fuel flow to avoid blow out or high transient temperatures in the turbine [53]. The right hand graphs illustrates how the area for the combustion stability curve decreases when combustion pressure is lowered from design point. This shows how a sub-optimal operation of a compressor will influence and limit the operational combustion area, resulting in sub-

optimal expansion and a lower thermal efficiency. Operating at different loads directly influence the exhaust temperature and exhaust mass flow. The flame temperature varies within the regulations for maximum NO<sub>x</sub> and minimum CO emissions [58] .



**Figure 6.5 Combustion stability curve and the effect of combustion pressure [59]**

## 6.2. Steam turbine

During part-load operation the waste heat from the gas turbine exhaust will differ. To be able to match this variation in heat, most steam turbines in bottoming cycles are operated with sliding pressure mode [51], see Figure 6.6. Sliding pressure mode was used in all Epsilon Professional simulations for the steam turbine component. This operation mode allows the live steam pressure to gradually decrease down to approximately 50 % pressure level at full ST load. A control valve fixes the pressure level for operation below 50 %.

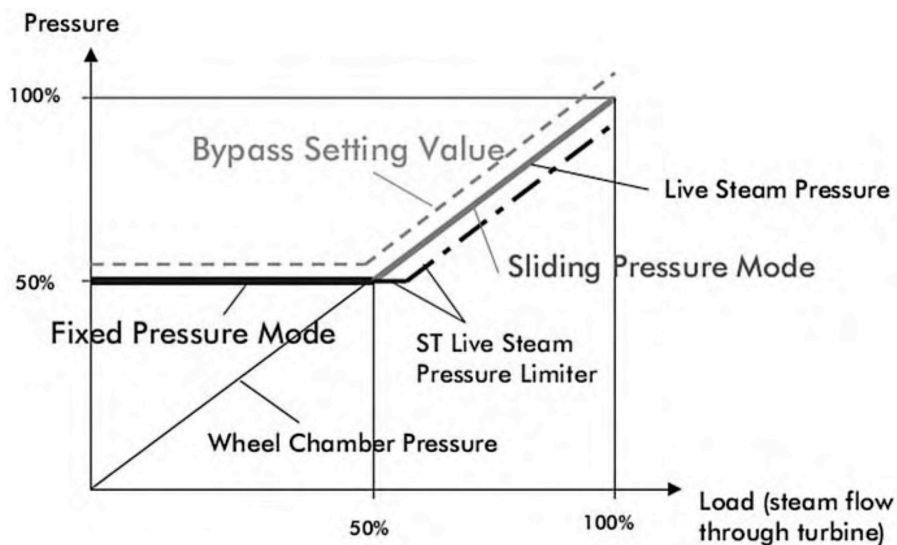


**Figure 6.6 Sliding pressure operation diagram [51]**



Steam turbines can also be operated at a constant inlet pressure using throttle control. A control valve is then fitted before the turbine inlet and controls inlet conditions for the steam. This method of operation was not chosen for the simulations.

To determine the swallowing capacity for the turbine in off-design operation, Stodolas Law is commonly used [47]. Stodolas Law is given by equation (6.3) for a turbine stage with no extraction points [51]. The suffix 0 represents the design point for the ST. The  $(n_v + 1) / n_v$  term is the relation for polytropic pressure-volume exponent from section 3.3. All steam turbines in the simulation were configured to use inlet pressure correction by Stodolas law in process calculations.

$$\frac{\dot{m}}{\dot{m}_0} = \frac{P_{inlet}}{P_{outlet}} \sqrt{\frac{P_{inlet,0} v_{inlet,0}}{P_{inlet} v_{inlet}}} \sqrt{\frac{1 - \left[ \frac{P_{outlet}}{P_{inlet}} \right]^{\frac{n_v+1}{n_v}}}{1 - \left[ \frac{P_{outlet,0}}{P_{inlet,0}} \right]^{\frac{n_v+1}{n_v}}}} \quad (6.3)$$

During part-load operation the efficiency of the turbine does not change a lot. The velocity triangles through the turbine are experience only small variation, and consequently the volume flow are kept within a limited range at part-load operation [47]. In Epsilon Professional the steam turbine efficiency characteristic is adjusted with variation in volume flow, see Figure 6.7.

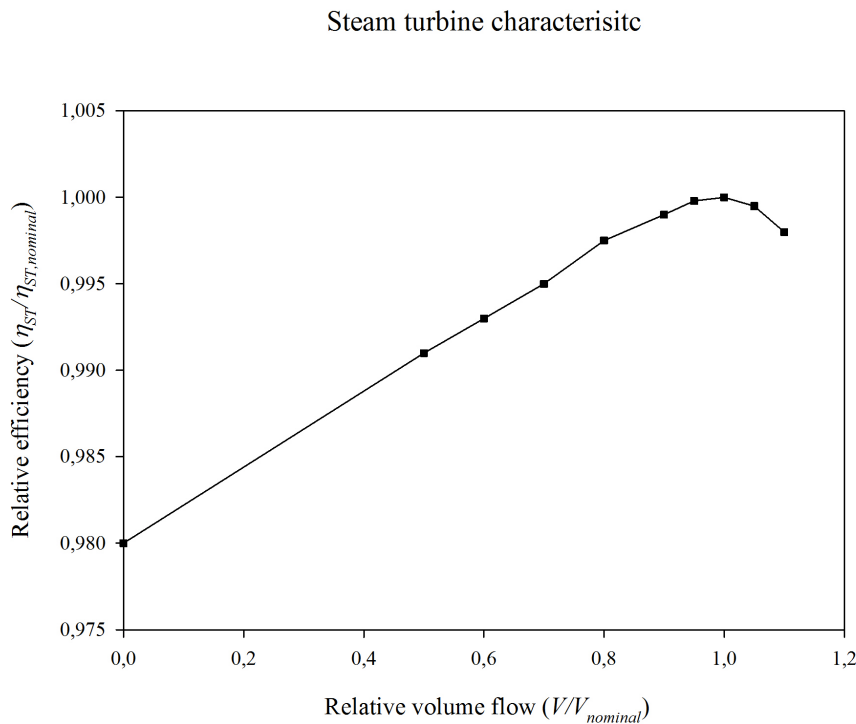


**Figure 6.7 ST efficiency correction characteristic from Epsilon Professional**

### 6.3. Heat recovery steam generator

There exist some operation conditions that should be evaluated when performing off-design simulations on HRSGs. Firstly, it is important to maintain a suitable mass flow in order to maintain sufficient driving forces through the heat exchanger. At low GT load operation, mass flow of feedwater must be reduced to keep a sufficient level of superheating in the outgoing steam. In real plants the steam outlet temperature is controlled by a feedback loop, where the feedwater regulating valve is controlled by the steam temperature [50]. The second point is to maintain a stack temperature above the sulphur dew point of the exhaust. If the exhaust temperature were to fall below the sulphur dew point, corrosion on metal surfaces and pipes might follow [47]. This is not normally a problem for gas fired GT, but for start-up and backup system where heavier fuels are utilized, this must be addressed. The final point is to keep the inlet feedwater temperature above water dew point temperature in the exhaust. For exhaust gases in from gas turbines this value is approximate 40 °C [47]. A low feedwater inlet temperature could cause the water in the exhaust to condensate close to the surface of the piping. Condensed water could form droplets around the piping, containing acid components that would corrode the surface. As a rule of thumb, the industry uses feedwater temperatures above 60 °C, meaning that preheating of water from the feedwater tank might be necessary for a real system [47]. Another solution to avoid the problem is to use a high quality non-corrosive alloy for the lower part of the HRSG.

### 6.4. Pump

Figure 6.8 illustrates a typical characteristic curve for centrifugal pump performance for a given shaft rotational speed. The independent variable is the flow rate,  $Q^*$  and the dependent is the head delivered  $H$ . In this figure the efficiency curve and break horsepower are included to emphasize where the best efficiency point lies on the head curve. Pump with a fairly flat efficiency curve is desirable in order to maintain good operation over large flow [45]. Note that operation for very low flow rates is unstable, and that cavitation problems might occur for very large flow rates.

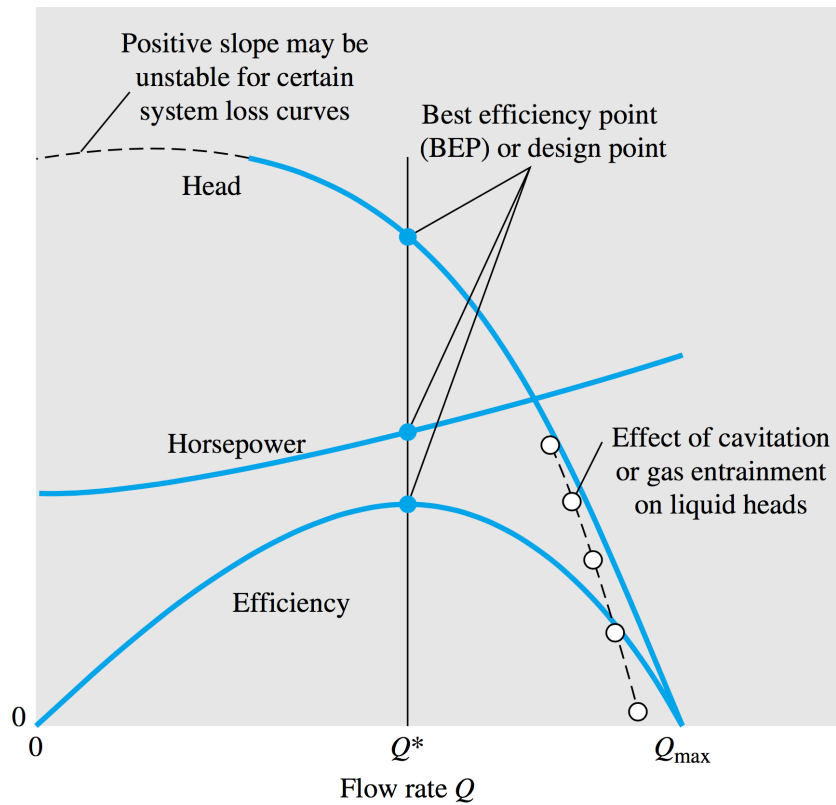


**Figure 6.8 Characteristic pump curve [45]**

In this chapter some off-design operation theory for the major parts in a combined cycle system has been presented. It is important to understand the thermodynamics behind this theory in order to interpret results accurately. In the next chapter simulation methodology and assumptions for the boundary conditions and cycles are presented.



## 7. Simulation methodology

This chapter describes the framework for the simulations. Firstly, some features in the software Ebsilon Professional will be described and an overview of the different simulation cases will be given. The subsequent sections will contain assumptions for the different boundary conditions and components in the cycles. Assumptions in section 7.2 are valid for all simulation, if not else specified in the individual cycle model description. In section 7.3, validation on the simulation method are presented. By comparing simulation results with real plant data and other simulation work, the method was validated. Section 7.4 and 7.5 presents the two cases simulated in this thesis with the chosen assumptions and parameters.

### 7.1. Ebsilon Professional V-10.6

This section will attempt to provide an overview of the calculation methodology and the most used features in the software. For additional description on specific topics surrounding the software, the reader may consult the “EBSILON Professional Online Help” localized inside the software.

#### Model options

Simulations were performed in the process simulations software Ebsilon Professional version 10 patch 6 [9]. In the software the simulations were carried out at steady state condition through calculative iterations with values from extensive fluid and material libraries. The following standards were used in the simulations specified in the model options window:

- Steam Table IAPWS-97
- Saltwater Lib-SeaWa (2009)
- Real gas formulation of Stodolas Law
- Real gas formulation for gases (N<sub>2</sub>, AR, O<sub>2</sub>, CO<sub>2</sub>, SO<sub>2</sub>, H<sub>2</sub>O), for other gases the ideal gas approach was used (ideal Cp value)

#### Graphical window

Cycles were designed in the graphical window with equipment components, measure points, boundary conditions and input values. The controller component was also used to vary parameters for a desired result, such as process heat extracted etc.

#### Optimization

For optimization of parameters the optimization module EbsOptimize was occasionally used. For simple optimization this module can be set to maximize a value dependent on a range of input values for one or several parameters. The module is based on an evolutionary (genetic) algorithm with a constant population size [9]. During design and construction of sub-profiles

the optimization function was used to optimize the mass flow at different GT loads. It was attempted to do optimization with more than one variable. However, during these optimizations attempts the software froze and a forced shutdown had to be carried out. This might have been due to user error, but not much time was spent to address the problem.

### **Ebsscript**

To ease the calculation procedure, automatic scripts were made to do calculation over a range of input values. Scripts were programmed in the Ebsscript editor window, and the software uses the programming language PASCAL along with some special customized functions. One of these functions used was the “ebsVar” variable. This data type enables direct connection between the scripts and the components in the graphical window. It was used to obtain specific values or model variables. The scripts were run through the Ebsscript editor window and results were programmed to export into Microsoft Excel.

### **Profiles**

For off-design simulations, the calculations are conducted in sub-profiles to the design profile. The sub-profiles contain the nominal values for the different component, and results are adjusted based on off-design specification for the given component. Typically this was characteristic curves and correction factors already implemented in the software. None of these were adjusted in any way. The hierocratic profile system made sure that simulations did not influence the design case. Profiles were made for different GT loads and supply temperature.

### **Calculation**

During calculation the software provided feedback for each step in the Ebsscript editor window. A limitation in this version of the software is the lack of explanation for warnings or errors that occurred when running scripts calculations. Consequently a reproduction of the exact calculation would have to be performed in the graphical window to see if the warnings were fatal to the results. In version 11 of the software, this limitation is fixed.

### **Off-design cases**

Following off-design simulations were carried out for this thesis:

- Four different supply temperatures were investigated for the two cycles
  - 100 [°C]
  - 120 [°C]
  - 150 [°C]
  - 175 [°C]
- Calculation was carried out for each 10 % step for GT load in the range 40 -100 %
- In the extraction steam turbine cycle, process heat was varied from 0 to maximum allowed.

## Sensitivity analysis

The sensitivity analysis was conducted by varying one of the parameters in the cycles, while keeping all other inputs constant. In chapter 8 the chosen parameters for the sensitivity analysis are listed with input value range.

### 7.2. General assumptions

#### 7.2.1. Ambient conditions

The boundary conditions for all the cycles are presented in Table 7.1. Their values have been obtained by evaluation the recommendations for power plant modeling assumptions [47] and studies with similar simulations towards offshore power generation [52, 58]. The values are considered to be representative for Norwegian offshore conditions.

**Table 7.1 Boundary Conditions Assumptions**

<b>Boundary Conditions</b>	
Ambient temperature $T_{amb.}$	[°C] 15
Ambient pressure $P_{amb.}$	[bar] 1.013
Ambient relative humidity	[%] 60
Cooling system	[-] Direct water system
Cooling medium	[-] Seawater
Cooling inlet temperature $T_{cw,in}$	[°C] 10
Max cooling temperature difference $\Delta T_{cw}$	[°C] 10
Cooling water pressure $P_{cw,in}$	[bar] 2

### 7.2.2. Gas turbine

The gas turbine GE LM2500+G4 was chosen as a topping cycle for the simulations. Operational values for the gas turbine were obtained from the “Gas Turbine Library” developed by VTU Energy [60] for the Epsilon Professional software. The library contains individual gas turbine operation characteristics in accordance with industry standards for gas turbine acceptance, namely ISO2314 and ASME PTC22 [60]. Models were developed in cooperation with the gas turbine manufacturers, which provided real operation data. This also eliminates the need for additional GT validation. Unfortunately the VTU GT library does not contain or allow extraction of the characteristic lines discussed in section 6.1.

To maintain operational flexibility offshore, gas turbines are seldom operated at maximum load [48]. A gas turbine operating load of 70 % was chosen for the design cases to allow flexibility in power generation. In the off-design simulations the variation in GT exhaust temperature affects the bottoming cycle performance. Graphs are provided in the appendices for exhaust temperature, power output and mass flow at different loads, see Figure A.1-A.3. The outlet pressure was set to 1.045 bar, in order to cover up for subsequent pressure loss in the OTSG. The exiting exhaust still maintained a stack pressure above ambient pressure. For simplicity the fuel input was selected to be pure methane. It is common for offshore installations to use some of the export gas as fuel, and the composition might vary depending on topside processing. The chosen parameters and design conditions for the GE LM2500+G4 are summarized in Table 7.2.

**Table 7.2 GE LM2500 +G4 Parameters**

<b>Gas Turbine</b>		
Model Type	[-]	GE LM2500 +G4
GT fuel	[-]	Methane
Lower Heating Value	[kJ/kg]	50047
GT inlet pressure drop $\Delta P_{GT,inlet}$	[bar]	0.010
GT outlet pressure $\Delta P_{GT,ex}$	[bar]	1.045
Design point load	[%]	70
GT exhaust mass flow $\dot{m}_{GT,ex}$	[kg/s]	78.8
GT exhaust temperature $T_{GT,ex}$	[°C]	532
Power output design point	[MW]	22.5



### 7.2.3. Heat recovery steam generator

By the discussion in section 5.3, a Once Through Steam Generator was chosen to be the most suitable option for the simulations. Epsilon Professional V-10.6 does not include a specific component for such a type of heat exchanger, but an attempt was made to reconfigure other components. In the models three components (number 71) were specified to act as an economizer, evaporator and a superheater. Together they represented the OTSG. Although this may seem like a more traditional HRSG, the off-design configurations of these components allow the vaporization point to float within the three components. Thus, allowing it to operate similarly to an OTSG. At design point the economizer was configured to deliver saturated water at the outlet, the evaporator was configured to deliver saturated steam on the hot side, and the superheater was configured to have an upper terminal difference of 30 K. These configurations corresponds to the following specification commands (FSPEC) in Epsilon Professional:

- 16: Economizer given: T1, H2=H(saturated water), T3 or T4
- 28: Evaporator M2(saturated steam)
- 32: Superheater given. DTN:upper temperature difference

The upper terminal difference of 30 K was chosen to provide sufficient thermal driving forces. Nord and Bolland [52] argued that a pinch point temperature difference of 25 K is necessary so that to size and weight are limited [52]. This argument is supported by Saravanomuttoo [53] who states that for an onshore power plant, minimum pinch point temperature difference of 20 K is necessary for the HRSG to be economically feasible. The 25 K then appears as a satisfactory assumption. The mass flow through the HRSG was optimized to provide a 25 K pinch point at design case. Pressure loss through the HRSG were chosen by the recommendations from Bolland [47], to be 25 mbar. Table 7.3 the assumptions and specifications are summarized.

**Table 7.3 OTSG simulation parameters**

<b>OTSG</b>			
Pressure drop exhaust	$\Delta P_{OTSG,ex}$	[bar]	0.04
Pressure drop fluid	$\Delta P_{OTSG,fluid}$	[bar]	0.75
Min. pinch point	$\Delta T_{PP}$	[°C]	25
Upper terminal difference		[°C]	30

#### 7.2.4. Steam turbine

Component 6 (steam turbine) were chosen to act as the steam turbine in the simulations. In Epsilon Professional the component has adjustable characteristic lines already implemented. These lines can be adjusted to better suit a real steam turbine. However, since no such data was available the characteristic from the software was used. The characteristic line corrects the efficiency of the turbine based on relative deviation from nominal volume flow. All simulations happened within the predefined area of operation. Live steam pressure was set to be 25 bar, corresponding to the recommendation of an optimization study for offshore steam bottoming cycles [55]. This value represented a good compromise between power output and operational flexibility of the system. During off-design simulation the steam turbine used the specification:

- FSPEC: P1 calculated by PINSET (by Stodolas equation)

By this specification the inlet pressure is calculated Stodolas equation, discussed in section 6.2, and the nominal values in from design point. Minimum allowed steam quality through the turbine was chosen to be 0.90. Isentropic efficiencies were chosen based on the recommendation from Bolland [47]. Table 7.4 summarizes the chosen parameters for the simulations.

**Table 7.4 Steam Turbine simulation parameters**

Live steam pressure $P_{HP,steam}$	[bar]	25
Minimum steam quality $x_{steam}$	[-]	0.90
Turbine isentropic efficiency first stage $\eta_{s,ST,HP}$	[-]	0.92
Turbine isentropic efficiency second stage $\eta_{s,ST,LP}$	[-]	0.88

### 7.2.5. Additional components

The condenser component is only valid for the extraction steam turbine cycle. It was configured to maintain a constant mass flow of cooling water during off-design simulation. By this, the variation in outlet pressure of the second turbine stage is dependent on the cooling water temperature. Pressure drop on the cooling water was set to be 0.1 bar. Further description on the condenser is given in the extraction steam turbine model description in section 7.4. The generator efficiency, and the isentropic pump efficiency, were set by the recommendations from Bolland [47]. Table 7.5 summarizes the parameters for pumps, generator, motor and condenser.

Process heat was extracted from the steam through two components (number 35) in series. The first component was specified to only remove the available superheat in the steam. For a real plant this would preferably not be the way to do desuperheating. Water could be sprayed into the steam flow through injectors in the pipe to reduce the temperature. This would exploit the available superheat into useful steam for process heating. This procedure was not carried out in the process models, as no injection component suitable for this operation was found in the Epsilon component library. By the definition in equation (3.46) usable process heat was defined as the latent heat of steam. This was extracted in the second heat consumer component configured to deliver saturated water at the outlet.

**Table 7.5 Additional machinery simulation parameters**

<b>Pumps</b>		
Isentropic efficiency $\eta_{s,pump}$	[-]	0.7
<b>Efficiencies</b>		
Generator efficiency $\eta_{gen}$	[-]	0.985
Mechanical efficiency $\eta_{mech}$	[-]	0.996
<b>Condenser</b>		
Cooling-water pressure drop	[bar]	0.1

### 7.3. Validation

As cogenerative facilities are highly site specific it was determined to perform validation on an existing plant. The facility chosen for validation was the Oseberg D cogenerative offshore facility. Layout of the built cycle can be seen in Figure 7.1. Reference values were used from the paper “Energy optimization on Offshore Installations with emphasis on Offshore Combined Cycle plants” by Kloster [12], and provided validation work on the same facility by Nord for the paper “Design and off-design simulations of combined cycles for offshore oil and gas installations”. In the paper Nord and Bolland [58] states that validation result was within 0.1 % error of the real data provided, thus a satisfactory basis for comparison and validation.

In Table 7.6 the power output from the validation are presented along with references. The results correspond to reference values with accuracy above 99%. It is then concluded that the systematic method for simulation is valid within a reasonable error limit. Heat transfer diagram (Q-T) for the HRSG and a temperature-entropy (T-s) process diagram are enclosed in the appendices, see Figure A.4 and Figure A.5. However, there are uncertainties as no real life data from the system were available, and some simplifications were done compared to the previous validation work. Noticeable errors or simplifications are:

- Pump work is lower than reference case
- Feedwater tank is neglected for simplicity
- The cycle is simulated as a closed loop with no mass flows exiting or entering the bottoming cycle

**Table 7.6 Validation results**

<b>Design point (Max power, No process heat)</b>		
P. Kloster paper [12]	[KW]	15 800
Lars O. Nord simulation	[KW]	15 800
Ebsilon Professional V-10-6 simulation	[KW]	15 811

As for the Gas Turbine used in this thesis, no validation was carried out. As stated in section 7.2.2 Ebsilon Professional uses the Gas Turbine Library developed by VTU Energy, and it was assumed to be sufficient validation.

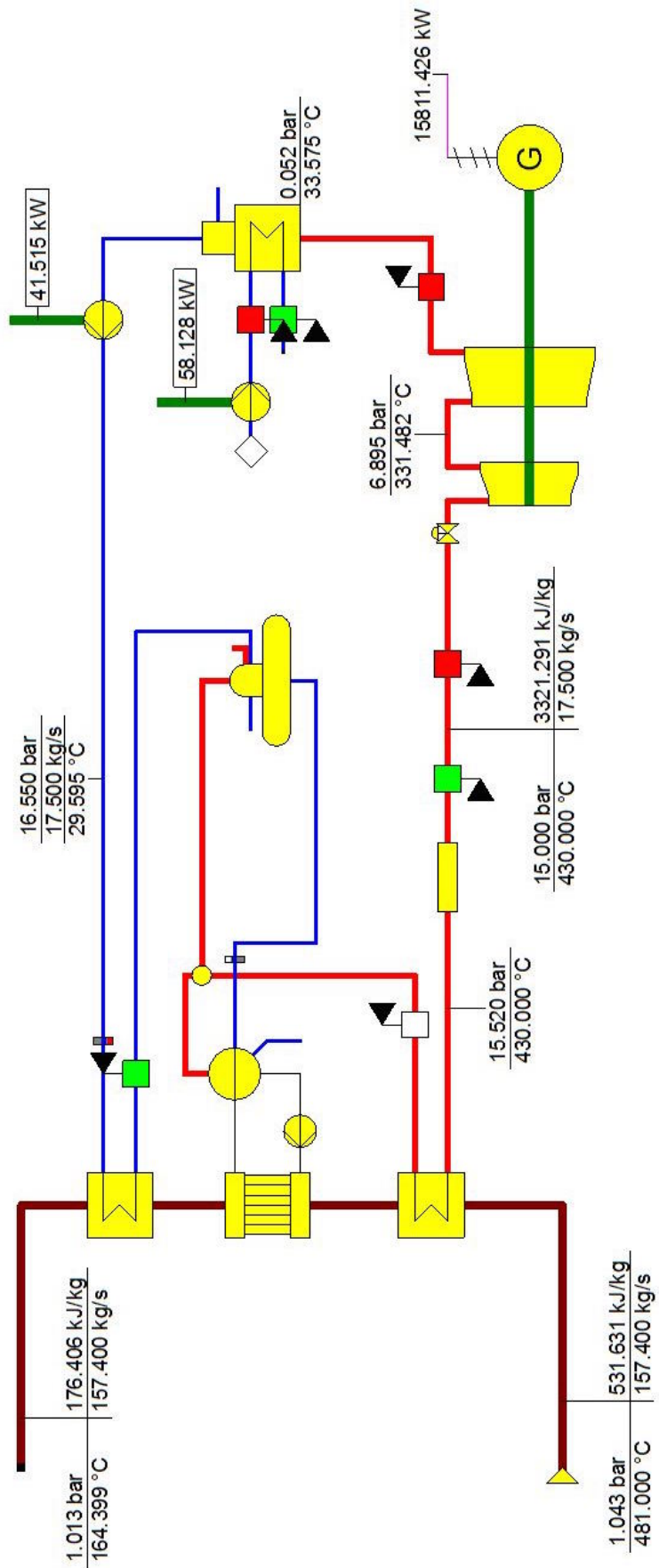


Figure 7.1 Oseberg D validation simulation

#### 7.4. Extraction steam turbine model description

In Figure 7.2 the Extraction steam turbine cycle is shown at design point from the Epsilon Professional graphical window. The extraction steam turbine is built up by two steam turbines (component 6) working in series, where steam can be extracted from the piping between the two. Epsilon Professional does not have a turbine component that allows for extraction between inlet and outlet pressure of the component. The illustrated design was chosen after studying examples and consulting recommendations in the help guide. Live steam pressure was set to 25 bar and steam was extracted at 10 bar between the stages. This introduced a loss when extracting steam at pressure levels far below this value. However, this was considered to be the best approach for steam extraction. Process heat at design point was set to be 5.0 MW. This was set based on an evaluation of the maximum allowed extraction in the system, which turned out to be 10.5 MW. This maximum value was due to upper limit of deviation in mass flow were reached (further discussed in section 8.1.2).

Simulations were carried out in the different sub-profiles categorized by the GT load. Since the cycle does not include the water treatment facility or a storage tank, the control of mass flow had to be optimized manually before simulations. The LP pump and motor was set to operate in local off-design, corresponding to maximum mass flow at 100 % GT load. This was done to stay within the pump characteristic during simulations. Given the 10 °C allowed increase in cooling water through the condenser, a 20 °C upper temperature difference between the condensing steam and cooling water was chosen. This would provide sufficient driving force and reduce the size of the condenser compared to an onshore solution. This resulted in condensation at 40 °C, corresponding to a pressure level of 0.07 bar at design. Table 7.7 summarizes the parameters.

**Table 7.7 Extraction steam turbine parameters**

<b>Extraction steam turbine cycle</b>		
Pressure 1 <sup>st</sup> ST $P_{HP,Steam}$	[bar]	25
Pressure 2 <sup>nd</sup> ST $P_{LP,Steam}$	[bar]	10
Mass flow $\dot{m}_{steam}$	[kg/s]	9.86
Condensing pressure $P_{cond.}$	[bar]	0.07
Extracted Process Heat $\dot{Q}_{vap}$	[MW]	5.0

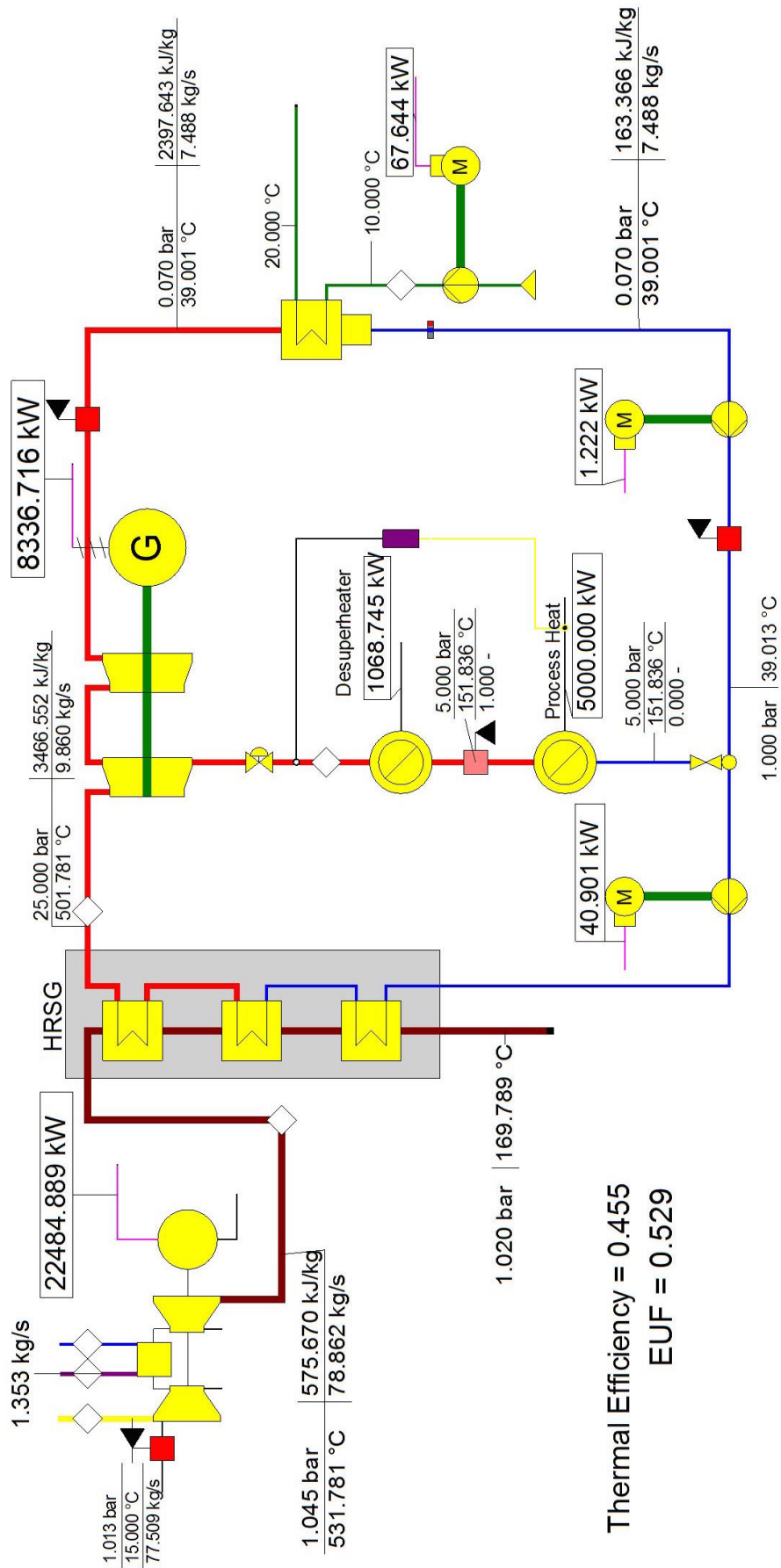


Figure 7.2 Extraction steam turbine cycle – Epsilon Professional model

## 7.5. Backpressure steam turbine model description

In Figure 7.3 the backpressure steam turbine cycle is shown at design point from Epsilon Professional graphical window. The steam turbine was modeled with one steam turbine component and a backpressure of 2 bar at design point. Exit pressure level was chosen after evaluation of some off-design testing that showed that 2 bar gave an acceptable supply temperature without reducing the electrical power output of the bottoming cycle too much. The reduction in electrical power output of a backpressure level of 5 bar was 30 % compared to the 2 bar case.

All steam from the turbine continues directly to the process heat extraction. The returning saturated water has a temperature of 120 °C, which is unrealistically high if the water is coming from water treatment facility, storage tank and or processes. An aftercooler was installed in the closed cycle design to lower the temperature down to 60 °C. This temperature was set based on the discussion in section 6.3. Table 7.8 summarizes the specific set parameters.

**Table 7.8 Backpressure steam turbine cycle parameters**

<b>Backpressure steam turbine cycle</b>		
Backpressure design $P_{BP}$	[bar]	2
Supply temperature $T_s$	[°C]	120
Mass flow $\dot{m}_{steam}$	[kg/s]	9.86
Exit temp after cooler $T_{out,aftercooler}$	[°C]	60



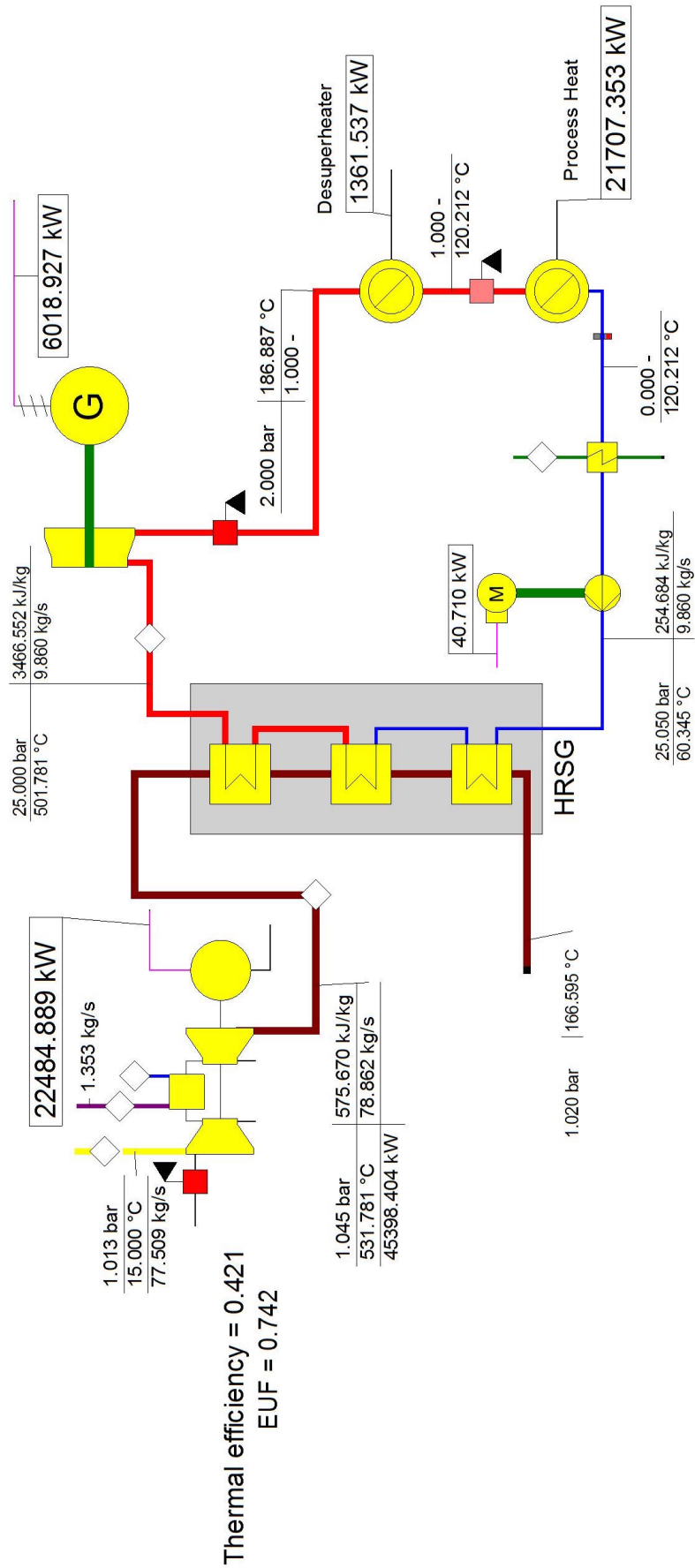


Figure 7.3 Backpressure steam turbine cycle – Epsilon Professional model



# 8. Results and discussion

This chapter contains the results from the simulations carried out in this thesis. It is divided into four parts. In the first part, results from the extraction steam turbine cycle simulations are presented. It includes obtained values from design case, off-design cases and sensitivity analysis. Trends and observations from the results are explained and discussed. In the second part, results from the backpressure steam turbine cycle simulations are presented in a similar manner. The chapter then compares CO<sub>2</sub> emission rates and taxation rates for the cycles to a simple cycle reference model. Finally, observations from the first three parts are compared and discussed in relation to the context presented in chapter 2.

## 8.1. Extraction steam turbine cycle

### 8.1.1. Design case

In Figure 8.1 the energy balance for the results at design is illustrated in a pie chart. The combined cycle obtained a power output of 30.8 MW. This was a 37 % increase in electric output compared to a simple cycle GE LM2500+G4. The steam quality at the turbine exit was calculated to be 0.93, which is above the defined minimum limit. As determined in section 7.4, the process heat output was set to 5.0 MW. Overall amount of energy extracted between the turbine stages was 7.5 MW. A loss due to desuperheating was calculated to 1.1 MW. This is a very large value, but some of this energy could have been retrieved by the modification discussed in section 7.2.5. The last unaccounted 1.4 MW is re-injected in the cycle as saturated water and does not show up as a loss in this energy balance.

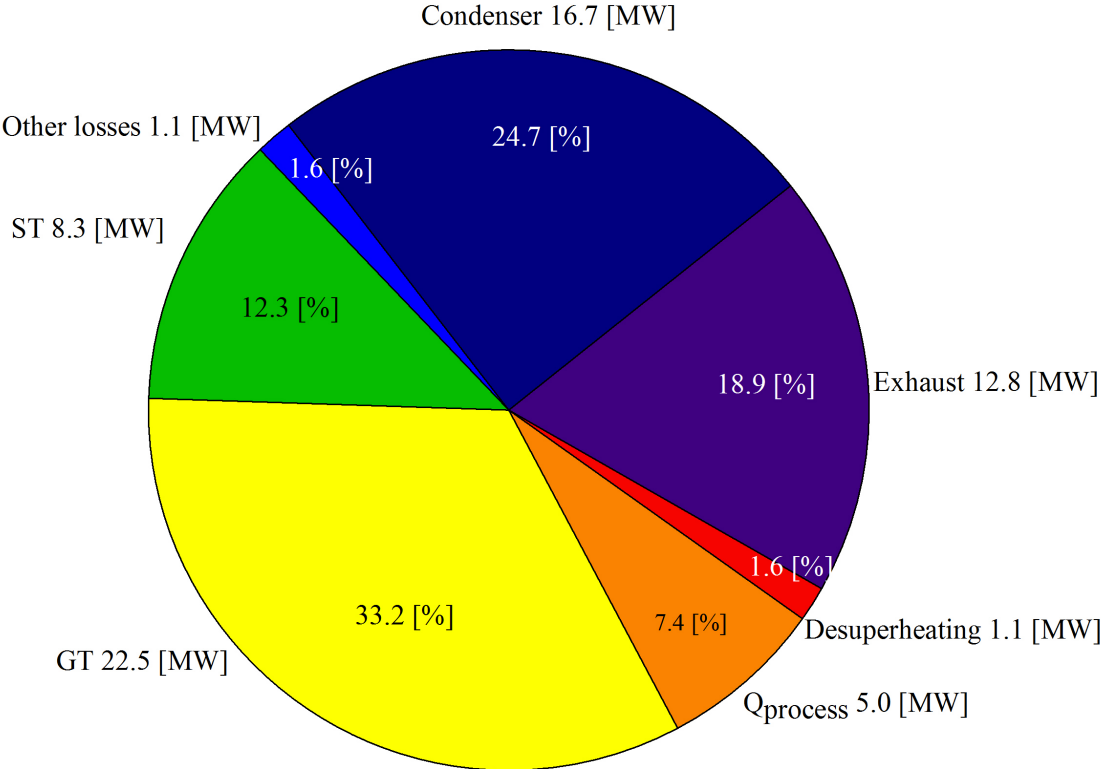


Figure 8.1 Energy balance for the extraction steam turbine cycle at design

Other losses throughout the cycle added up to 1.1 MW. This number also includes all pump work throughout the cycle. Lastly, a substantial amount of heat is rejected in the condenser (16.7 MW) and lost in the exhaust (12.8 MW). Still, the low temperature of this energy makes it difficult to exploit. Overall, this resulted in a net thermal efficiency of 45.5 % at design. This was increase of 12.2 % compared to a simple cycle configuration with the same GT. With the 5 MW of process heat, the *EUF* reached a value of 52.9 %. All results stated above are listed in Table 8.1 below.

In Figure 8.2 and Figure 8.3 the T-Q and T-s diagram is presented for the design case of the bottom cycle. Notice how steam is extracted in the T-S diagram and desuperheating is rejected at a constant pressure line.

**Table 8.1 Results for extraction steam turbine cycle at design case**

<b>Gas Turbine</b>		
Fuel: Methane $\dot{m}_{CH_4}$	[kg/s]	1.35
<i>LHV</i>	[kJ/kg]	50015
Gross Power Output $\dot{W}_{GT}$	[MW]	22.5
Mass flow exhaust $\dot{m}_{exhaust}$	[kg/s]	78.9
Exhaust temperature $T_{exhaust}$	[°C]	532
<b>HRSG</b>		
Efficiency $\eta_{HRSG}$	[%]	69.0
Live Steam temperature $T_{live,steam}$	[°C]	502
Mass flow steam $\dot{m}_{steam}$	[kg]	9.9
Stack temperature $T_{stack}$	[°C]	170
<b>Steam Turbine</b>		
Power Output $\dot{W}_{ST}$	[MW]	8.3
Rankine Cycle efficiency $\eta_{SRC}$	[%]	18.9
Steam quality outlet $x$	[-]	0.93
Process Heat Extraction $\dot{Q}_{process}$	[MW]	5.0
<b>Plant</b>		
Net power output $\dot{W}_{net,plant}$	[MW]	30.7
Thermal efficiency $\eta_{net,plant}$	[%]	45.5
<i>EUF</i>	[%]	52.9

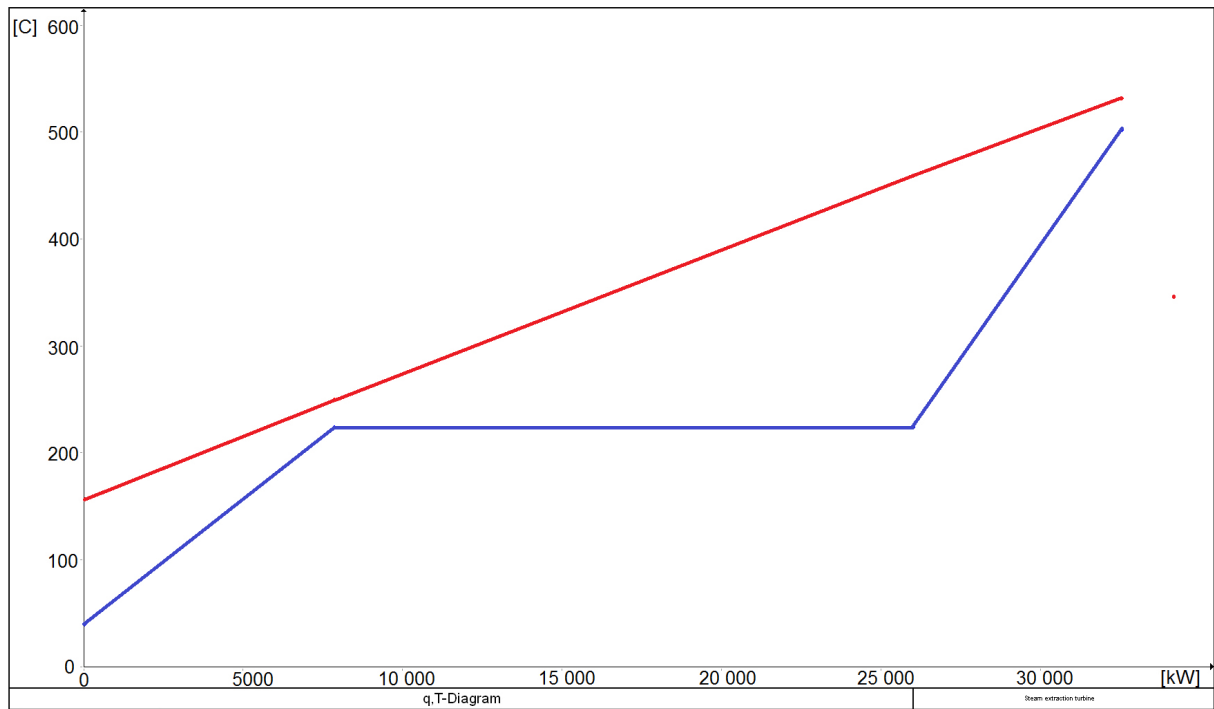


Figure 8.2 T-Q diagram for HRSG in extraction steam turbine cycle

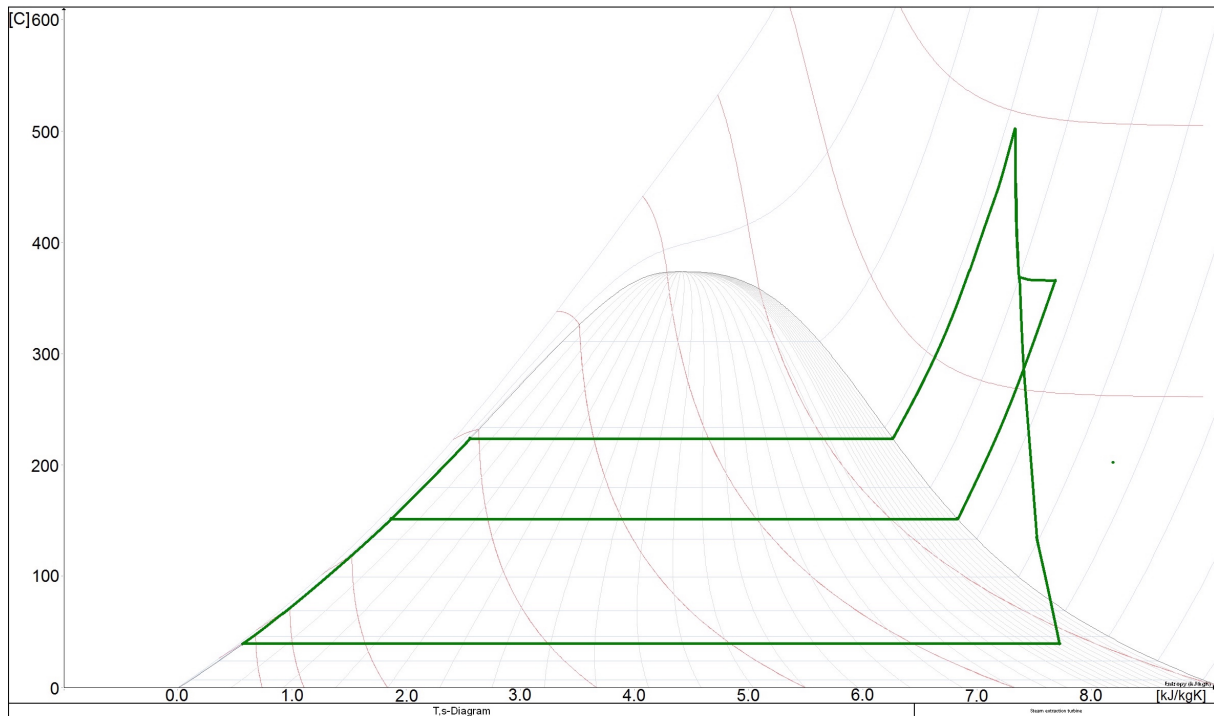
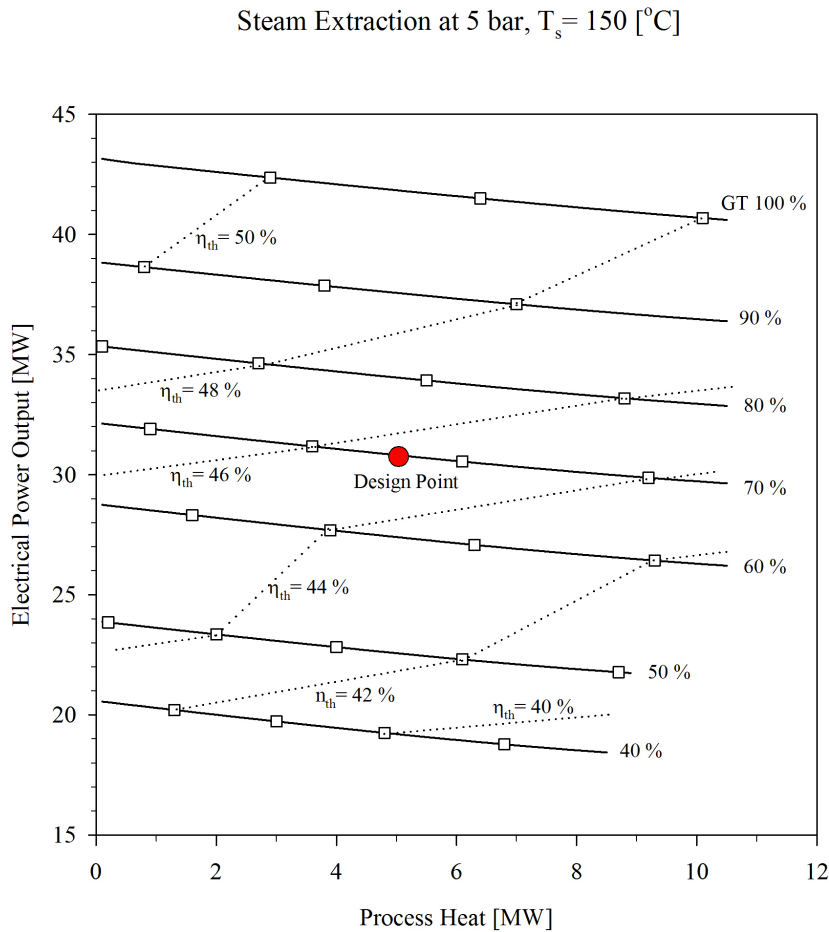


Figure 8.3 T-s diagram for extraction steam turbine cycle

### 8.1.2. Off-design

Off-design simulations were carried out for the supply temperature cases. At each GT, heat was extraction from zero to maximum allowed value. In Figure 8.4 the results for a supply temperature of 150 °C are shown in a diagram illustrating the window of operation. Net electrical power output  $\dot{W}_{net,plant}$  from the CC is plotted against extracted process heat  $\dot{Q}_{process}$ . Each solid line represents a given GT load, equivalent to a constant fuel input. A table of fuel consumption at the different loads is provided in Table A.1 in the appendices. The white squares marks net thermal efficiency points of the plant, and the dotted lines are drawn between the squares to illustrate the trend. The red dot indicates the design case of the plant presented in section 8.1.1. Values for the endpoints on the solid lines are summarized in Table 8.2.



**Figure 8.4 Operational area for extraction of steam at 5 [bar]**

It can be observed from the diagram and table that a maximum process heat extraction of 10.5 MW is achievable. An upper limit occurred when maximum allowed deviation from nominal mass flow in the steam turbine was reached. In Epsilon Professional this limit is set to 46 % deviation. For 50 and 40 % GT load, the extraction of process heat was limited by the pressure level reaching 5 bar in the piping between the turbines. The extraction of steam

decreases the pressure in the continuing flow through the second turbine stage. When the value fell below the minimum required delivery pressure, the control valve was locked into that position and prevented any further extraction.

Between 90-100 % GT load there is a bigger gap between the solid lines, than between the following lines. The reason for the difference was a drop in the gas turbine exhaust temperature appearing at 100-90 % GT load (see Figure A.1 in the appendices). The exhaust temperature drop resulted in a ~1.0 MW difference in steam turbine output. This difference maintained for all the supply temperature cases. From 90-60 % load the exhaust temperature for the gas turbine increased. This caused a very stable power output from the steam turbine for operation within this range, seen by the numbers in Table 8.2. Another characteristic alteration occurred between the lines for 60-50 % GT load. An approximate drop of 1.3 MW in steam turbine output was reported for operation through this area. As seen in Figure A.1 the exhaust temperature experiences a new drop for operation below 60 % GT load. The steam turbine maintained a stable power output through operation at 40–50 % GT load, due to a slight increase in exhaust temperature. Table 8.2 displays the obtained results at the extremities for different GT loads.

**Table 8.2 Off-design results for extraction steam turbine 5 [bar] T<sub>s</sub> 150 [°C]**

GT Load	No extraction		Full Extraction			
	$\dot{W}_{ST}$	$\eta_{net,plant}$	$\dot{W}_{ST}$	$\dot{Q}_{process,heat}$	$\eta_{net,plant}$	<i>EU</i> F
100	10.8	50.9 %	8.3	10.5	47.9 %	60.5 %
90	9.8	50.2 %	7.4	10.5	47.1 %	60.8 %
80	9.6	47.3 %	7.1	10.5	45.5 %	60.3 %
70	9.6	47.3 %	7.2	10.5	43.7 %	59.3 %
60	9.5	45.7 %	7.0	10.5	41.6 %	58.5 %
50	8.0	45.0 %	5.8	8.9	41.0 %	58.0 %
40	7.9	42.7 %	5.8	8.5	38.3 %	56.2 %

The *EU*F for the system was very stable at maximum extraction and only experienced a decrease of 4.3 % over the whole range of GT loads. Due to stable power outputs from the steam bottoming cycle, net thermal efficiency was more affected by the variation in gas turbines thermal efficiency at different loads.

Results from the off-design simulations at different supply temperatures can be found in the appendices section (A.IV). Diagrams for possible window of operation and tabulated results are provided for all the cases, similarly as to Figure 8.4 and Table 8.5. Some of the results are supplemented with a short comment. However, the major trends in the diagrams are identical to what have been described above. In the next section the sensitivity analysis performed on the 150 °C supply temperature case will be presented.

### 8.1.3. Sensitivity analysis

With the purpose of investigating the systems sensitivity to different parameters, a number of inputs were varied over a range of values. Selected parameters are listed in Table 8.3 provided with design case value and selected range. Input deviations are all within a relative change of  $\pm 15\%$  from design case. At some of the parameters the input range was limited. This occurred either by limitations in the software or by reaching an end of sensible input number. Further details are provided under the individual parameter description.

**Table 8.3 Selected input parameters for the sensitivity analysis of the extraction steam turbine cycle.**

<b>Input Parameter</b>	<b>Range</b>	<b>Design</b>
Ambient temp. $T_{amb}$ [°C]	-25 – 40	15
Cooling water temp. $T_{CW}$ [°C]	1 – 35	10
Pinch point temp. $\Delta T_{PinchPoint}$ [°C]	5 - 35	25
Isentropic efficiency 1 <sup>st</sup> Turbine stage $\eta_{ST,HP}$ [-]	0.80 – 0.98	0.92
Isentropic efficiency 2 <sup>nd</sup> turbine stage $\eta_{ST,LP}$ [-]	0.80 – 0.98	0.88
GT exhaust pressure $P_{GT,exhaust}$ [bar]	1.035 – 1.075	1.045

In Figure 8.5 and Figure 8.6 all parameters are displayed in a joint diagrams where thermal efficiency is plotted against the relative change from the design case. Real values of selected inputs are typed next to some chosen plots. The diagrams are quite useful in the way that one can easily tell how sensitive the system is to one parameter compared to another. If the line has a sharp slope the parameter has a large influence on system performance for a small relative change. By this, one can determine which key parameters to provide extra attention in a real system designing procedure. From the figures it was observed that efficiency of the second turbine stage had a larger affect on output than the first stage. Another interesting observation was how change in pinch point temperature difference corresponded almost identically to the changes in cooling water temperature. This might suggest that the penalty by higher cooling water temperature at the site can be recovered by a lower pinch point temperature difference in the HRSG design. It was noticed that ambient temperature had a major affect on the operation of the cycle, and seasoned output variation should be expected for operation on the NCS. On the following pages the individual plots are displayed and discussed.



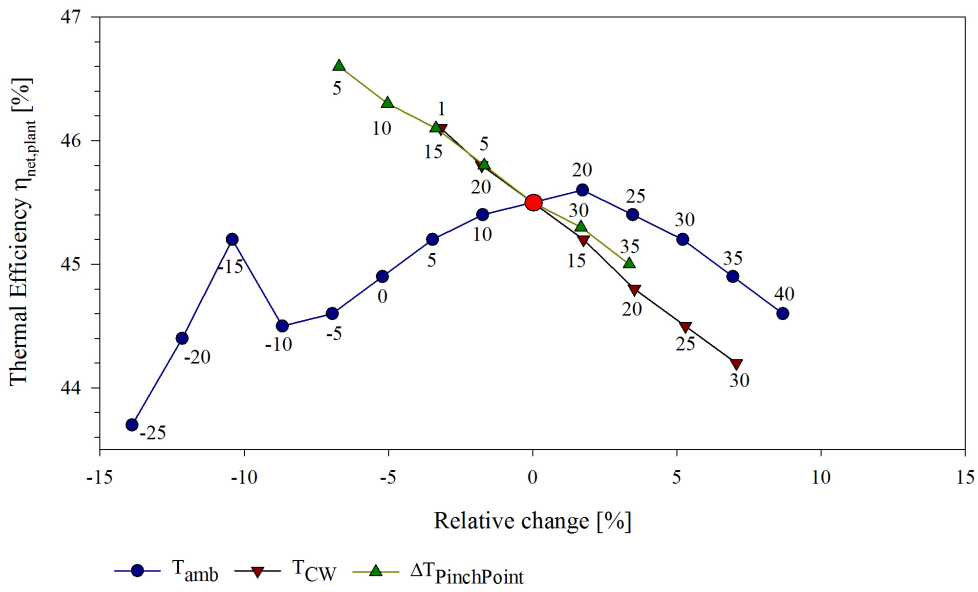


Figure 8.5 Effect of input parameters (1) – Extraction steam turbine cycle

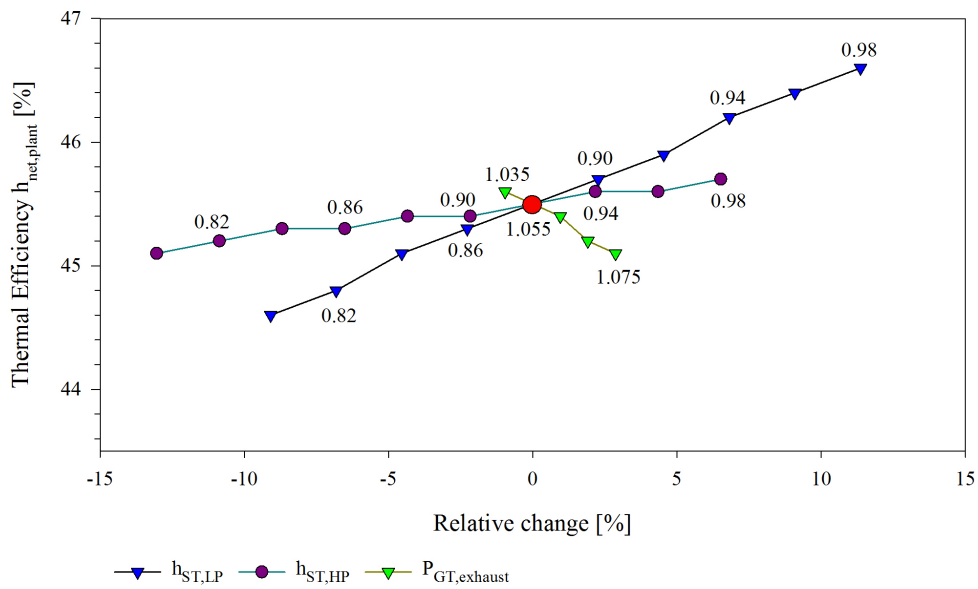
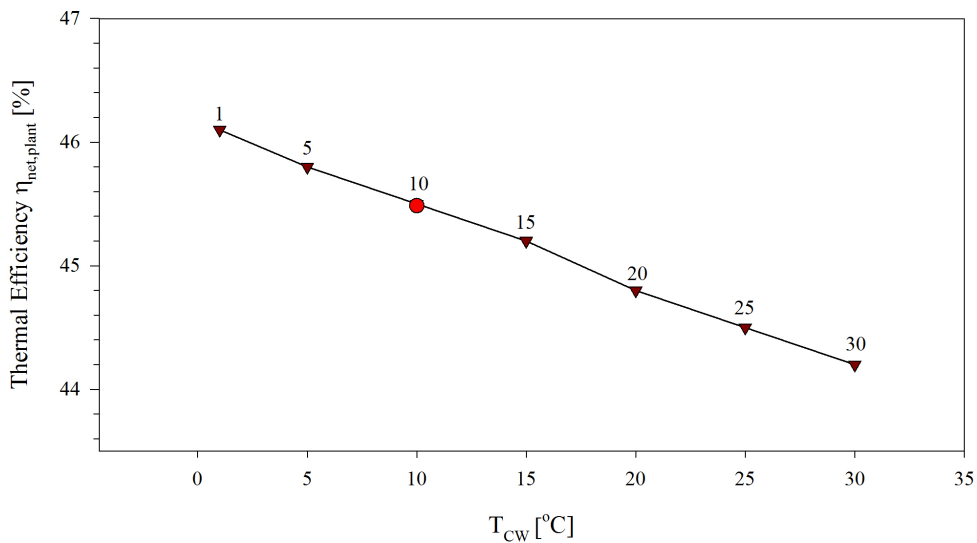


Figure 8.6 Effect of input parameters (2) – Extraction steam turbine cycle

## Cooling water temperature

In the model, inlet cooling water temperature determines the pressure level in the condenser, and consequently the exit pressure of the steam turbine. As stated in section 7.2.5, a 20 °C temperature difference was chosen to ensure sufficient driving forces through the condenser. Figure 8.7 illustrates how a decrease in cooling water temperature increases the net power output. The opposite occurs for increase in temperature and the resulting line is an almost linear function. The cold extremity showed a thermal efficiency increase of 0.6 %, while the upper temperature would decrease the net thermal efficiency by 1.25 %. However, the system is unlikely to experience such large changes in temperature as cooling water is lifted unto the installations from depths where temperatures are more consistent [47].



**Figure 8.7 Sensitivity plot for cooling water temperature – Extraction steam turbine cycle**

## Ambient temperature

Ambient temperature changes directly influences the GT through the VTU-library component. During operation at lower ambient temperatures the GT produces more power, illustrated in Figure A.3 in the appendices. However, the amount of available heat in the exhaust is reduced and this has a great impact on the bottoming cycle. The result is a decline in overall net thermal efficiency for all ambient temperature, except in the range 15-22 °C. In this range the system delivers a rather stable power output, maintain its net thermal efficiency. Results could suggest a necessity to adjust the mass flow of feedwater dependent on the ambient temperature in order to maintain a desired output. At -15 °C there is a quite noticeable increase in thermal efficiency before the value rapidly declines when approaching -20 °C. The explanation for this sudden change is an unexpected large drop in fuel consumption of the GT. In table Table A.2 in the appendices, power outputs and fuel consumption for the surrounding ambient temperatures are listed. Further details to why the GTs fuel consumption experiences such a large drop, was not available in the VTU Gas Turbine library in Epsilon Professional.

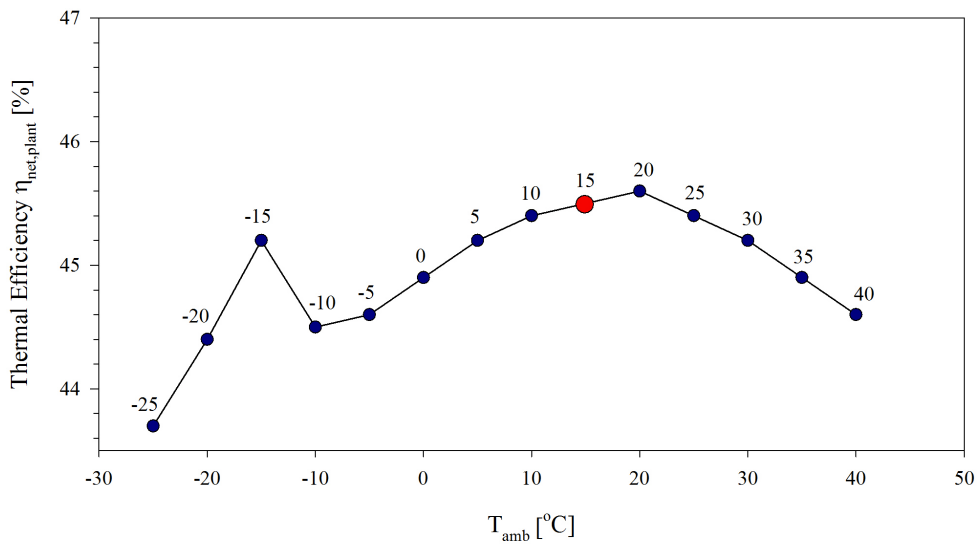


**Figure 8.8 Sensitivity plot for ambient temperature – Extraction steam turbine cycle**

### Pinch point temperature difference

The pinch point temperature difference is a parameter that directly influences the generated amount of steam, and is determined when optimizing the design of the plant. Because of the predefined pinch point temperature difference, the sensitivity analysis can be used to see how the system would have been for a different temperature difference. As seen in Figure 8.9, the relation between net thermal efficiency and pinch point temperature difference is linear. A value of 5 °C would increase the net thermal efficiency with 1.1 %, while a 35 °C would decrease the efficiency by 0.5 %.

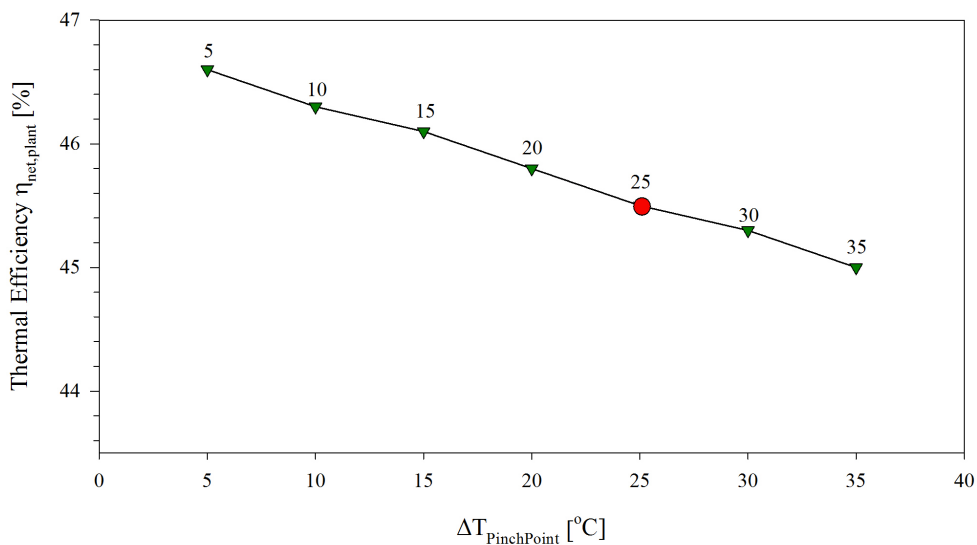


**Figure 8.9 Sensitivity plot for pinch point temperature – Extraction steam turbine cycle**

**Exhaust Pressure GT**

The change in gas turbine exhaust pressure was varied between the minimal value that still maintained above ambient pressure through the stack (1.035 bar), and the maximum allowed value set by the VTU-library (1.080 bar). An error message occurred when exhaust pressure exceeded this value. Changing the exhaust pressure of the GT did not affect the bottoming cycle in any way, thus maintaining stable ST outputs for all inputs. By decreasing the exhaust pressure, the net thermal efficiency was raised by 0.1 %. A pressure increase of 0.030 bar reduced the net thermal efficiency with 0.4 %. These numbers suggest that no necessary improvements should be made from current design case. It could have been interesting to see the reduction in net thermal efficiency at higher exhaust pressure, but the VTU library component stopped that analysis.

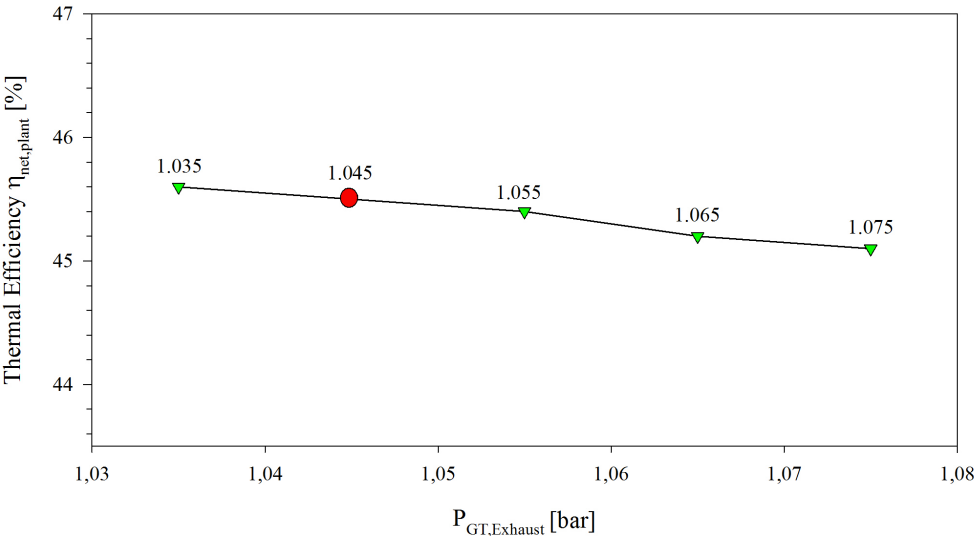


**Figure 8.10 Sensitivity plot for GT exhaust pressure – Extraction steam turbine cycle**

**Isentropic efficiency of turbines stages**

In Figure 8.11 and Figure 8.12 the changes in isentropic efficiency have been plotted for the two turbine stages. It was observed by the purple plots in Figure 8.11, that net thermal efficiency is within 1.0 % difference for all efficiency inputs in the first turbine stage. Interestingly, plots for the second stage showed a larger change in the net thermal efficiency over the input values. The difference between the extremities was 2.2 %. This suggests focus on the second turbine stage is important as much of the energy extracted occurs in the related pressure levels.

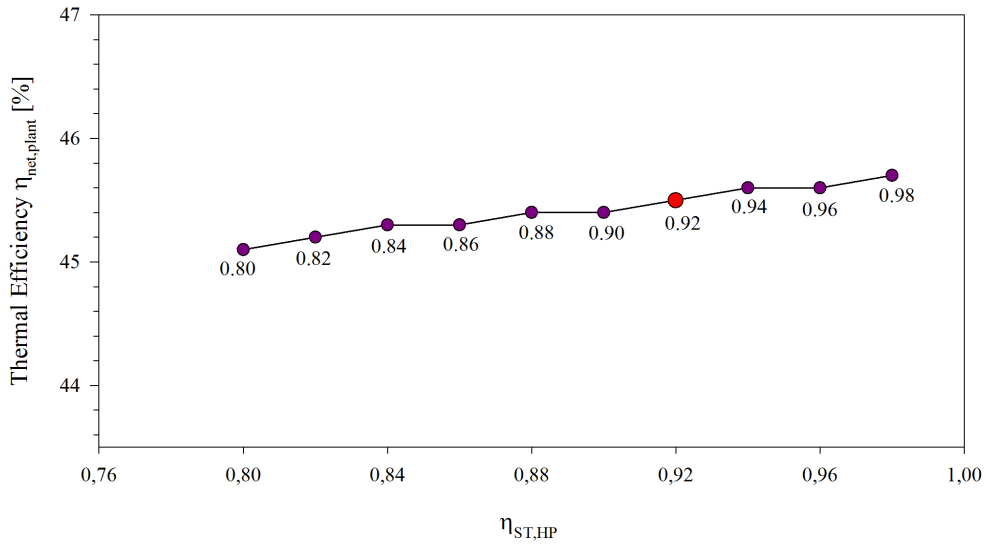


**Figure 8.11** Sensitivity plot for 1<sup>st</sup> stage ST efficiency – Extraction steam turbine cycle

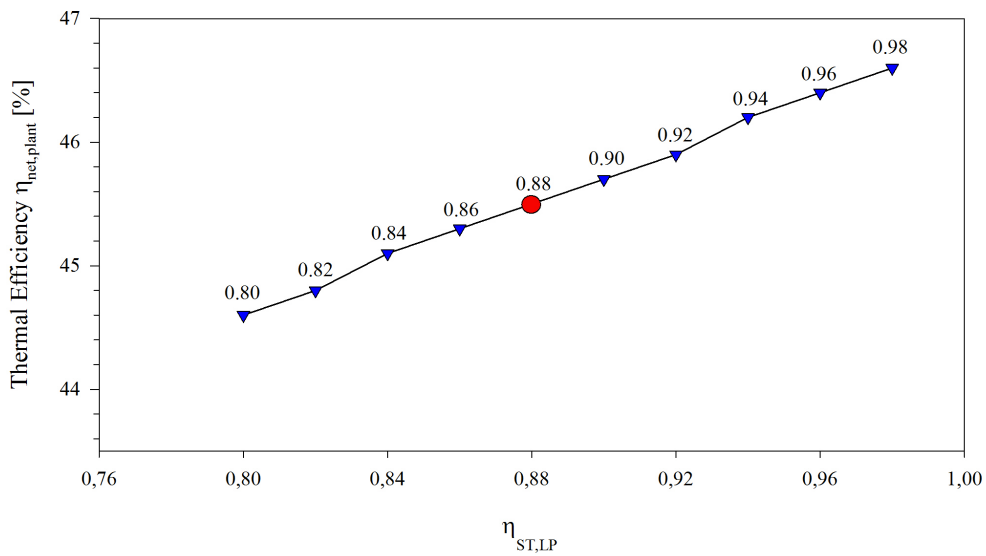


**Figure 8.12** Sensitivity plot for 2<sup>nd</sup> stage ST efficiency – Extraction steam turbine cycle

## 8.2. Backpressure steam turbine cycle

### 8.2.1. Design case

In the backpressure steam turbine cycle the electrical power output from the steam turbine was calculated to be 6.0 MW. The net electrical power output from the cycle was then 28.5 MW, corresponding to a net thermal efficiency of 42.1 %. This was an increase of 8.8 % in thermal efficiency compared to a simple cycle GE LM2500+G4 configuration. The loss due to desuperheating was calculated to 1.4 MW. With the modification discussed in section 7.2.5 some of this loss can be retrieved for a real plant. Process heat extracted from the cycle reaches a value of 21.7 MW at a supply temperature of 120 °C. This is over four times the amount of process heat supplied by the extraction steam turbine at design. The *EU*F of the combined cycle reached a value of 74.2 %. The aftercooler reduced the temperature of the returning saturated water down to 60 °C, removing 2.5 MW of energy from the flow. Exhaust losses were similar to the extraction steam turbine cycle (12.6 MW), and the other losses added up to a total of 1.0 MW. All results for design case are summarized in Table 8.4. In Figure 8.14 the T-Q diagram for the OTSG is shown, and the T-s diagram for the cycle can be seen in Figure 8.15.

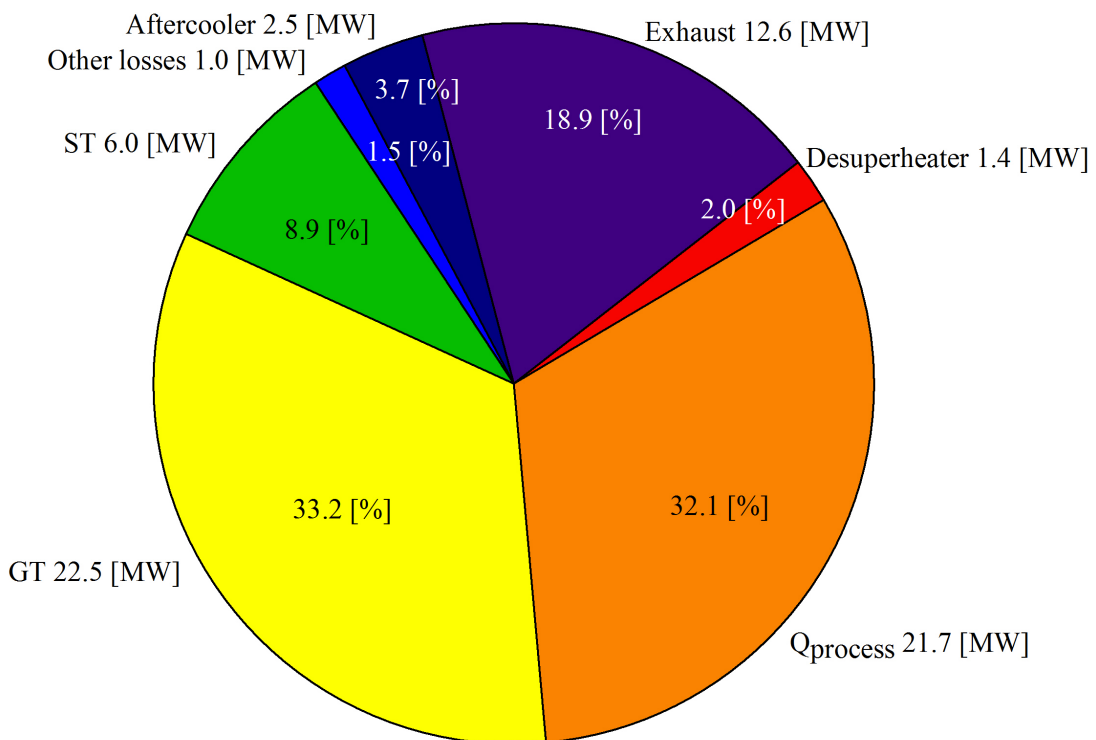


Figure 8.13 Energy balance for backpressure steam turbine cycle at design

**Table 8.4 Results for backpressure steam turbine at design point**

<b>Gas Turbine</b>		
Fuel: Methane $\dot{m}_{CH_4}$	[kg/s]	1.35
$LHV$	[kJ/kg]	50015
Gross Power Output $\dot{W}_{GT}$	[MW]	22.5
Mass flow exhaust $\dot{m}_{exhaust}$	[kg/s]	78.9
Exhaust temperature $T_{exhaust}$	[°C]	532
<b>HRSG</b>		
Efficiency $\eta_{HRSG}$	[%]	69.7
Live Steam temperature $T_{live,steam}$	[°C]	502
Mass flow steam $\dot{m}_{steam}$	[kg]	9.8
Stack temperature $T_{stack}$	[°C]	167
<b>Steam Turbine</b>		
Power Output $\dot{W}_{ST}$	[MW]	6.0
Rankine Cycle efficiency $\eta_{SRC}$	[%]	13.2
Steam quality outlet $x$	[-]	1.00
Process Heat Extraction $\dot{Q}_{process}$	[MW]	21.7
<b>Plant</b>		
Net power output $\dot{W}_{net,plant}$	[MW]	28.5
Thermal efficiency $\eta_{net,plant}$	[%]	42.1
$EU\!F$	[%]	74.2

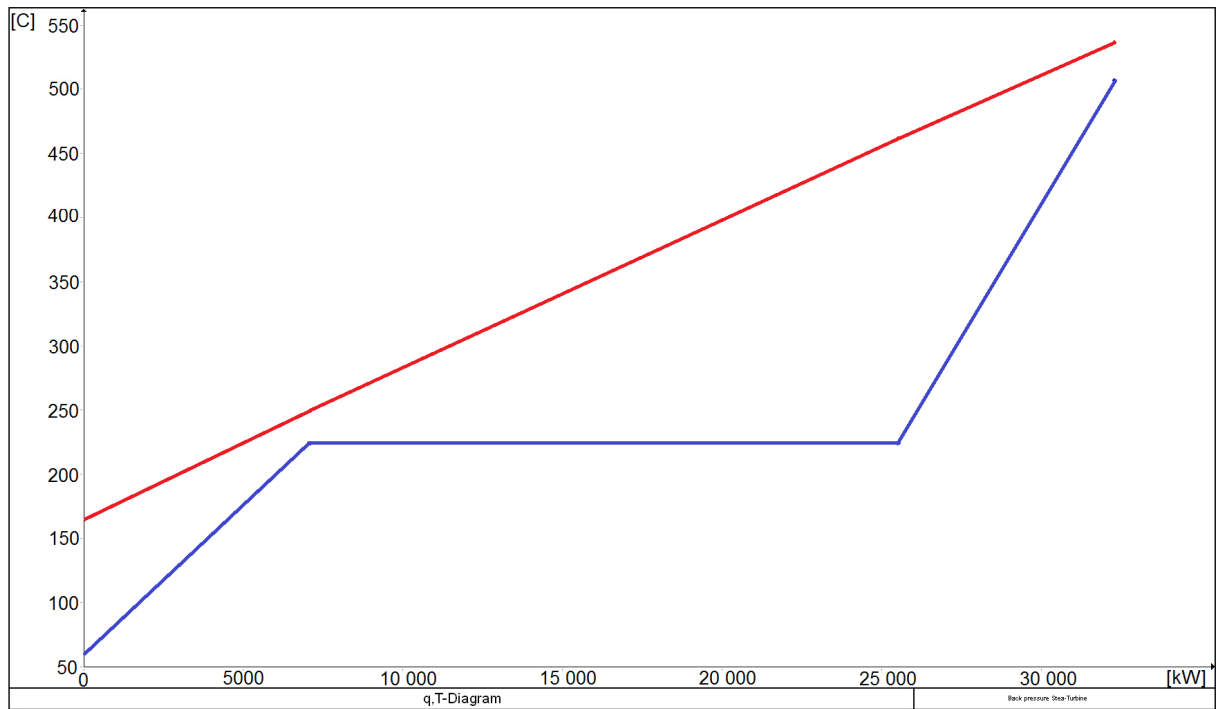


Figure 8.14 T-Q diagram for the HRSG in backpressure steam turbine cycle

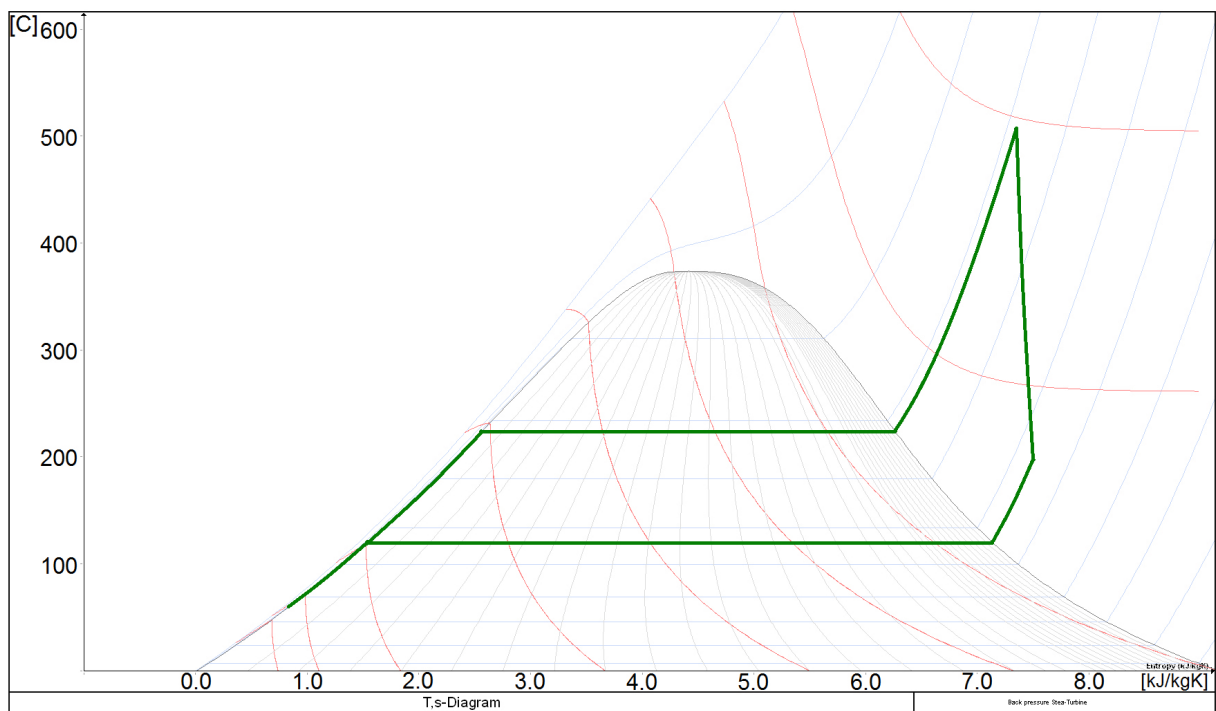


Figure 8.15 T-s diagram for backpressure steam turbine cycle



### 8.2.2. Off-design cases

Figure 2.1 shows the line of operation for the backpressure steam turbine cycle at 120 °C supply temperature. Noticeable shifts in the curve are the distance observed between 100–90 % GT loads, and again between 60–50 %. The explanation for this is the reduction in the gas turbine exhaust temperature seen by in Figure A.1 in the appendices. These observations were similar to the ones seen in the extraction steam turbine cycle, discussed in section 8.1.2. The major difference is the additional drop in process heat, due to the fixed relation between power output and process heat in the bottoming cycle. Results for values along the line of operation are summarized in Table 8.5.

Backpressure Steam Turbine 2 [bar],  $T_s = 120$  [°C]

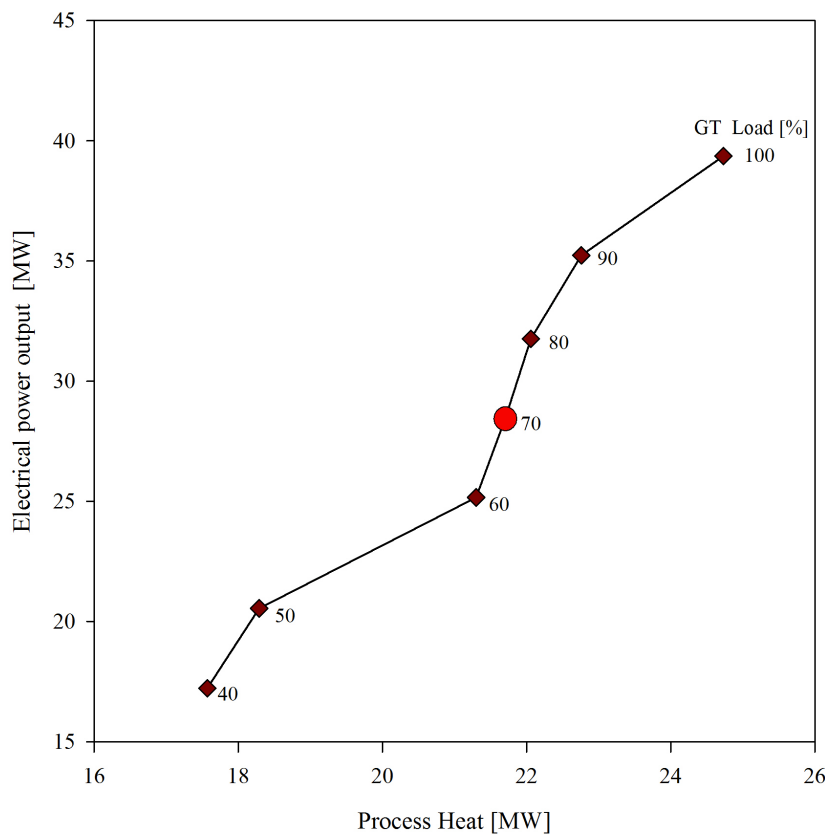


Figure 8.16 Operational line for backpressure steam turbine at 2 [bar]  $T_s$  120 [°C]

From 60–90 % GT load the steam turbine output was very stable, providing a power output between 6.0–6.4 MW. This suggests that deviations in power demand can be met by quick load variations on the GT, while maintaining a stable power output from the bottoming cycle. Delivered amount of process heat is also very consistent for operation in this range. Process heat varied from 21.3 to 22.8 MW. The major change in net thermal efficiency for the cycle was mostly due to variations in GT efficiency. *EU*F maintained a stable value of approximately 70 % for the range, which suggests a very good utilization of the fuel combusted.

At maximum GT load the system is able to deliver 7.1 MW of electricity and 24.7 MW of process heat. Maximum net thermal efficiency was calculated to be 46.6 % with an *EUF* of 72.2 %. The thermal efficiency is not particularly good compared to other designs, but the amount of process heat might be sufficient to cover the heat requirement of the whole installation if supply temperature is below 120 °C.

**Table 8.5 Results for backpressure steam turbine 2 [Bar]  $T_s$  120 [°C]**

GT load	$\dot{W}_{GT}$ [MW]	$\dot{W}_{ST}$ [MW]	$\dot{Q}_{process,heat}$ [MW]	$\eta_{net,plant}$	<i>EUF</i>
100 %	32.3	7.1	24.7	46.6 %	72.2 %
90 %	29.0	6.3	22.8	45.7 %	71.6 %
80 %	25.8	6.1	22.1	44.2 %	71.0 %
70 %	22.5	6.0	21.7	42.1 %	70.1 %
60 %	19.2	6.0	21.3	40.1 %	69.8 %
50 %	15.9	4.7	18.3	38.9 %	69.1 %
40 %	12.7	4.6	17.6	36.0 %	67.9 %

Off-design results for the other supply temperatures cases can be found in the appendices (A.IV) with short comments. Simulations showed a high penalty in power output for systems with a higher process heat supply temperature. A power reduction from the steam turbine of approximate 2 and 3 MW was observed in the 150 and 175 °C cases, when compared to the 120 °C case. Installing steam turbines with such low power outputs does not seem like a financial feasible option. Nevertheless, the supply of process heat was more consistent with a difference of only 2 MW between the 100 and 175 °C cases. Comparable diagrams of steam turbine power output and process heat for all the off-design cases, can be seen in Figure A.12 and Figure A.13 in the appendices.

### 8.2.3. Sensitivity analysis

To investigate the sensitivity of net thermal efficiency for the plant, 5 input parameters were varied. Selected parameters are listed in Table 8.6 with design case value and range of input for the sensitivity analysis. All input values are within  $\pm 15\%$  relative change from nominal value. At some of the parameters the input range was limited. This occurred either by limitations in the software or by reaching an end of sensible input number. Further details are provided under the individual parameter description.

**Table 8.6 Selected parameters for sensitivity analysis of backpressure steam turbine cycle**

<b>Input parameter</b>	<b>Range</b>	<b>Design case</b>
Ambient temp. $T_{amb}$ [°C]	-25 – 40	15
Isentropic efficiency ST $\eta_{ST,HP}$ [-]	0.80 – 0.98	0.92
GT exhaust pressure $P_{GT,exhaust}$ [bar]	1.035 – 1.075	1.045
Pinch point temp. $T_{PinchPoint}$ [°C]	5 – 35	25
Feedwater inlet temp. $T_{FW}$ [°C]	40 – 90	60

In Figure 8.17 and Figure 8.18 all parameters are displayed in a joint diagrams where thermal efficiency is plotted against the relative change from the design case. Real values of selected inputs are typed next to some chosen plots. From the figures it was observed that isentropic efficiency input of the turbine had a larger impact than change in ambient temperature. The parameter that influenced the system most for a small relative change was the pinch point temperature. The feedwater temperature did not affect the system in any way. On the following pages the individual plots are displayed and discussed.

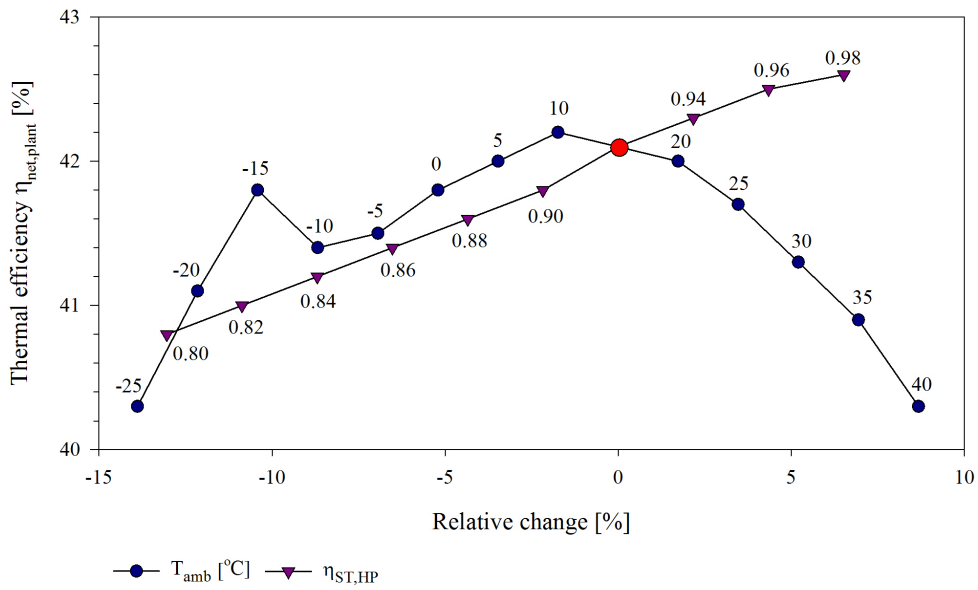


Figure 8.17 Effect of input parameters (1) - Backpressure steam turbine cycle

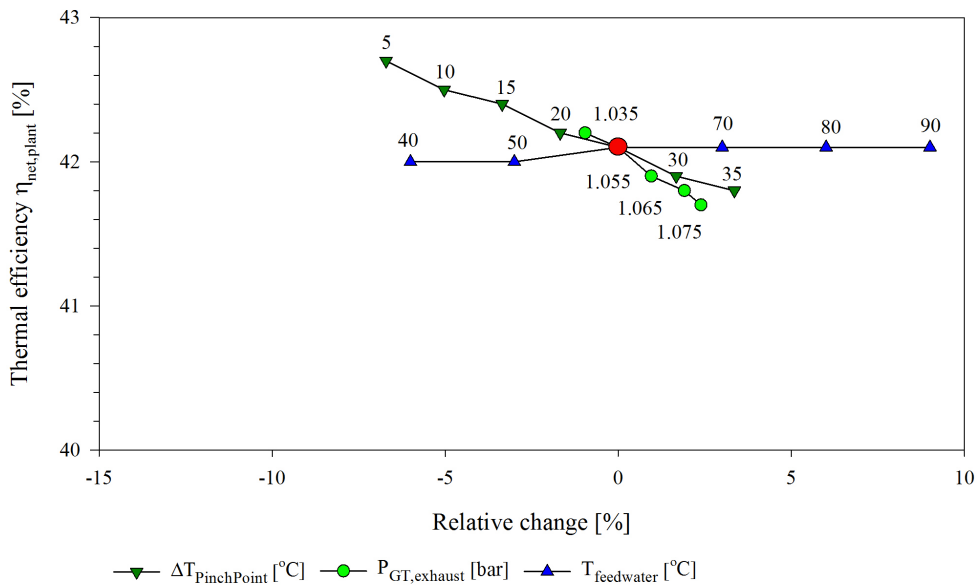


Figure 8.18 Effect of input parameters (2) - Backpressure steam turbine

## Ambient temperature

By the VTU gas turbine library component, changes in ambient temperature also resulted in changes for the inlet mass flow of air and fuel. The graph in Figure 8.19 shows a steady net thermal efficiency around 42 % for the temperature range 5-20 °C. Outside this range the system produces less power and reaches approximately the same penalty of -1.7 % in net thermal efficiency for the two extremities. For detailed explanation of the odd result at -15 °C, please see comment in section 8.1.3.

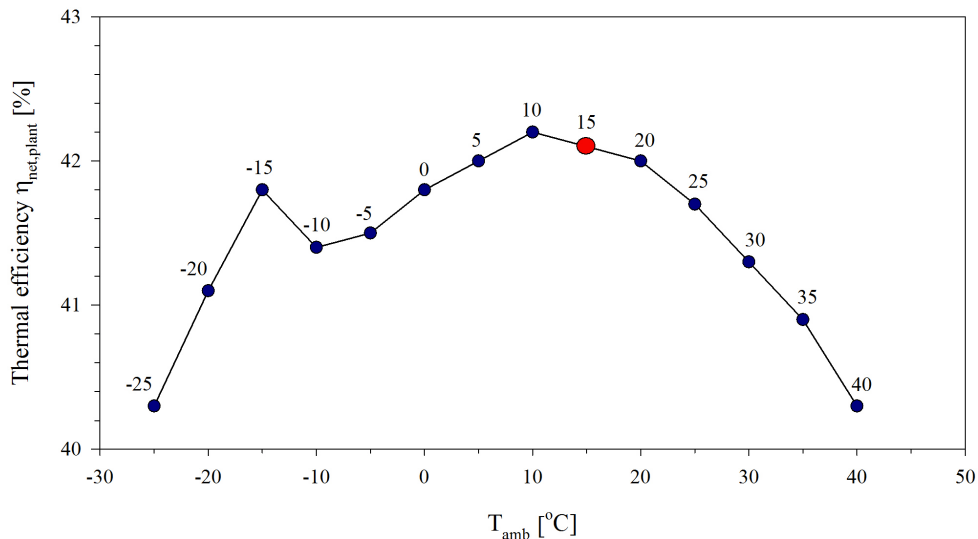


Figure 8.19 Sensitivity analysis ambient temperature - Backpressure steam turbine cycle

## Isentropic efficiency steam turbine

The effect of the isentropic efficiency of the steam turbine was investigated for the input values 0.80 – 0.98. The lower extremity showed a reduction in net thermal efficiency of 1.3 %, while the upper extremity showed an increase of 0.5 %. The graph illustrates a linear trend for the input values.

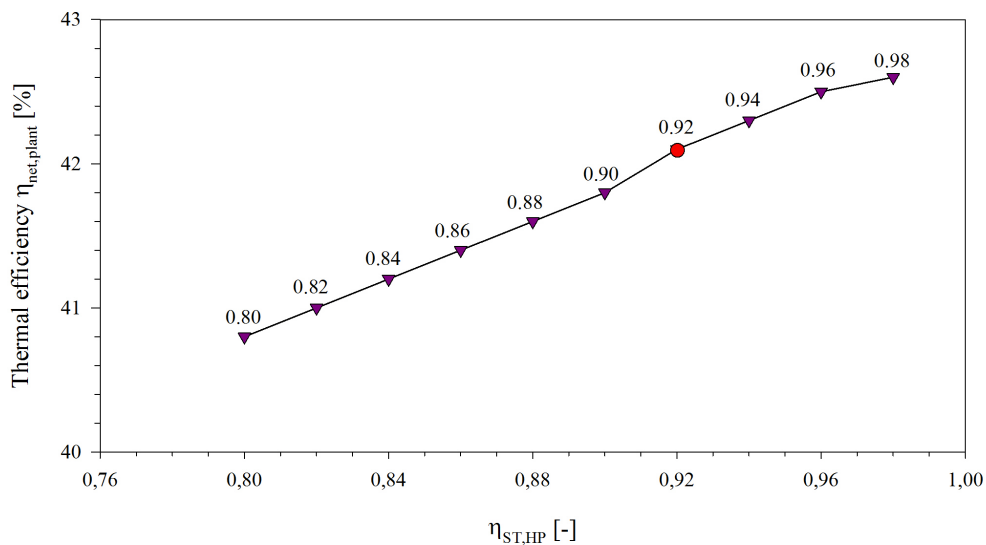
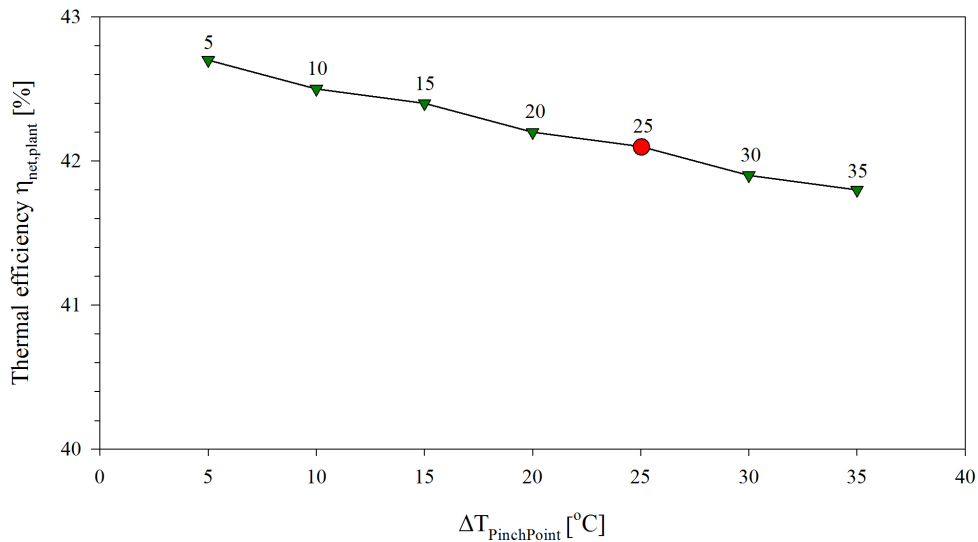


Figure 8.20 Sensitivity plot for ST efficiency - Backpressure steam turbine cycle

## Pinch point temperature difference

A sensitivity analysis on the pinch point temperature difference can illustrate how much the design is restricted by the set value. Figure 8.9 shows that a net thermal efficiency increase of 0.6 % can be achieved with a 5 °C pinch point. A pinch point of 35 °C would reduce the net thermal efficiency by 0.25 %.



**Figure 8.21 Sensitivity plot pinch point temperature difference - Backpressure steam turbine cycle**

## Gas turbine exhaust pressure

The same restrictions to changes in gas turbine exhaust pressure were present for the backpressure steam turbine as in the extraction turbine sensitivity analysis. Further explanation on the restrictions is seen in section 8.1.3. Highest achievable increase in net thermal efficiency was 0.1 %, and maximum increase of pressure level reduced the net thermal efficiency with 0.4 %. These values are similar to the extraction steam turbine case.

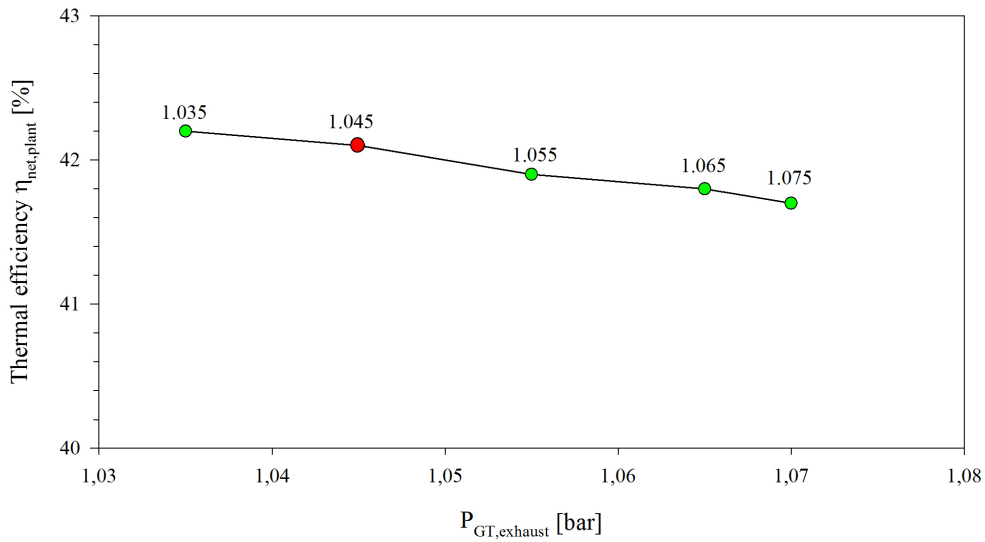


**Figure 8.22 Sensitivity plot exhaust gas pressure - Backpressure steam turbine cycle**

### Feedwater temperature

The temperature of feedwater was adjusted through the aftercooler component. Figure 8.23 shows that only an incremental change of 0.1 % in net thermal efficiency for all input values 40-90 °C. These results illustrates that the feedwater temperature does not affect the amount of steam generated through the HRSG at given design. Still, feedwater temperature should be kept at 60 °C due to risk of corrosion, see section 6.3.

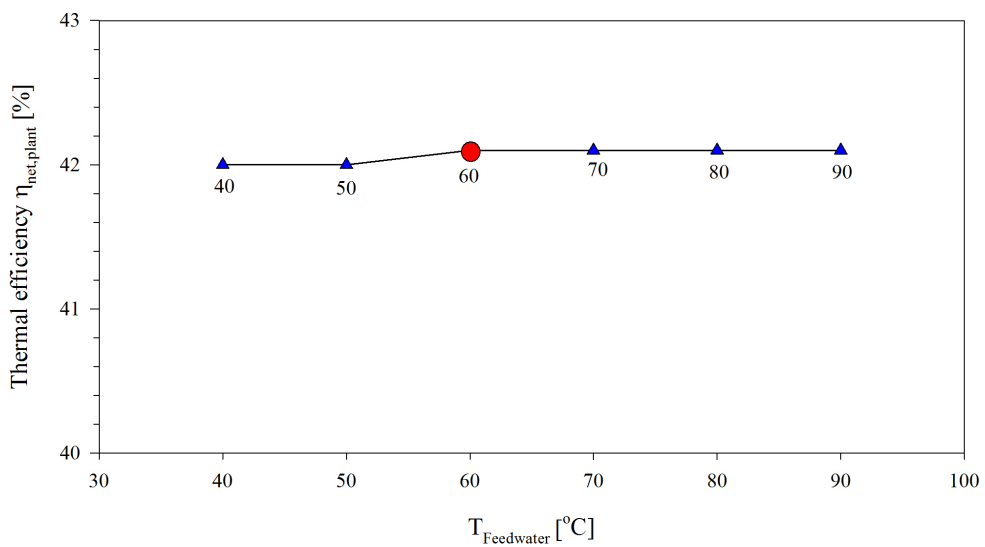


**Figure 8.23 Sensitivity plot for feedwater temperature - Backpressure steam turbine cycle**

### 8.3. Emission and taxation

In this section the potential reductions in CO<sub>2</sub> emission and taxation cost are investigated. Calculations were only carried out at design point for the cycles, as a real life integration and comparison were outside the scope of this thesis. The results are based primarily on electrical production, as no reference case for cost of heat generation offshore was carried found.

#### Reference case

The reference case was calculated with a simple cycle using GE LM2500+G4 for electrical power production. Annual number of operational hours was assumed to be 8000 hours at 70 % load on the GT. This resulted in an annual electric power output of 18 000 MWh. On this load the amount of CO<sub>2</sub> in the exhaust, calculated by Epsilon Professional, is 3.79 kg/s, resulting in an annual emission of 109 008 ton/year. The emission ratio was calculated by equation (3.48) to be 606 kg/MWh. As explained in section 2.5, CO<sub>2</sub> taxation on the NCS is calculated based on fuel consumption. Annual fuel consumption was calculated to 3896 ton/year, resulting in an annual taxation fee of 57 400 000 kr/year. The CO<sub>2</sub> taxation fee per megawatt hour produced was then calculated with equation (3.50), to be 319 kr/MWh. All the results are summarized in Table 8.7 below.

**Table 8.7 Reference case – LM2500+G4 annual emission and taxation**

<b>Simple Cycle LM2500 +G4</b>		
Operational load	70	[%]
Power Output $\dot{W}_{GT}$	22.5	[MW]
Annual operating hours	8000	[h/year]
Annual power output $\dot{W}_{annual,GT}$	180000	[MWh/year]
Annual CO <sub>2</sub> emission $\dot{m}_{CO_2,exhaust}$	109 019	[ton/year]
Emission rate $ER_{power}$	606	[kg/MWh]
Annual fuel consumption (CH <sub>4</sub> )	3896	[ton/year]
Density Methane $\rho_{CH_4}$	0.6785	[kg/sm <sup>3</sup> ]
Taxation rate $l$	1.00	[kr/sm <sup>3</sup> ]
Annual taxation cost	57.4	[Mkr/year]
$CO_{2,tax}$	319	[kr/MWh]



## Relative CO<sub>2</sub> emission rate

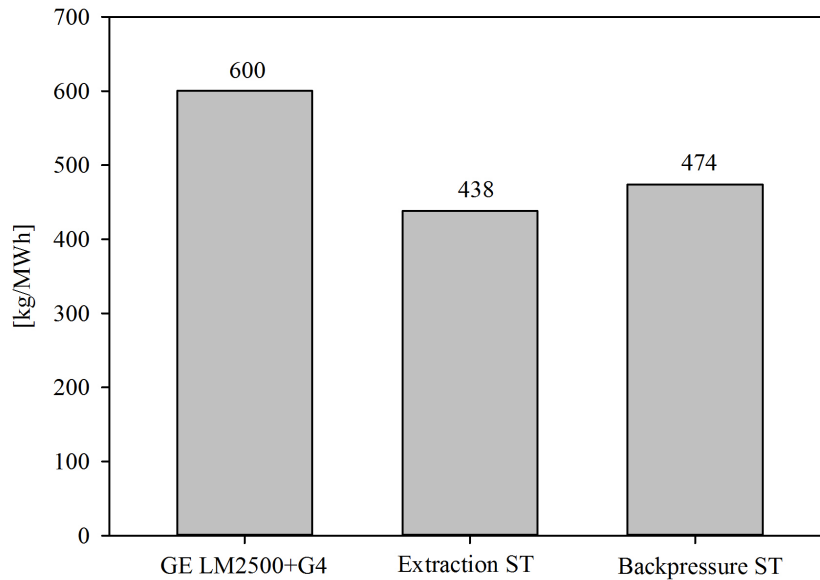


**Figure 8.24 CO<sub>2</sub> emission rate**

The emission rate is a useful parameter in the way that it shows the possible reduction in emissions per megawatt hour produced. This makes it easy to compare against other setups and technologies. With the steam bottoming cycle the amount of produced power is increased per kg of emitted CO<sub>2</sub>. In simple other words, the system delivers more useable products with the same amount of input.

In Figure 8.24 the emission rates for the reference case and the two steam bottoming options are presented. The extraction steam turbine cycle reduces the emission rate *ER* by 27 % compared to the reference case. This resulted in an *ER* of 438 kg/MWh. The backpressure steam turbine cycle reduced *ER* with 21 %, equivalent to 126 kg/MWh. The result was 474 kg/MWh. These number shows that a relative reduction in emission levels are achievable for electrical power generation. By implementing one of the bottoming cycles an operator can reduce emissions by at least 1/5 for the simple comparison showed here. A comparison with variation in load and operational strategies are suggested in further works.

## Taxation cost

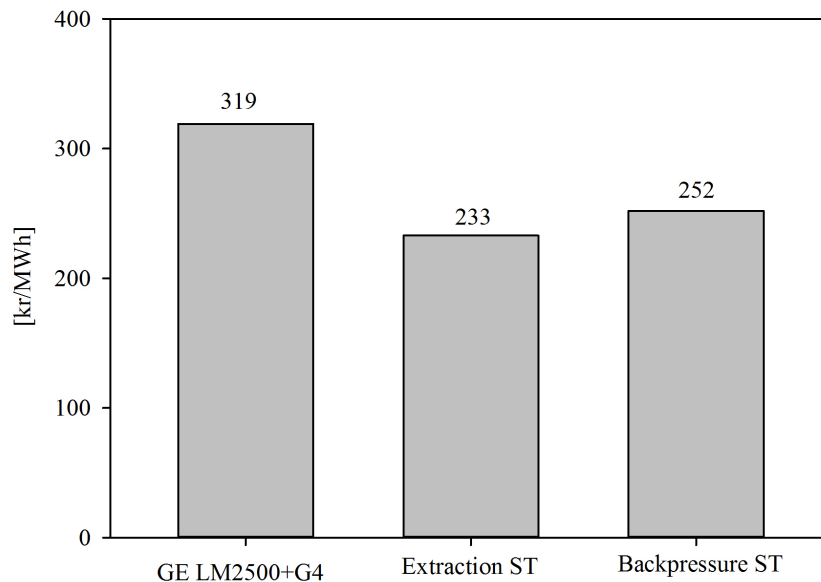


**Figure 8.25 CO<sub>2</sub> taxation cost per MWh**

Potential saving in taxation cost may be one of the primary drivers for further implementation of combined cycles on the NCS. In the reference case the annual taxation cost of fuel combustion was calculated to be 57.4 million kroner per year. This is a significant amount considering that many facilities have more than one GT operating at all time through the year. In Figure 8.25 the relative CO<sub>2</sub> taxation cost are shown for both steam bottoming cycles compared to the simple cycle reference case. The numbers are derived from numbers presented in Figure 8.24 This means that the relative change to the reference case is the same for taxation cost as it is for *ER*. The numbers are interesting as they are easy to implement in financial analysis for the cost of produced power. However, a full detailed analysis of installation, equipment, operation, maintenance and decommissioning should be conducted before choosing the technological options. The numbers show that one can expect significant reductions in the CO<sub>2</sub> taxation cost. For the simulations and the reference case, methane has been used as fuel for simplistic reasons. Note that the values presented in this section must be adjusted if another fuel is utilized on the offshore installation.

## 8.4. Discussion

Simulations of the extraction steam turbine cycle revealed interesting characteristics in operation. Firstly, the power output of 8.0 MW at 70 % GT load increased the thermal efficiency by 13.3 %. The effect on the efficiency decreased for higher GT loads, yet the steam turbine delivered very stable power outputs for a large operational window. As seen in the off-design results the system is very flexible in its heat and power output. Process heat could easily be varied from 0 to 10.5 MW for a range of GT loads. Such operational flexibility would potentially ease the implementation process onto existing facilities. The value of the net thermal efficiency is in the expected range when comparing to work by Nord and Bolland [52], and ranged from 38.3 up to 50.9 %. However, the system was only able to obtain an *EU*F of 60.8 % at maximum. This might not be enough to outdo the competitive WHRU configuration. From chapter 2 it was stated that offshore production from a gas reservoir would require less process heat, and in that context the extraction steam turbine could prove a suitable option. For such an installation the extraction steam turbine could provide the needed steam for reboiling of amine in CO<sub>2</sub> removal. However, the current system design proved unsuited to provide steam to reboiling of condensate and regeneration of TEG for dehydration. This was due to the high temperature requirement in the range of 200 °C, corresponding to an extraction pressure level of 16 bar. In order to supply such temperatures steam could be extracted in front of the turbine or from the OTSG at saturated steam condition. At design point the emission rate was reduced by 27 % per MWh, making the system interesting from both an environmental and economical viewpoint.

The backpressure steam turbine cycle did not deliver as much power as the extraction steam turbine with its 6 MW output in design case. Be that as it may, the process heat delivered is substantially higher with 22 MW at 120 °C. In the off-design cases with supply temperatures of 150 and 175 °C, the penalty in power output is very high compared to the 120 °C case. This made the backpressure steam cycle an unsuitable option for such temperatures, thus the 120 °C was chosen as the design case. The 100 and 120 °C simulations delivered enough power to be an attractive solution compared to installing a WHRU with hot oil. The amount of process heat generated could potentially be sufficient to cover up for all required pre heating of well flow in separation trains. Thus, the backpressure steam cycle could be a suitable option for oil producing facilities with high demand for process heating. Additionally the cycle could handle water treatment (boiling of seawater) and flue gas heating. Heating requirements at temperatures above this level would have to require steam extraction prior to the turbine. A large drawback for the backpressure steam cycle was the fixed relation between generated heat and power. This restricted operational flexibility, although a bypass piping and valve could be installed to allow for continuous process heating while the steam turbine was out of operation. The reduction in *ER* was calculated to be 21 [%] at design condition compared to a simple cycle configuration. This is 5 [%] lower than the extraction steam turbine cycle, but the backpressure system makes up for it with a high *EU*F of 74.2 %.

Off-design operation of the two cycles was very stable for both of cycles from 60–90 % GT load. Best points of efficiency for the bottoming cycles were both at design conditions. Best

net performances for the plants were at 100 % GT load. Both plants proved sensitive to the variations in exhaust temperature, suggesting that controlling mass flow of feedwater to maintain a high exhaust temperature is important. Sensitivity analysis showed that seasonal variation in outputs could be expected for both plants. The analysis also revealed that choosing of pinch point temperature difference had a large impact on both cycles. In Table 8.8 the major positives and negative for the cycles are listed. Thus, the table offers some answers to the research question of this thesis. In the authors' mind, the backpressure steam turbine cycle seems like the more suitable option of the two.

**Table 8.8 Summarized overview of major positives and negatives for the cycles**

---

<b>Extraction steam turbine cycle</b>	
+ Flexible heat/power relation	- Limited process heat generation for high supply temperatures ( $\geq 150$ [°C])
+ High power output	- Amount of process heat properly not enough to supply an entire installation
+ 13.3% increase in net thermal efficiency	- <i>EUF</i> 52.9%
+ Can have several extraction points	
+ 27 % reduction in <i>ER</i> compared to SC	
+ Stable power output for a large range of GT loads	
<b>Backpressure steam turbine cycle</b>	
+ High generation of process heat	- Very low power output when supply temperature is high ( $\geq 120$ [°C])
+ 8.8 % increase in net thermal efficiency	- Fixed heat/power relation
+ <i>EUF</i> 74.2%	
+ 21 % reduction in <i>ER</i> compared to SC	
+ Stable power output for a large range of GT loads	

---

## 9. Conclusions and further work

This last chapter is devoted to the final conclusions of the simulation work and research activities disclosed in this thesis. Lastly, the chapter provides some suggestions for further works on the cycles and topics presented in the thesis.

### 9.1. Concluding remarks

In this thesis the operation of two different configurations of the steam rankine cycle have been simulated, with the aim of answering the research question: “*What are the positives and negatives of the backpressure- and extraction steam turbine for offshore combined cycle operation?*” Simulations of the combined cycles were carried out in Epsilon Professional and based on the results some observations were made. In line with the objectives operation were investigated at design, off-design and sensitivity analysis carried out.

By installing a bottoming cycle on the GE LM2500+G4 the results suggest that the net thermal efficiency can be noticeably increased. At design point the best performer of the two options was the extraction steam turbine that delivered 8.3 MW of power, achieving a net thermal efficiency of 45.5 % for the plant. This constitutes an increase of 13.3 % compared to the GE LM2500+G4 running at 70 % load. The backpressure steam turbine cycle obtained a power output of 6.0 MW, resulting in a net thermal efficiency of 42.1 % for the plant. Despite the extraction steam turbine achieving best results in power output, the delivered process heat is approximately four times higher for the backpressure steam turbine cycle. This makes it a highly attractive alternative for offshore facilities with large demand for process heat below 120 °C. Oil producing facilities with high demand for process heat in the separation trains could potentially be an ideal fit. The penalty in power output makes backpressure steam turbines unattractive for integration in systems with high temperature process heat demands. For such installations, the extraction steam turbine could be a more interesting alternative, although the amount of process heat required should be considerably lower and not above 150 °C. A gas producing installation on a gas reservoir could prove more suitable. None of the cycles were found suitable in delivering process heat at high temperatures without modifications to extract steam prior to the turbines.

Both systems delivered very stable outputs for GT load in the range of 60-90%. Simulations showed that the steam bottoming cycle output is closely connected to exhaust temperature from the GT. The extraction steam turbine illustrated a very good flexibility that could ease the implementation to a real life system. The biggest drawback for the backpressure steam turbine is the fixed power and heat relation, which could prove more difficult to implement. Reductions in relative emissions and CO<sub>2</sub> taxation cost are directly linked with the net power output from the cycles. Simulations showed reduction in emissions was achievable compared to a simple cycle configuration. A reduction of 26 % and 21 % in CO<sub>2</sub> emissions per MWh produced were found for the extraction and backpressure steam turbine respectively. These

numbers illustrate that reduction in GHG emissions from the NCS can be achieved with available bottoming cycle technology.

In order to meet the future emission reduction targets, there is a need to address emission levels from power generations offshore. The cogenerative combined cycle could prove a suitable solution to provide required heat and power demand where onshore power supply is not economically feasible. Consequently, this report can tell us something about the suitability of combined cycles with steam for offshore heat and power generation facilities. In order to meet future targets in CO<sub>2</sub> emission reduction, the combined cycle could prove an appropriate option to provide required heat and power demand.

## **9.2. Further work**

In regards to the cycles described in this thesis, a study of transient behavior is suggested for further study and would be a natural continuation of the work presented. Dynamic behavior of the system could potentially reveal problems that require necessary adjustments in the design case. A study could include startup, shutdown and changes in heat and power demand. If real time data on required heat and power demand for a facility was available, a transient behavior study could be extended to include optimization of operational strategy. This could maximize fuel savings and plant efficiency. The operational area diagrams could prove useful for preliminary estimation in such an analysis.

Simulations of a cogenerative combined cycle with lower temperature in available waste heat would be interesting to examine. A comparison between the results for different exhaust temperatures could provide an indication of what temperature region a steam bottoming cycle could prove applicable. In this thesis it was always assumed that a singular gas turbine would act as the topping cycle. An evident alternative would be to have several gas turbines connected to a singular HRSG. Increased power output of the bottoming cycle could potentially remove the necessity of a gas turbine, if the offshore installation has several gas turbines installed. Transient behavior would be important to provide satisfactory results on system availability and operability.

A case study of integration with the topside processing system and production equipment would also be very useful. Potential bottlenecks that influences design could be determined, and restrictive events in the operational windows could be detected. Lastly, extending the cogenerative combined cycle system further with CO<sub>2</sub> capture and storage technology, is something the author finds extremely interesting. As the reboiler in the CO<sub>2</sub> capture plant requires process heat from steam or other sources, integration with one of the cycles investigated in this thesis could be attractive. The captured CO<sub>2</sub> could potentially be reinjected into producing reservoirs for enhanced oil and gas recovery.

## Bibliography

- [1] Norwegian Petroleum Directorate, *Facts 2014: The Norwegian Petroleum Sector*. 2014.
- [2] Norwegian Petroleum Directorate, Norwegian Pollution Control Authority, and Norwegian Energy Directorate, *Power from onshore to the norwegian continental shell*. 2008.
- [3] Ministry of Finance. *Tax and Customs 2014*. 2014 [cited 2014 22.10]; Available from: <http://www.regjeringen.no/nb/dep/fin/dok/regpubl/prop/2013-2014/prop-1-ls-20132014/7/9.html?id=741145>.
- [4] Ministry Of Climate And Environment, *Meld.St.21 Norwegian Climate Politic*. 2012.
- [5] SINTEF. *EFFORT Goals and Objectives*. 2012 [cited 2014 23.10]; Available from: <http://www.sintef.no/Projectweb/Effort/Goals-and-objectives/>.
- [6] SINTEF. *COMPACTS*. 2015 [cited 2015 03.05]; Available from: <https://http://www.sintef.no/projectweb/compacts/>.
- [7] DNV. *OPera Offshore power system for the new era*. 2012 [cited 2014 23.10]; Available from: [http://www.dnv.com/binaries/opera\\_brochure\\_tcm4-527124.pdf](http://www.dnv.com/binaries/opera_brochure_tcm4-527124.pdf).
- [8] Hetland, J., Kvamsdal, H.M., Haugen, G., Major, F., Kårstad, V., and Tjellander, G., *Integrating a full carbon capture scheme onto a 450 MWe NGCC electric power generation hub for offshore operations: Presenting the Sevan GTW concept*. *Applied Energy*, 2009. **86**(11): p. 2298-2307.
- [9] STEAG, *Epsilon Professional 10.6*. 2014.
- [10] Badeer, G.H., *GE's LM2500+G4 Aeroderivative Gas Turbine for Marine and Industrial Applications*. 2005.
- [11] Mazzetti, M.J. *EFFORT - Recovering Wasted Heat*. 2014 27.08 [cited 2015 03.05]; Available from: <http://www.ons.no/2014/tv/centre-court-programme/>.
- [12] Kloster, P., *Energy Optimization on Offshore Installations with Emphasis on Offshore Combined Cycle Plants*, in *Offshore Europe Conference*. 1999, Society of Petroleum Engineers Inc. : Aberdeen Scotland.
- [13] Norwegian Petroleum Directorate, *Status report for environmental friendly technology*. 2011.
- [14] Ministry of Petroleum and Energy, *Proposal to eletrification of Utsirahøyden*. 2014.
- [15] Statoil, *Johan Sverdrup-Feltet PUD del II - Konsekvensutredning*. 2014.
- [16] SAFETEC, *Kunnskapsutvikling - Elektrisk kraft fra land, reservekraft og nødkraft*. 2015.
- [17] Ngyen, T.-V., Tock, L., Brauhaus, P., Maréchal, F., and Elmegaard, B., *Oil and gas platforms with steam bottoming cycles: System integration and thermoenviromomic evaluation*. *Applied Energy*, 2014. **131**: p. 222-237.
- [18] Bothamley, M., *Offshore Processing Options for Oil Platforms*, in *SPE Annual Technical Conference and Exhibition*. 2004, Society of Petroleum Engineers Inc. : Houston, USA.

- [19] Nguyen, T.-V., Fülöp, T.G., Breuhaus, P., and Elmegaard, B., *Life performance of oil and gas platforms: Site integration and thermodynamic evaluation*. Energy, 2014. **73**: p. 282-301.
- [20] Campbell, J.M., *Gas Conditioning and Processing, Vol.2: The Equipment Modules*. 1992: Campbell Petroleum Series.
- [21] Wall, M., Lee, R., and Frost, S., *Offshore gas turbines (and major driven equipment) integrity and inspection guidance notes*. 2006.
- [22] Campbell, J.M., *Gas Conditioning and Processing, Vol.4: Gas treating and Sulphur Recovery*. 4th ed. 2006: Cambell Petroleum Series.
- [23] Voldsund, M., Nguyen, T.-V., Elmegaard, B., Ertesvåg, I.S., RøsJORde, A., Jøssang, K., and Kjelstrup, S., *Exergy destruction and losses on four North Sea offshore platforms: A comparative study on the oil and gas processing plant*. Energy, 2013(74): p. 45-58.
- [24] Nguyen, T.-V., Pierobon, L., Elmegaard, B., Haglind, F., Breuhaus, P., and Voldsund, M., *Exergetic assessment of energy systems on Northe Sea oil and gas platforms*. Energy 62 2013: p. 23-36.
- [25] Pinczewski, V., *Reservoir Engineering I*. 2013, School of Petroleum Engineering: University of New South Wales.
- [26] Norwegian Petroleum Directorate, Statoil, OLF, Hydro, and Conoco Phillips, *Improved energy management offshore*. 2004.
- [27] Cholet, H., *Well Production Practical Handbook*. 2008: Editions Technip.
- [28] Norwegian Petroleum Directorate. *CO2 Storage Atlas of Tthe Norwegian Continental Shelf*. 2014 [cited 2015 24.05]; Available from: <http://www.npd.no/Publikasjoner/Rapporter/CO2-samleatlas/Preface/>.
- [29] Vanner, R., *Energy use in the offshore oil and gas production: Trends and Drivers for efficiency from 1975 to 2025*. 2005, Policy studies Institute.
- [30] Voldsund, M., Nguyen, T.-V., Elmegaard, B., Ertesvåg, I.S., and Kjelstrup, S., *Thermodynamic Performance Indicators for Offshore Oil and Gas Processing: Application to Four North Sea Facilities*. 2014: Oil and Gas Facilities. p. 51-63.
- [31] Svalheim, S. and King, D.C., *Life of Field Energy Performance*, in *Offshore Europe 2003*. 2003, Society of Petroleum Engineers: Aberdeen.
- [32] SSB Statistics Norway. *Emissions of greenhouse gases, 1990-2013, final figures*. 2015 [cited 2015 24.05]; Available from: <http://www.ssb.no/en/natur-og-miljo/statistikker/klimagassn/aar-endelige>.
- [33] IPCC. *Direct Global Warming Potentials*. 2007 [cited 2014 22.10]; Available from: [http://www.ipcc.ch/publications\\_and\\_data/ar4/wg1/en/ch2s2-10-2.html](http://www.ipcc.ch/publications_and_data/ar4/wg1/en/ch2s2-10-2.html).
- [34] United Nations Framework Convention on Climate Change. *Kyoto Protocol to the United Nations Framework Convention on Climate Change*. 2014 [cited 2014 22.10]; Available from: [http://unfccc.int/essential\\_background/kyoto\\_protocol/items/1678.php](http://unfccc.int/essential_background/kyoto_protocol/items/1678.php).



- [35] Ministry of Finance. *Why the government purchases 20 millions emission licenses by 2012*. 2011 [cited 2014 22.10]; Available from: <http://www.regjeringen.no/en/dep/fin/Selected-topics/Sustainable-development/statens-kvotekjop-2/hvorfor-skal-staten-kjope-25-30-millione.html?id=588003>.
- [36] United Nations. *Doha amendment to the Kyoto Protocol*. 2012 [cited 2015 23.05]; Available from: [http://unfccc.int/files/kyoto\\_protocol/application/pdf/kp\\_doha\\_amendment\\_english.pdf](http://unfccc.int/files/kyoto_protocol/application/pdf/kp_doha_amendment_english.pdf).
- [37] Ministry of Finance. *National Budget 2015 - Tax rates*. 2015 [cited 2015 28.05]; Available from: <http://www.statsbudsjettet.no/Statsbudsjettet-2015/Artikler/Avgiftssatser-2015/>.
- [38] Aibel. *StatoilHydro awards 58 MUSD Oseberg EPCI contract to Aibel*. 2015 [cited 2015 03.05]; Available from: <http://aibel.com/en/news-and-media/press-releases/statoilhydro-awards-58-musd-oseberg-epci-contract-to-aibel>.
- [39] HRS. *News - April 2012*. 2015 [cited 2015 03.05]; Available from: <http://heatrecoveryolutions.co.uk/index.php/news/>.
- [40] Henschel, S., Rygg, V., and Lauvdal, T., *Long-Term Stability of a Combined Cycle Plant and Two Interconnected Oil Platforms*, in *International Conference on Power System Transients*. 2001: Rio de Janeiro.
- [41] Moran, M.J. and Shapiro, H.N., *Fundamentals of Engineering Thermodynamics*. Vol. 6th Edition. 2010: John Wiley & Sons, Inc.
- [42] Bakken, L.E., *Thermodynamics, Compression and Expansion Processes*. 2014, Norwegian University of Science and Technology.
- [43] Shultz, J.M., *The Polytropic Analysis of Centrifugal Compressors*. *Journal of Engineering for Power* 1962.
- [44] Incropera, DeWitt, Bergman, and Lavine, *Fundamentals of Heat and Mass Transfer*. 6th ed. 2006: Wiley.
- [45] White, F.M., *Fluid Mechanics*. 4 ed. 1998: WCB McGraw-Hill.
- [46] Horlock, J.H., *Cogeneration - Combined Heat and Power (CHP)*. 1997: Krieger Publisher Company.
- [47] Bolland, O., *Thermal power generation*. 2009, Department of Energy and Process Engineering - NTNU.
- [48] Norwegian Petroleum Directorate. *Block diagram of NOx-dutiable equipment*. 2014 [cited 2014 10.11]; Available from: <http://www.npd.no/global/norsk/3-publikasjoner/rapporter/oversiktskjema-motorer-og-turbiner.xlsx>.
- [49] General Electric, *LM2500+ G4 Marine Turbine Data Sheet*. 2014.
- [50] Boyce, D.M.P., *Handbok for cogeneration and combined cycle power plants*. 2002: Asme Press.
- [51] Kehlhofer, R., Hannemann, F., Stirnimann, F., and Rukes, B., *Combined-Cycle Gas and Steam Turbine Power Plants*. 3rd ed. 2009: PennWell Corporation.
- [52] Nord, L.O. and Bolland, O., *Steam bottoming cycles offshore - Challenges and possibilities*. *Journal of Power Technologies* 92, 2012(3): p. 201 - 207.

- [53] Saravanamuttoo, H., Rogers, G., Cohen, H., and Straznicky, P., *Gas Turbine Theory*. 6th ed. 2009: Pearson Prentice Hall.
- [54] Pierobon, L., Kandepu, R., and Haglind, F., *Waste heat recovery for offshore applications*, in *ASME 2012 International Mechanical Engineering Congress & Exposition*. 2012: Houston, Texas, USA.
- [55] Nord, L.O., Bolland, O., and Martelli, E., *Weight and power optimization of steam bottoming cycle for offshore oil and gas installations*. 2014.
- [56] Athey, R.E., Martin, B.J., and Spencer, E., *Condensate Oxygen Control In A Combined Cycle System Without A Conventional Deaerator - Test Results*, in *Electric Power Research Institute Condenser Technology Conference*. 1990: Boston, Massachusetts. p. 1-8.
- [57] Evulet, A.T., *GE Oil & Gas - Gas Turbine Combustion Technologies*, in *CORE Symposium*. 2011: Houston.
- [58] Nord, L.O. and Bolland, O., *Design and off-design simulations of combined cycles for offshore oil and gas installations*. *Applied Energy* 2013. **54**(1).
- [59] Lieuwen, T. and Yang, V., *Combustion Instabilities in Gas Turbine Engines - Operational Experience, Fundamental Mechanisms, and Modeling*. Vol. 210. 2005: American Institute of Aeronautics and Astronautics.
- [60] VTU Energy, *Gas Turbine Library for Epsilon Professional*. 2014.

# A. Appendices

## I. GE LM 2500+G4 Diagrams

Figures are marked with design point for the combined cycles.

Exhaust temperature change for different loads at ambient temp 15 [°C]

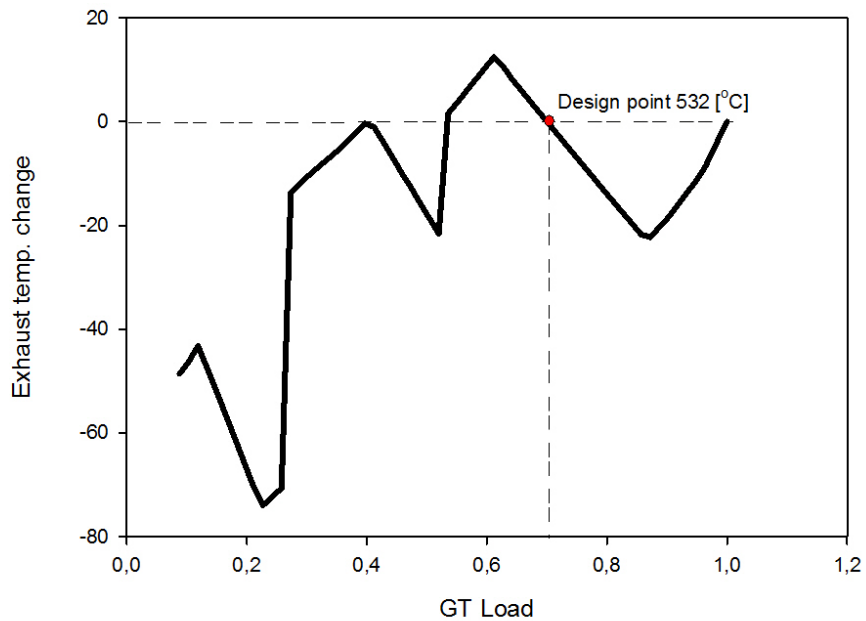


Figure A.1 GE LM2500+G4 Load vs. Exhaust temperature diagram

Exhaust mass flow change for different load at ambient temperature 15 [°C]

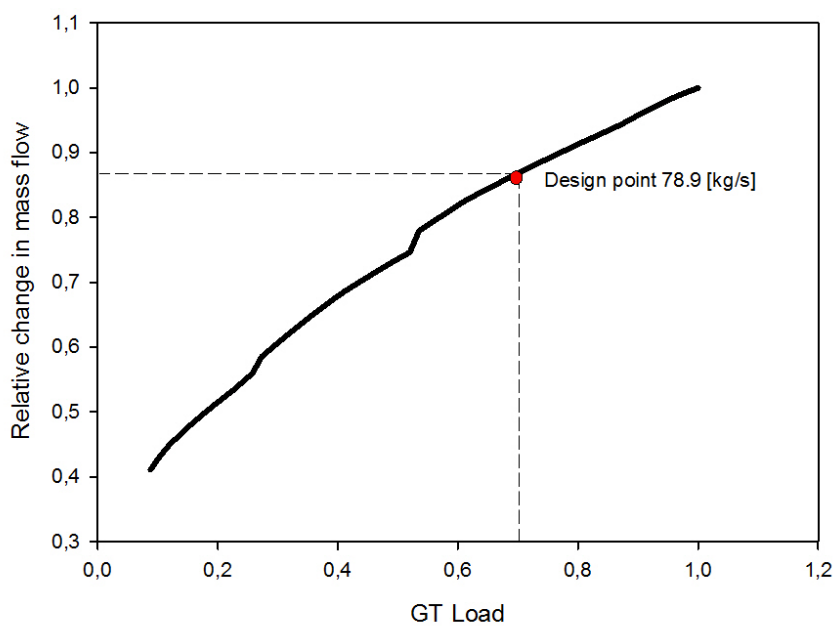


Figure A.2 GE LM2500+G4 Load vs. Exhaust mass flow

GE LM2500+ G4

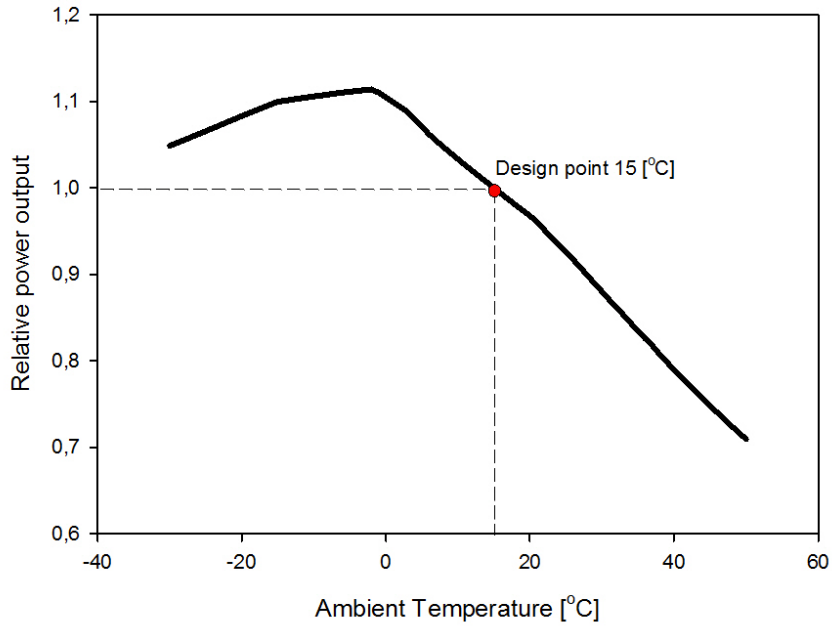


Figure A.3 GE LM2500+G4 Power output for different ambient temperatures

Table A.1 GE LM2500+G4 power output, fuel consumption and thermal efficiency at different loads

Load [%]	$\dot{W}_{GT}$ [MW]	$\dot{m}_{fuel}$ [kg/s]	$\eta_{GT}$ [%]
100	32.3	1.690	38.2
90	29.0	1.541	37.7
80	25.8	1.439	35.8
70	22.5	1.353	33.2
60	19.2	1.254	30.6
50	15.9	1.057	30.1
40	12.7	0.958	26.4

Table A.2 GE LM2500+G4 operational behavior for low ambient temperatures

$T_{amb.}$ [°C]	$\dot{W}_{GT}$ [MW]	$\dot{W}_{ST}$ [MW]	$\dot{m}_{fuel}$ [kg/s]	$\dot{m}_{air}$ [kg/s]
-20	24.60	6.92	1.432	82.73
-15	24.95	6.86	1.422	86.79
-10	25.26	7.94	1.499	88.32

## II. Diagrams Validation Simulation

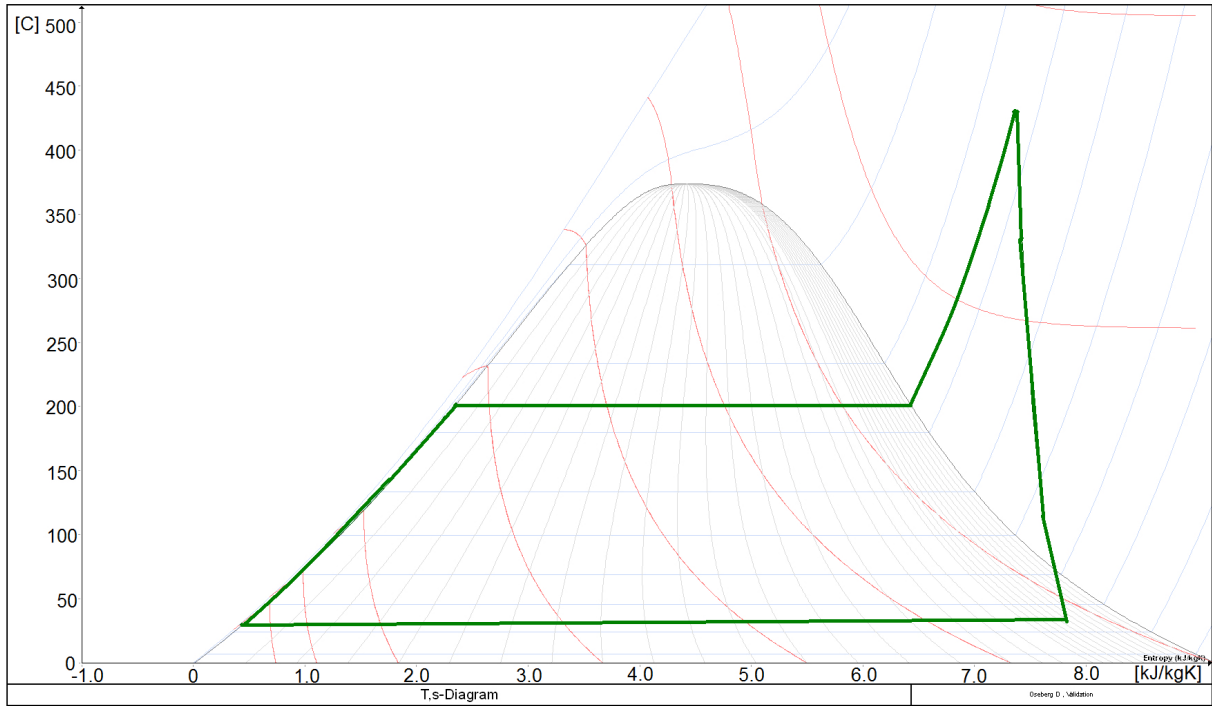


Figure A.4 T-s diagram Oseberg-D simulation

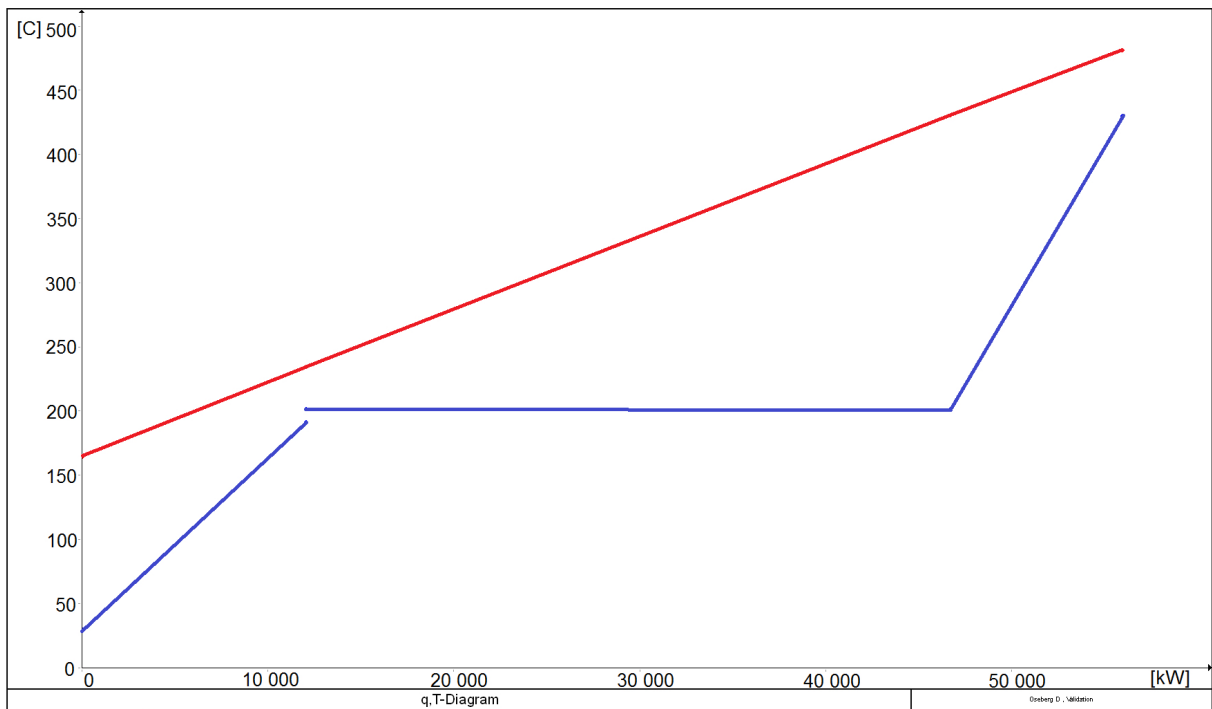


Figure A.5 HRSG Q-T diagram Oseberg-D simulation

### III. Extraction steam turbine cycle – additional results

Steam Extraction at 1 [bar]  $T_s = 100$  [°C]

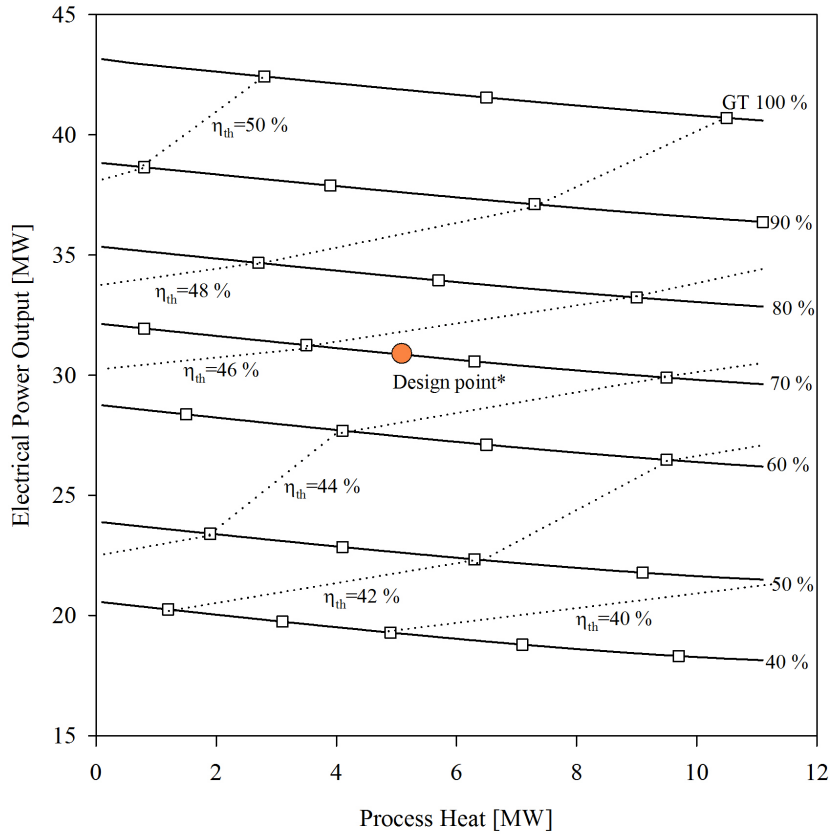


Figure A.6 Operational area for extraction steam turbine cycle at 1 [bar]  $T_s$  100 [°C]

The limiting factor for all lines of operation was the maximum deviation in mass flow through the steam turbine.

Table A.3 Off-design results for extraction steam turbine 1 [bar]  $T_s$  100 [°C]

GT Load	No Extraction		Full Extraction			
	$\dot{W}_{ST}$ [MW]	$\eta_{net,plant}$	$\dot{W}_{ST}$ [MW]	$\dot{Q}_{process,heat}$ [MW]	$\eta_{net,plant}$	$EUF$
100 %	10.8	50.9 %	8.3	11.1	47.9 %	61.2 %
90 %	9.8	50.2 %	7.4	11.2	47.0 %	61.6 %
80 %	9.6	48.9 %	7.1	11.3	45.5 %	61.1 %
70 %	9.6	47.3 %	7.1	11.3	43.6 %	60.2 %
60 %	9.5	45.6 %	7.0	11.4	41.6 %	59.5 %
50 %	8.0	44.9 %	5.6	11.3	40.5 %	61.7 %
40 %	7.9	42.6 %	5.5	11.6	37.6 %	61.0 %

Steam Extraction 2 [bar]  $T_s = 120$  [°C]

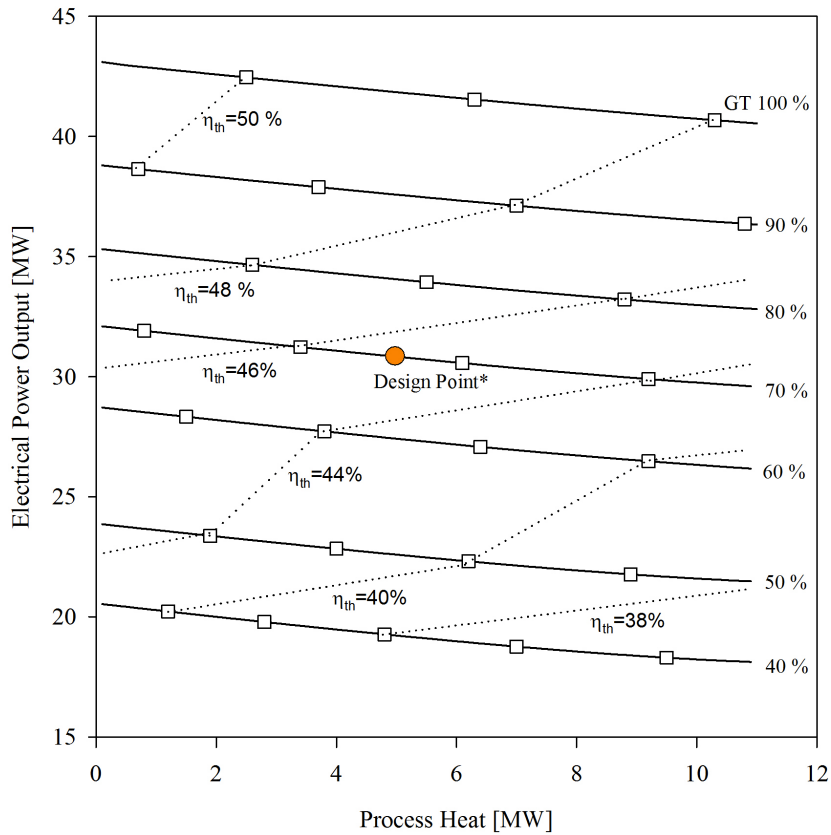


Figure A.7 Operational area for extraction steam turbine at 2 [bar]  $T_s$  120 [°C]

The limiting factor for all lines of operation was the maximum deviation in mass flow through the steam turbine.

Table A.4 Off-design results for extraction steam turbine 2 [bar]  $T_s$  120 [°C]

GT Load	No Extraction		Full Extraction			
	$\dot{W}_{ST}$ [MW]	$\dot{\eta}_{net,plant}$	$\dot{W}_{ST}$ [MW]	$\dot{Q}_{process,heat}$ [MW]	$\eta_{net,plant}$	<i>EU</i> F
100 %	10.8	50.8 %	8.2	11.0	47.8 %	61.0 %
90 %	9.8	50.2 %	7.3	11.0	47.0 %	61.4 %
80 %	9.6	48.9 %	7.1	11.0	45.4 %	60.8 %
70 %	9.6	47.2 %	7.1	10.9	43.6 %	59.8 %
60 %	9.5	45.6 %	7.0	10.9	41.5 %	59.1 %
50 %	8.0	44.9 %	5.6	10.9	40.4 %	61.3 %
40 %	7.9	42.6 %	5.5	10.9	37.6 %	60.6 %

Steam Extraction at 8 [bar],  $T_s = 175$  [°C]

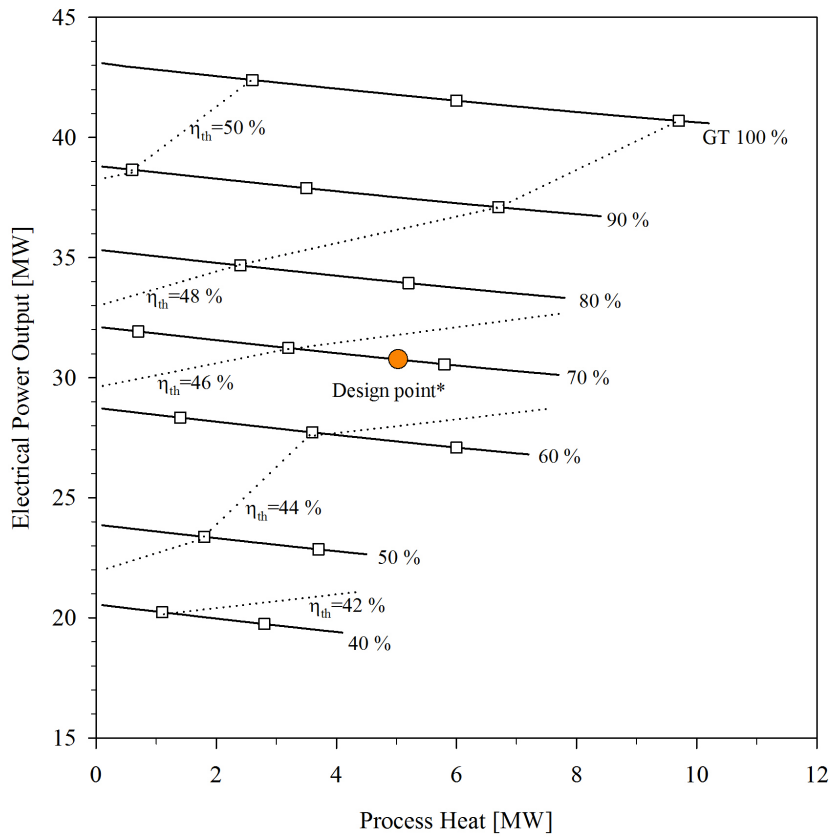


Figure A.8 Operational area for extraction steam turbine at 8 [bar]

Limiting factor is the decrease in pressure between the steam turbine stages.

Table A.5 Off-design results for extraction steam turbine 8 [bar]  $T_s$  175 [°C]

GT Load	No Extraction		Full Extraction			
	$\dot{W}_{ST}$ [MW]	$\eta_{net,plant}$	$\dot{W}_{ST}$ [MW]	$\dot{Q}_{process,heat}$ [MW]	$\eta_{net,plant}$	<i>EU</i> F
100 %	10.8	50.8 %	8.3	10.2	47.9 %	60.1 %
90 %	9.8	50.2 %	7.7	8.4	47.5 %	58.5 %
80 %	9.6	48.9 %	7.6	7.8	46.2 %	57.1 %
70 %	9.6	47.3 %	7.6	7.7	44.4 %	55.9 %
60 %	9.5	45.6 %	7.6	7.3	42.6 %	54.3 %
50 %	7.9	44.9 %	6.7	4.5	42.7 %	51.3 %
40 %	7.9	42.6 %	6.7	4.1	40.3 %	49.0 %



#### IV. Backpressure steam turbine cycle –Additional results

**Table A.6 Off-design results for backpressure steam turbine 1 [Bar] T<sub>s</sub> 100 [°C]**

GT load	$\dot{W}_{GT}$ [MW]	$\dot{W}_{ST}$ [MW]	$\dot{Q}_{process,heat}$ [MW]	$\eta_{net,plant}$	<i>EU</i> F
100 %	32.3	8.4	25.4	48.1 %	78.1 %
90 %	29.0	7.4	23.3	47.2 %	77.5 %
80 %	25.8	7.2	22.6	45.7 %	77.1 %
70 %	22.5	7.1	22.3	43.6 %	76.5 %
60 %	19.2	7.1	21.8	41.9 %	76.7 %
50 %	15.9	5.7	18.8	40.7 %	76.2 %
40 %	12.7	5.5	18.0	37.9 %	75.5 %

**Table A.7 Off-design results for backpressure steam turbine 5 [Bar] T<sub>s</sub> 150 [°C]**

GT load	$\dot{W}_{GT}$ [MW]	$\dot{W}_{ST}$ [MW]	$\dot{Q}_{process,heat}$ [MW]	$\eta_{net,plant}$	<i>EU</i> F
100 %	32.3	5.1	23.7	44.2 %	72.2 %
90 %	29.0	4.4	21.8	43.3 %	71.6 %
80 %	25.8	4.2	21.1	41.6 %	71.0 %
70 %	22.5	4.2	20.8	39.4 %	70.1 %
60 %	19.2	4.2	20.4	37.2 %	69.8 %
50 %	15.9	3.1	17.5	36.0 %	69.1 %
40 %	12.7	3.1	16.8	32.8 %	67.9 %

**Table A.8 Off-design results for backpressure steam turbine 8 [Bar] T<sub>s</sub> 175 [°C]**

GT load	$\dot{W}_{GT}$ [MW]	$\dot{W}_{ST}$ [MW]	$\dot{Q}_{process,heat}$ [MW]	$\eta_{net,plant}$	<i>EU</i> F
100 %	32.3	4.0	23.0	42.8 %	70.1 %
90 %	29.0	3.3	21.2	41.9 %	69.4 %
80 %	25.8	3.2	20.5	40.2 %	68.7 %
70 %	22.5	3.2	20.2	37.9 %	67.7 %
60 %	19.2	3.2	19.8	35.6 %	67.2 %
50 %	15.9	2.3	17.0	34.4 %	66.6 %
40 %	12.7	2.2	16.3	31.0 %	65.1 %

Backpressure steam turbine cycle 1 [bar]  $T_s$  100 [°C]

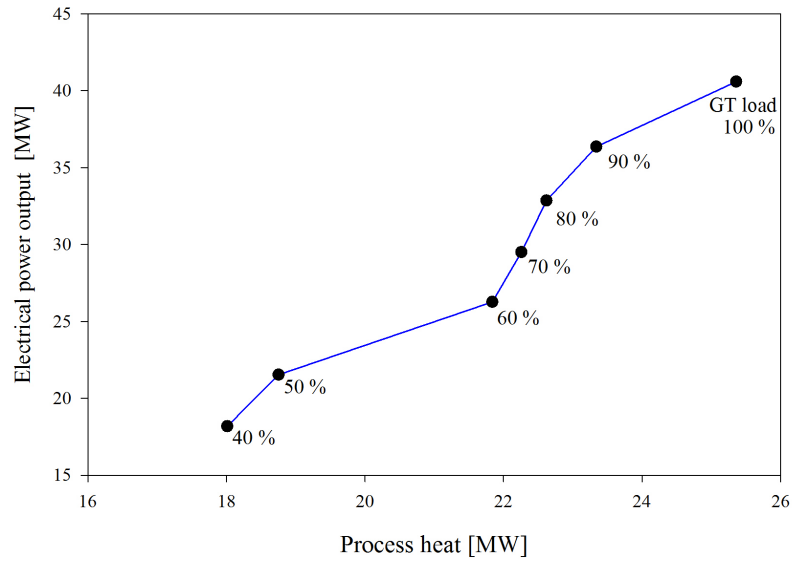


Figure A.9 Operational line for backpressure steam turbine at 1 [bar]

Backpressure steam turbine cycle 5 [bar]  $T_s$  150 [°C]

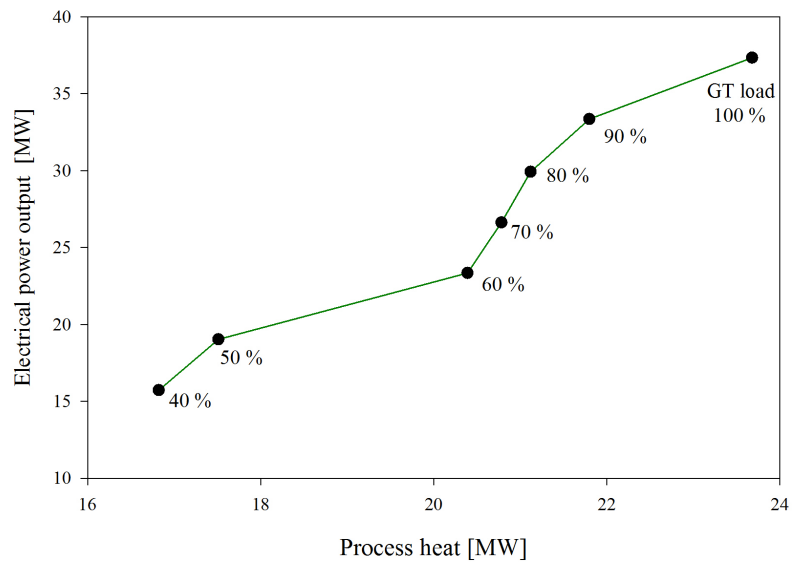


Figure A.10 Operational line for backpressure steam turbine at 5 [bar]

Backpressure steam turbine cycle 8 [bar]  $T_s$  175 [°C]

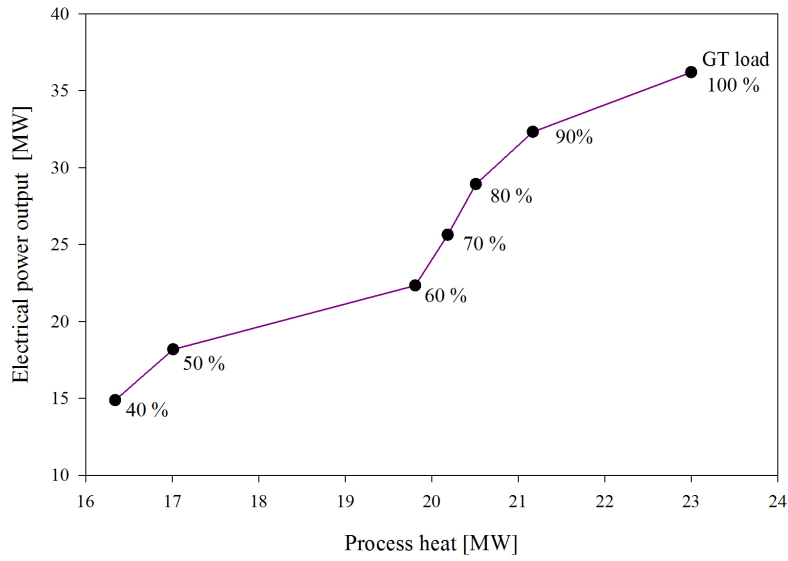


Figure A.11 Operational line for backpressure steam turbine at 8 [bar]

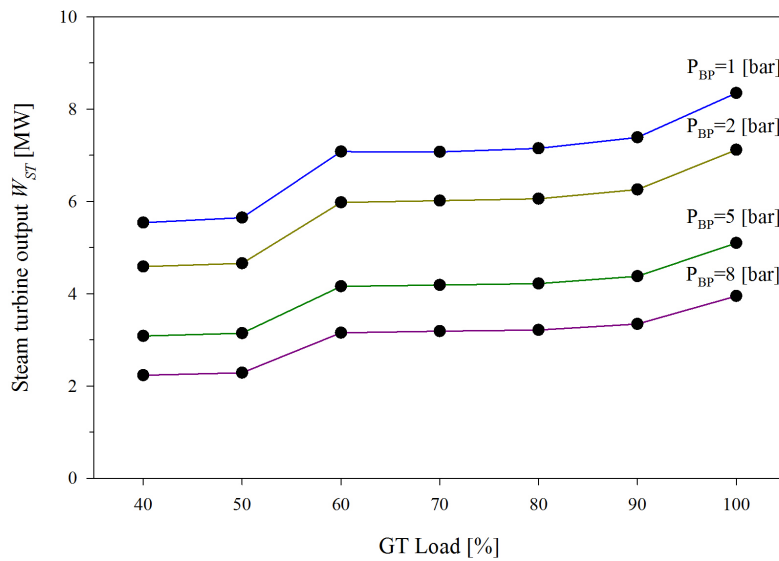
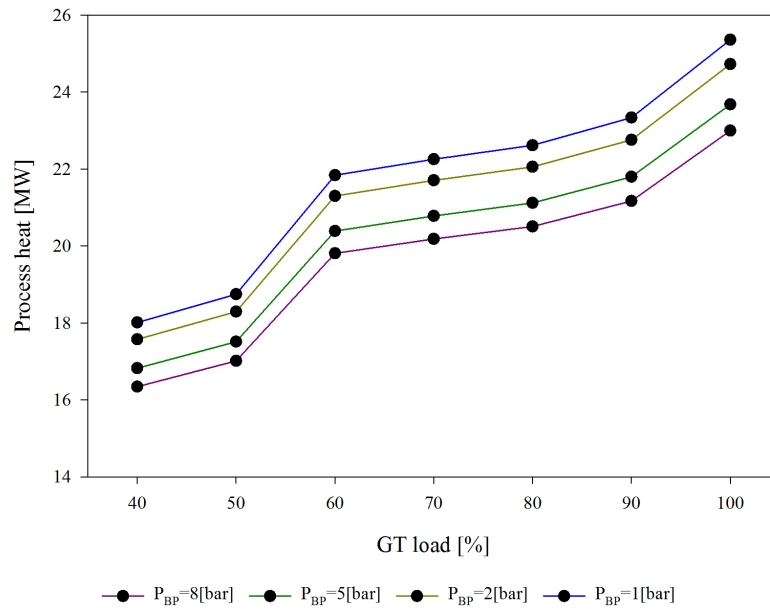


Figure A.12 Backpressure steam turbine cycle - Steam turbine output vs. GT load - All backpressure levels



**Figure A.13 Backpressure steam turbine cycle – Process heat vs. GT load - All backpressure levels**